Tracking Vascular Function as a Marker of Aortic Stenosis Progression and Outcome: Engineering, Vascular Medicine, and Population Studies

A thesis submitted by

Jonathan Brown

in partial fulfillment of the requirements for the degree of

PhD

in

Clinical and Translational Science

Tufts University

Graduate School of Biomedical Sciences

May 2023

Advisor: Benjamin S. Wessler, MD, MS

Abstract

Background: Aortic Stenosis (AS) is a common type of valvular heart disease that if left untreated carries significant morbidity and mortality. The long-held view that AS is a disease of only the aortic valve (AV) is being increasingly displaced by the understanding that the left ventricle (LV) must contend with multiple loads beyond just the stenotic AV. A critical but historically overlooked load in AS is the vascular system. We undertook a series of studies to investigate the effect of vascular function on the progression of AS and patient centered outcomes post aortic valve replacement (AVR).

Methods: We developed and validated a novel method to assess patient specific vascular parameters derived from simulated aortic input impedance. We then used this method to calculate vascular parameters over time in a large set of AS patients followed at Tufts Medical Center (TMC) from 2006-2021. Time to event models were fitted to determine the association between vascular parameters and time to AVR. Finally, we calculated vascular parameters from patients enrolled in the Placement of Aortic Transcatheter Valves (PARTNER) II prior to Transcatheter Aortic Valve Replacement (TAVR). We then fitted and assessed the incremental predictive ability of vascular parameters in predicting post-TAVR quality of life outcomes (QOL). This model was then externally validated in patients undergoing TAVR at TMC.

Results: In validation analysis comparing patient specific simulation-based vascular impedance to non-invasively measured impedance, correlation between methods across a range of vascular parameters varied between $R^2 = 0.40$ to 0.99. A tendency was seen

toward underestimation of pressure waveforms in point-by-point comparison of measured and simulated waveforms with an overall mean difference of 4.01 mmHg. A similar trend was seen in vascular parameters. Using this novel method, we found in patients followed for AS at TMC, that increases in baseline total wave intensity parameters to be associated with increased hazard of AVR (characteristic impedance HR: 0.74 95% CI: 0.58, 0.95, total forward wave intensity HR: 1.74 95% CI: 1.47, 2.06, total backward wave intensity HR: 1.23 95% CI: 1.05, 1.44 per SD). However, vascular parameters were not found to enhance predictive discrimination in post-TAVR QOL outcomes compared to models without vascular parameters (AUC: STS Risk Score + Vascular Parameters: 0.66 vs. STS Risk Score: 0.65 $p = 0.17$).

Conclusion: Simulation-based vascular parameters have the potential to allow for exploration of the effect of vascular function on the progression of AS in larger populations. Baseline vascular state is associated with the progression of AS to the point of need for AVR and may provide means of early detection of symptom emergence. However, at the point when TAVR is required, vascular parameters and ultimately function have little additional predictive benefit with respect to discrimination of post-TAVR outcomes over clinical parameters that do not include vascular impedance metrics.

Support

This work was performed in the Edelman Laboratory at the Massachusetts Institute of Technology and supported by grants to Elazer R. Edelman Poitras Professor of Medical Engineering and Science and Director, Institute of Medical Engineering and Science

Dedication

To My family

Acknowledgments

My journey from where I started to where I am now would not have been possible without the endless support and encouragement of my family, colleagues, and friends. First and foremost, I must thank my thesis advisors Professor Elazer Edelman and Professor Benjamin Wessler. Their constant encouragement, guidance, mentorship, and willingness to speak and problem solve anytime I needed was a constant source of strength during my Ph.D. In particular I'd must extend a huge thank you to Professor Edelman for his constant and unwavering support both before and during my Ph.D. I could have never imagined when I walked into the Edelman laboratory almost 10 years ago that this is where it would take me. You have truly been the central guiding figure for me during this transformative experience. I also have to express gratitude to my thesis committee as a whole, Professors Edelman and Wessler as well as Professor David Kent and Professor Norma Terrin. Without their support and insight, this work would not have come together as well as it did.

Additionally, to all those over the years in the Edelman lab who taught me how to be the best engineer, scientist, and showed me all the secrets of MIT. I am especially grateful to have met Brett Boval during my first week in lab. His insights and indulging me in my Patriots fandom were much appreciated as well as showing me all the west coast had to offer. I also have to thank Professor Claire Conway for humoring my "you know what's interesting" lunch chats and being the best social secretary, I could have ever asked for. I additionally need to thank Reuven Dashevsky for his friendship over the past 17 years, keeping me out of trouble, and my yearly bag of Reese's pieces.

Finally, I need to thank my family for their continuous support. To my parents who have always encouraged and supported me. To my siblings Daniel and Ariella for putting up with me all these years and always being willing to play catch with the koosh ball on Shabbat. To Ralph for making sure I got outside each and every day no matter how cold or hot it was outside or how tired I was. To my daughter Plia who arrived in the last year of this work and regardless of how hard the day was, always brought a smile to my face. And finally, to my wife Shira without whom this Ph.D. would have never been a reality. We got married the same month as I started my Ph.D. and I know this work has taken over our lives the last few years, but I would never have wanted to go on this journey with anyone else.

Table of Contents

List of Tables

List of Figures

List of Copyrighted Material Used

Parker, K. H. An introduction to wave intensity analysis. *Med Biol Eng Comput* **47**, 175–188 (2009).

List of Abbreviations

AS: Aortic Stenosis
AVR: Aortic Valve Replacement
KCCQ: Kansas City Cardiomyopathy Questionnaire
NYHA: New York Heart Association Class
SAVR: Surgical Aortic Valve Replacement
TAVR: Transcatheter Aortic Valve Replacement
TMC: Tufts Medical Center
WIA: Wave Intensity Analysis
WSA: Wave Separation Analysis

Chapter 1 Introduction

Aortic stenosis (AS) is a common, highly morbid and, deadly form of degenerative valvular heart disease that, if left untreated, results in an estimated 50% mortality two years after the emergence of symptoms[1–4]. The prevalence of moderate to severe AS increases with age reaching a peak in the over 75 years of age subset. Prevalence of moderate or severe AS has been found to be between 2.8% and 4.5% in those over the age of 65 in the United States (US) National Heart Lung and Blood and Olmsted County, Minnesota cohort studies of more than 28,000 subjects[5]. In 2021 there was an estimated 56 million adults in the US over the age of 65[6]. With the aging of the US population[7] it is projected that there will be 90 million Americans over the age of 65 by 2030 and over 5 million adults with AS.

The aortic valve (AV) was first described by Leonardo Da Vinci in 1512[8]. But it wasn't until 1633 that French physician Lazare Riviere described what was probably the first report of AS[9]. Despite more than 300 years of study it wasn't until 1960 that a treatment for the end stage of the disease was successfully developed[10].

AS is unique in that there are no interventions to slow progression and no medical interventions to mitigate symptoms[11]. Even patients in whom the disease is detected early are simply put on a course of "watchful waiting" as the only action. Patients undergo successive echocardiograms to track progression and only once the disease has reached its peak severity and symptoms emerge, are they offered a surgical Aortic Valve

Replacement (AVR). However, given the lack of early interventional strategies accurate tracking and understanding of factors that affect disease progression is key.

1.1 Pathology of Aortic Stenosis

Traditionally AS has been understood as a disease where an increasing burden of calcific deposits located on the AV causes a reduction in leaflet motion and AV narrowing. This results in an inability of the AV to open fully during systole. This restriction primarily acts as a resistance to forward blood flow and an increase in pressure proximal to the AV. To maintain adequate distal organ perfusion downstream of the left ventricle (LV), pressure in the LV must rise to overcome the increased resistance brought on by the stenosis of the valve. The classic teaching is that as long as the rise in pressure between the LV and aorta is adequate, distal organ perfusion is maintained and symptoms are not present. However, once the pressure generated by the LV is insufficient, symptoms begin to emerge.

The delineation of load opposing the left ventricle is multifactorial. In addition to the pressure drop across the stenotic valve, the systemic vasculature downstream of the valve imposes an additional resistance that reflects the combined effects of large and small vessel tone and caliber modulation. Every artery from the largest, the aorta, to the smallest arteriole, constricts and dilates to direct flow and in doing so imposes local flow impedances that track with vessel diameter raised to the 4^{th} power following Hagen-Poiseuille relation. This load is often defined simply as the brachial blood pressure, but

such characterization neglects the delineation of the pulsatile and steady components of cardiovascular system.

1.2 Quantification of Aortic Stenosis Severity

The severity of AS is primarily defined by severity of symptoms[12] and echocardiographic[13] parameters, but there is no continuous or linear relationship of these metrics with outcomes, only broad classification. Typically, echocardiographic parameters of peak aortic valve velocity (Vmax), mean aortic valve gradient (MG), and aortic valve area (AVA) classify patients into mild (Vmax: ≤2.5 m/s), moderate (Vmax: 2.6-2.9 m/s, MG: < 20 mmHg, AVA: > 1.5 cm^2) or severe classes (Vmax: ≥4 m/s, MG: ≥ 40, AVA: < 1 cm^2). Additionally, patients with severe AS can also be classified as symptomatic or asymptomatic. There is no one metric that is dominant in a predictive capacity leading to an ever increasing array of proposed measures and normalizations, compounded by the discordance in metric indication of severity in the same patients [14,15]. Imaging modalities such as magnetic resonance (MR), and computed tomography[16] (CT) have higher resolution when it comes to delineating anatomic structures, hemodynamic parameters[17] and degree of calcification. However, logistical and cost issues have limited these imaging types to the research space only. These hurdles additionally preclude the use of these techniques for longitudinal tracking.

1.3 Natural History of Aortic Stenosis

The natural history of AS has been greatly influenced by observations made by Ross and Braunwald[18] on post-mortem studies conducted in the 1950's and 60's. They described a

long latent asymptomatic period as valvular obstruction increases, due to a narrowing AV, up to the point of symptom presentation and a steep increase in mortality. The key symptoms identified once severe AS presented were angina, syncope, and congestive heart failure conferring five, three and two years on average until death. While these studies were an important step in defining the natural history of AS, they were done in an era when rheumatic disease was a significant contributor to the pathology of AS. This study was also based on chart reviews of only 10 patients and whose average age was 63. AS is today a disease of octogenarians, and rheumatic fever is virtually unseen in the US. The vast majority of AS cases are caused by the calcific degeneration that comes with aging.

The rate of AS progression varies widely. In prospective cohort studies conducted in Norway over a 14-year timespan found the mean rate of progression to be 3.2 mmHg/year with an standard deviation (SD) of 2.36 mmHg. For those with moderate AS or greater progression was 4.5 mmHg/year, indicating a non-linear progression of the disease[19]. Progression has also been measured in randomized control trials. The Simvastatin and Ezetimibe in Aortic Stenosis (SEAS) trial tested the effects of cholesterol lowering medication on the progression of calcific AS in mild to moderate patients. Patients were followed for a median of 52.2 months – with an annualized mean gradient change of 2.7 mmHg/year with no benefit seen on slowing the progression of AS with medication.

Survival in the modern area of surgical and transcatheter intervention has also been studied extensively. Perhaps the last natural history study of severe AS survival, due to the advent of TAVR, begin in 2007, as part of the Placement of Aortic Transcatheter Valves (PARTNER) I trial. In this trial patients with severe symptomatic AS who were not candidates for Surgical Aortic Valve Replacement (SAVR) were randomized to either TAVR or medical management. At 1 year the survival rate in the medical management group was 50.7%[4]. More recent large-scale studies conducted on the National Echocardiographic Database of Australia (NEDA), using modern echocardiographic metrics to stratify AS by severity showed that 5-year all-cause mortality in the mild AS population approaching 45%. Interestingly the moderate and severe groups displayed similar 5 year mortality figures (Moderate: 61.4% Severe: 64.6%)[20]. Together these results, with the variable rates of progression and known poor mortality without treatment suggest that current markers of progression and recommendations for tracking and intervention are still lacking.

1.4 Treatment of AS

The joint task force of the American College of Cardiology/American Heart Association recommends either SAVR or TAVR based on two primary criteria, hemodynamic parameters meeting severe AS and symptoms[21]. In those without symptoms, and normal LV function, survival is similar to age matched controls[21]. Thus, identification of symptoms early is a key component to ensuring good outcomes. Patients with mild or moderate AS are simply followed while hemodynamic severity or symptoms emerge to a point where treatment is recommended.

Currently no therapies exist to slow or stop the progression of calcific AS, with replacement being the only option. The first successfully prosthetic AV replacement for a stenotic valve was performed by Dwight Harken in 1960 at the Peter Bent Brigham Hospital in Boston[10]. These first ball-and-cage valve devices were eventually replaced with bioprosthetic bovine pericardium for the leaflet material reducing device complications and failure. SAVR had been the mainstay for treatment of AS until the advent of TAVR in 2002[9,22].

TAVR, similar to the deployment of coronary stents, is a type of minimally invasive surgery facilitated by catheterization. In TAVR the valve stent frame and leaflet material are crimped onto a catheter. The catheter is advanced to the AV position and expanded, either via a balloon or a self-expanding shape memory alloy. The minimally invasive nature of TAVR has led to a revolution in treatment, allowing those at high surgical risk or those who would otherwise not be candidates for SAVR to still receive treatment. While TAVR has opened treatment to a new large set of patients and has matched or exhibited superior survival at 1 year compared to SAVR, some drawbacks have been identified. Namely up to 1/3 of patients report no improvement in quality of life (QOL) or have died at 1 year post-TAVR[23,24]. While some prediction models have attempted to identify predictors for poor outcomes, overall performance of these models has been poor[25].

1.5 Pathology of Ventricular Afterload in Aortic Stenosis

Throughout the course of AS, the AV stiffens, and the force required to eject blood forward increases slowly but drastically over time. This resistance further causes alterations during the cardiac cycle. In particular, the rise in pressure is matched by a rise in wall thickness as dictated by the need to limit wall stress which as defined by Laplace's relationship and is related to the pressure by the quotient of LV chamber radius and thickness. The morphological changes feed into altered timing of the cardiac cycle (need for increased contraction times with greater ventricular mass and afterload, and increased ejection time through the stenosed orifice) increase ventricular work and greater myocardial oxygen demand. When this work requirement cannot be met clinical symptoms, classically seen as angina, syncope, and congestive heart failure become manifest.

As noted above a major component of this system that has been often seen as a secondary issue is the "second" load imposed on the LV, in addition to that of the stiffened AV, the systemic vasculature. It is become increasingly recognized that ventricular afterload maybe a determinant of outcomes for patients with AS that has been ill explored[26]. In principle this load is the result of two distinct but additive forces: the valve and the vasculature. However, little is known about the vascular contribution to global hemodynamic afterload, in part because in the past invasive catheterization was required for full assessment, and because of the complexity of this load which bears frequency dependence and requires more sophisticated mathematical characterization than linear and lumped parametric analysis. Hence, we still lack the ability to delineate if the dominant global afterload being

seen by the LV is a function of the stenosed valve, stiffened vasculature, or, most likely, a combination of the two and how this combination changes over time.

The gold standard for investigating vascular function and its effect on afterload is through evaluation of pressure and flow waveforms produced by the LV in the aorta. The morphology of the aortic pressure and flow waveforms in turn are influenced by the pumping of the LV and properties of the vascular system. Due to the compliant nature of this system, a highly dynamic response is seen in these waveforms. During the systolic portion of the cardiac cycle not only must the LV overcome the "static" pressure in the aorta to pump blood forward, but it must also contend with an increase of pressure due to a phenomenon known as wave reflection[27]. During each cardiac cycle, a pressure wave is produced and travels distally to the LV. At each branch point along the vascular network be it the carotid, renal, or femoral arteries among others, the pressure waveform "reflects backward" to the LV. Reflection is therefore tied to individual vascular anatomy and to the material properties of the vasculature which is by its nature are dominated by non-linear distensibility and second-order dynamics.

The reflected or backward pressure wave plus the forward wave is the systolic pressure we measure in typical office or home blood pressure monitor. Typically, using invasive methods we measure the pressure and flow in the central aortic position just above the AV. The initial upstroke in both the pressure and flow waveforms can be seen early in systolic period where wave reflection is absent, as the pressure waveform hasn't had time to travel downstream and reflect back to the LV. This can be further noted in that the peak pressure

in the aorta occurs *after* flow has peaked. A set of metrics resulting from analysis of *aortic input impedance* has the ability to quantify the magnitude and timing of the reflected wave that increases LV load as well as overall vascular stiffness and function.

1.6 Vascular Parameters

1.6.1 Vascular Impedance

Clinicians have classically thought in terms of vascular resistance and while this is helpful a lumped parametric view of overall vascular state (e.g., in a Ohmic manner relating pressure drops to net flow or cardiac output and an overall systemic vascular resistance) such a perspective does injustice to the mechanisms at play. Resistance is the response to steady or non-oscillatory flow – it is impedance that defines the limitations on the speed of pulsatile flow. Impedance incorporates the properties of the vascular system itself with widely varying viscoelastic and non-rigid properties. In the strictest sense, impedance is the relationship between pulsatile pressure and pulsatile flow recorded in the time domain taken at any point along the vascular tree. However, impedance can also integrate all of the properties and flow impediment of the vasculature downstream of the measurement location. In practice this means the most convenient site for measurement in the cardiovascular system is the central aortic position as this input impedance integrates all elements beyond the aortic valve.

Given the pulsatile, non-linear, viscoelastic and time varying nature of the pressure and flow waves generated in the LV and propagated within the vasculature, a frequency domain approach is often favored. Using this approach, the pressure and flow waveforms

are broken down into their component parts or "mini-waveforms" represented by an infinite set of successive of phasic sinusoidal waves. In practice the number of mini-waves or harmonics is limited only by the resolution of the measurement equipment. The decomposition from time domain pressure and flow waves to the frequency domain is done with Fourier analysis, and computationally with the Fast Fourier Transform. For each of the component waves or harmonics, we obtain an amplitude and phase. To obtain the impedance spectrum we relate the pressure to the flow to obtain the impedance amplitude and define the phase as the difference in alignment of the pressure and flow waveforms. Mathematically this can be written as

$$Z_i = \frac{|P_i|}{|Q_i|} \text{ and } \theta_i = (\beta_i - \phi_i)$$

where Z is impedance at the i^{th} harmonic, P is the pressure modulus, Q is the flow modulus, θ is the impedance phase, β is the pressure phase and ϕ the flow phase. It can be visually represented by plotting the modulus or harmonic amplitudes by the frequency and phase (Figure 1.1). From this spectrum we can now calculate several parameters that can fully describe the vascular system. The 0^{th} harmonic or amplitude at 0 Hz is equivalent to systematic vascular resistance (SVR) typically calculated as

$$SVR = \frac{MAP - CVP}{CO}$$

where MAP is mean arterial pressure, CVP is central venous pressure and CO is cardiac output. Values between 0 to 2 Hz are generally considered representing the pulsatile

components of the cardiovascular system. Finally, the average of higher frequency harmonics above 2 Hz are referred to as the characteristic impedance.

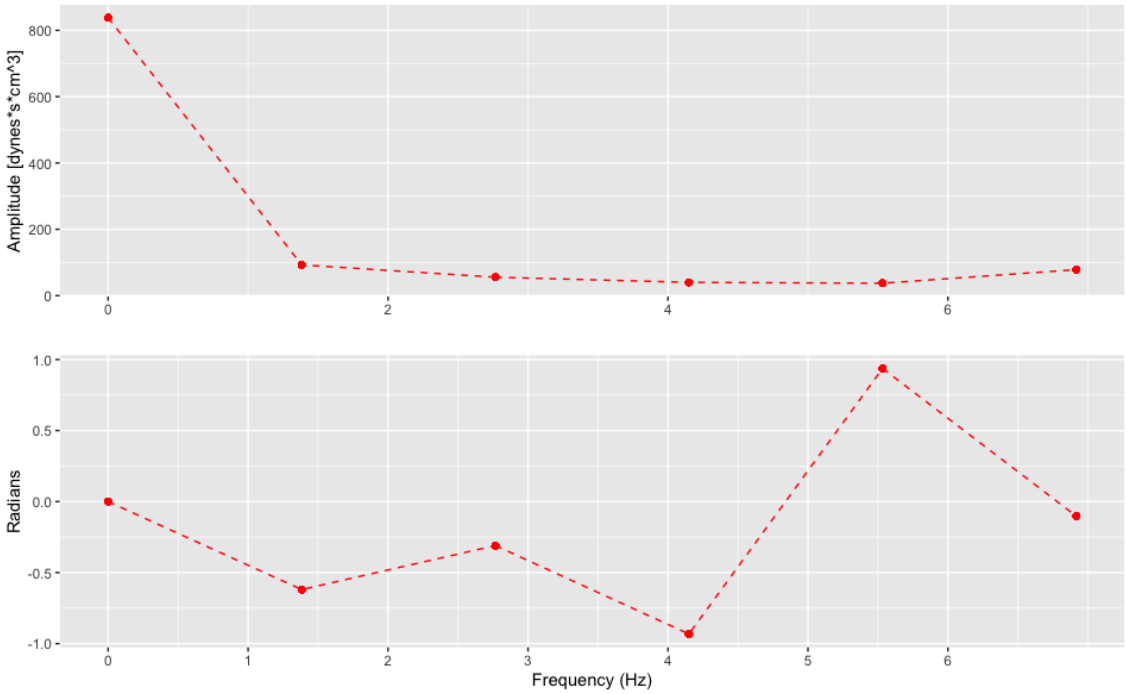

Figure 1.1 Representative plot of impedance amplitude and phase for an AS patient pre-TAVR.

Characteristic impedance is the relationship between pulsatile pressure and flow in the absence of any wave reflection effects. When measured in the central aortic position it can be thought of a metric of overall aortic stiffness and geometry.

1.6.2 Hydraulic Work

Additional but less studied parameters that can also be calculated from the impedance spectrum are steady and pulsatile hydraulic work. Pulsatile hydraulic work can be defined

as the energy lost in the vascular system to pulsation and steady work as the energy lost in maintaining steady blood flow[28,29]. These are defined as

$$Steady\ Hydraulic\ Work = Pressure_{Mean} * Flow_{Mean}$$

$$Pulsatile\ Hydraulic\ Work = \sum_{n=1}^{5} Pressure_n * Flow_n * \ |\cos(\theta_n)|$$

where n indicates the harmonic. Here we constrain these to the harmonic values up to 5 due to the data used for calculation of these parameters in our later studies.

1.6.3 Wave Intensity Analysis

A more recently developed method known as wave intensity analysis (WIA) can be used as an alternative to frequency domain Fourier based impedance. In contrast to traditional Fourier techniques examining blood pressure and flow as the summation of a set of sinusoidal waves, instead, the waves are seen as a set of successive small wavelets or wavefronts[30]. Each of these wavefronts combine to produce a single pressure wave. WIA allows for the examination of flux in energy per unit area of a vascular segment due to pressure waves that are either seen as originating antegrade from the LV or returning retrograde from the periphery due to wave reflection. Each forward and backward component can be further broken down into compression and expansion. The compression component in the forward case quantifies the pressure generated by the LV. The forward expansion wave component represents the slowing of the pressure wave by

the LV in late systole as well as integrating downstream ventricular-vascular coupling factors.

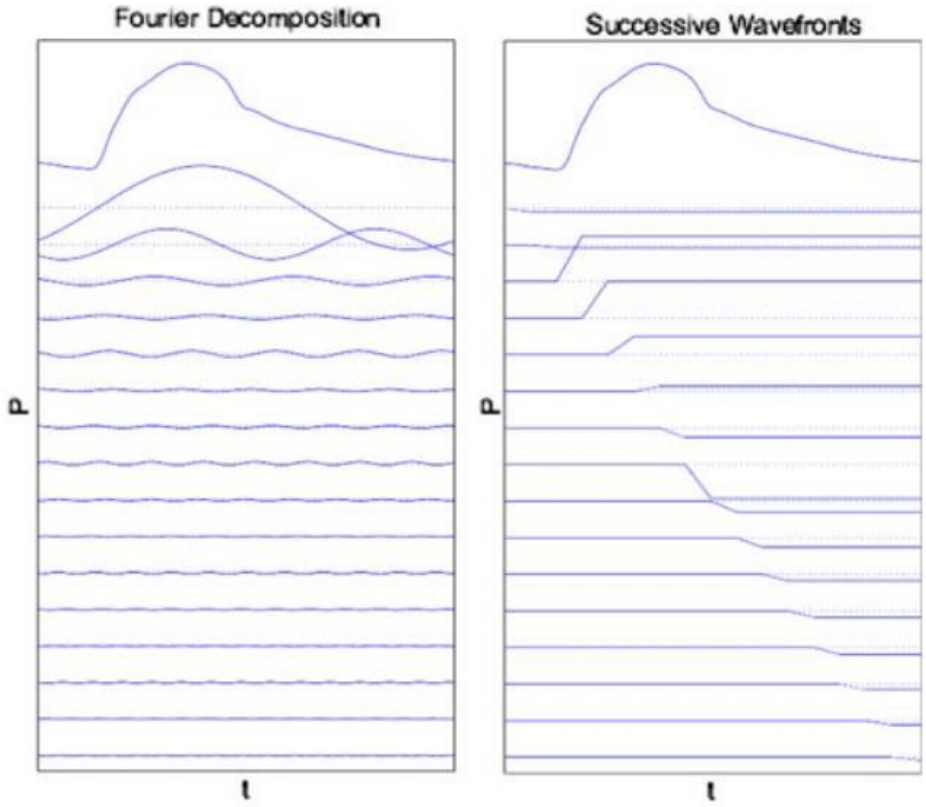

Figure 1.2. Examples of Fourier and Successive Wavefronts decomposition representations of a central aortic pressure waveform. Reprinted with permission Parker, K. H. An introduction to wave intensity analysis. Med Biol Eng Comput 47, 175–188 (2009).

WIA parameters are calculated by separating central aortic pressure waves into their forward and backward components using the water hammer or hydraulic-shock equations[31]. Finally, the wave intensity parameters can be calculated by taking the derivative of the corresponding forward and backward pressure and flow components and multiplying by each other. (Appendix 6.1)

1.7 Measurement of Vascular Parameters

Historically, invasive pressure and flow waveforms were needed to calculate impedance, or wave intensity parameters. The need for invasive catheterization[32,33] has limited regular assessment of vascular parameters and their potential integration into clinical care. More recently, echocardiography techniques[34,35] and non-invasive central pressure measurement devices have been used to calculate vascular impedance however, current non-invasive tools are expensive, require expertise, and consume significant time in an already packed clinical workflow. The need for specialized equipment and training has further limited large-scale research applications, as well as the ability to deploy these types of analysis into the clinical space. This has also limited longitudinal assessment. In practice this has limited the sample size of studies in the AS population to no more than 38 with the vast majority looking at change in metrics from pre to post-TAVR[32,33,35].

1.8 Vascular Impedance Simulation

A significant limitation in measurement of a range of vascular parameters is the need for invasive left heart catheterization or specialized non-invasive central pressure measurement equipment. This has limited the clinical understanding and implementation of these parameters into the clinical workflow. To overcome this, we set out to develop a novel method to simulate vascular impedance on a patient specific basis using routinely collected clinical echocardiographic data. Using the resulting raw impedance data, we can calculate and test the clinical association of a range of vascular parameters. Given that virtually all AS patients who come to clinical attention undergo routine

echocardiographic evaluation throughout their disease course, it might then be possible to track longitudinal changes in vascular parameters over time.

Blood pressure and flow waveforms in the central aortic position are required if we are to accurately measure vascular impedance. Blood flow captured during echocardiographic exams can be used as direct measure of overall flow. Blood pressure taken at the time of the exam can provide the systolic and diastolic pressures, or peak and trough of the brachial pressure waveform. But pressure waveform information must be extrapolated, and this cannot be inferred from the upper and lower bounds measured. As the human vascular impedance spectrums, amplitudes, and phases all fall within a set range we can propose a series of candidate central pressure waveforms from the impedance equation. Five hundred million of these candidate amplitude and phase combinations were generated. These covered the full range of physiologic and super-physiologic and states. Patient specific flow information from echocardiographic exams were then multiplied by the 500 hundred million candidate impedance values to obtain the full range of possible patient specific central aortic pressure waveforms. A well validated generalized transfer function was then to convert the central pressure waveform into a corresponding brachial pressure waveform[36]. Finally, a set of domain, bounding or convergence criteria were applied to this set to reduce the 500 million potential impedance/waveform combinations to converge upon a set of patient specific solutions. Patient specific criteria included the brachial blood pressure taken at the time of the echocardiographic exam. The results from this simulation workflow were then used to calculate a range of vascular parameters to

fully quantify vascular function. Further details and explanation of this method are explained and validated in Chapter 2.

1.9 Study Aims

Using this novel method outlined above we sought to study three primary objectives. First, we validated our novel method to simulate the vascular impedance spectrum and associated vascular parameters on a patient specific basis. Second, we applied this method to a longitudinal dataset of patients being followed for AS at a large tertiary medical center to define the association between changes in vascular parameters and time to AVR. Finally, we attempted to identify the incremental value in vascular parameters in predicting post-TAVR quality of life outcomes.

1.10 Data Sources

The data used for each of these aims comes from three data sources. The data used for the validation aim comes from a cohort of patients undergoing TAVR from 2 centers in Spain (HUMV, Santander) between 2019 and 2020. In addition to standard clinical data, concurrent pressure data was obtained using a central pressure measurement device (SphygmoCor XCEL, AtCor Medical Sydney, Australia), and flow data from standard clinical echocardiographic exams. These were used to calculate reference vascular impedance and associated vascular parameters. The second data source was a cohort of AS patients followed at Tufts Medical Center (Boston, MA). This dataset was generated from several individual sources of data. Firstly, all echocardiographic reports between 2006 and 2021 were analyzed with a natural language processing framework. This was

required as echocardiographic data prior to 2010 was not available in the standard clinical echocardiographic dataset. This data was then merged with all other echocardiographic data between 2010 and 2021. From this dataset patients were searched for any record of AS. This was defined as having a peak aortic valve velocity of greater than 2.5 m/s, a mean aortic valve gradient of 20 mmHg or greater, an aortic valve area of less than 1.5 cm^2 or a record of an AVR. All longitudinal echocardiographic data was then gathered and used for impedance simulations. Clinical and demographic data was obtained from the Tufts Research Data Warehouse. Outcome data for those patients who underwent TAVR or SAVR was obtained from the TMC site specific Society of Thoracic Surgeons/Transcatheter Valves (STS/TVT) registry. Finally, the last data source was patients enrolled in the Placement of AoRTic TraNscathetER Valves II (PARTNER II) clinical trial. The PARTNER II trial was a large, randomized control trial designed to test the safety and effectiveness of the Edwards SAPIEN XT TAVR valve in the high and intermediate surgical risk population.

Chapter 2 Clinical Validation of Non-Invasive Simulation Based Determination of Vascular Impedance in Patients Undergoing Transcatheter Aortic Valve Replacement

---

Brown JY, Fernandez GV, De la Torre Hernández JM, Murphy M, Wessler BW, Edelman ER. To be submitted to Annals of Biomedical Engineering

2.1 Introduction

Aortic Stenosis (AS) is detected in ~5% of people over 65, and its prevalence increase with age. The advent of new technologies such as Transcatheter Aortic Valve Replacement (TAVR) [37] for minimally invasive replacement and the observation that many patients have poor outcomes after aortic valve replacement (AVR) have prompted the search for enhanced diagnostics to identify disease early but also to determine potential benefit from intervention. Pressure drop across the valve is not sufficient to predict need for benefit from TAVR, and there is evidence that vascular afterload adds further physiologic and prognostic information to understanding AS[32,33,35]. Only 1/3 of patients who undergo TAVR receive clinical benefit,[23] 50% of patients post-TAVR are hypertensive, and paradoxically post-TAVR hypertension confers a significant mortality benefit over those that are normotensive[38]. Taken together, these observations motivate the need for a greater understanding of left ventricle (LV) vascular coupling that may be a key component to ensuring good outcomes post-TAVR.

Aortic input impedance provides the most comprehensive physiologic description of the interaction between the LV and vascular system. While the concept of input impedance has been in use since the early 1950s a significant hurdle to its wide spread implementation has been difficulty in measurement and calculation[27]. Traditional measurement of input impedance requires simultaneous central aortic blood pressure and blood flow through the aorta. Each of these time-based signals is then decomposed using signal processing techniques such as Fourier analysis[27]. For each decomposed harmonic the ratio of pressure and flow amplitudes are taken, and phases subtracted to obtain the

full frequency domain-based impedance spectrum. In the past, obtaining concurrent pressure and flow signals has required invasive catheterization which is not conducive to repeated measurements allowing for studies such as tracking disease progression. While non-invasive methods have been developed, namely using non-invasive central blood pressure devices and echocardiography[34,39] or Cardiac Magnetic Resonance[40] for blood flow, they require specialized equipment and training. They are also an additional time burden on the already overloaded clinical workflow, making routine use difficult. Furthermore, given the highly dynamic environment of the cardiovascular system and high dimensional nature of impedance, the direct relationship between various impedance parameters and clinical outcomes remains unclear in AS.

To allow for more accurate tracking of changes in impedance during the progression of AS, prior to TAVR, and the relationship to clinical outcomes, we sought to develop and validate a patient-specific simulation-based method to measure aortic input impedance[35]. Routine standard of care clinical echocardiographic data along with a simple brachial blood pressure measurement were used as inputs. Reference measured impedance was calculated using data from a non-invasive central pressure measurement device and echocardiograms. Our novel simulation-based method was validated in a cohort of AS patients undergoing TAVR.

2.2 Materials and Methods

2.2.1 Cohort

Patients undergoing TAVR were recruited from 2 centers in Spain (HUMV, Santander) between 2019 and 2020. Inclusion criteria were a diagnosis of severe symptomatic AS and suitable femoral access as determined by the local heart team. Patients not able to provide informed consent were excluded. The study was approved at each site, written and informed consent was obtained from all subjects.

2.2.2 Echocardiographic Data

Echocardiographic data were captured at baseline prior to the TAVR. Standard clinical echocardiographic views and metrics were captured describing LV, valvular, and hemodynamic states. Specific data extracted for use in the calculation of impedance was peak aortic valve velocity, acceleration time, heart rate, stroke volume, and aortic valve area (AVA). Stroke volume and AVA were calculated via standard continuity-based methods[41].

2.2.3 Non-Invasive Central Pressure Measurements

Non-Invasive central pressure measurements were captured using the SphygmoCor XCEL (AtCor Medical Sydney, Australia) system alongside echocardiographic data. Time-resolved central pressure waveforms were exported and saved for offline analysis for comparison against output central blood pressure waveforms from the Simulation-based vascular impedance (SBVI) method. Additionally, the standard brachial blood pressure was taken and recorded for use in the SBVI.

2.2.4 Vascular Impedance

Recorded vascular input impedance was calculated via the standard method[27]. Time resolved blood pressure and linear blood velocity flow waveform data were decomposed computationally into their Fourier harmonics via the Fast Fourier Transform (FFT). Input impedance amplitude values were calculated as the ratio of the pressure waveform amplitude at each harmonic to the flow amplitude. The impedance phase angles were calculated by subtracting the pressure and flow harmonic phase angles. Central aortic pressure waveform data was supplied from the SphygmoCor device. Linear velocity blood flow waveforms were generated using data extracted from echocardiographic exams using a 5^{th} order B-spline. Heart rate was used to define the signal period, peak aortic valve velocity, the peak of the flow waveform, and acceleration time, the time to peak flow. The ejection duration (ED) was determined by an optimization algorithm that iteratively tested a range of ED values until the area under the curve matched the stroke volume as recorded by echocardiography. Further details on blood flow waveform generation can be found in Appendix 6.2.1.

2.2.5 Simulation-Based Vascular Impedance

Simulation-based vascular impedance was calculated using an iterative method. Human vascular impedance spectrums, amplitudes, and phases fall within a set range. This range was defined based on values taken from literature both in normal[27,42] and AS patients[33–35]. With this knowledge, we created a set of candidate impedance spectrum amplitudes and phase values. This range was then expanded by 20% to ensure all physiologic and pathophysiologic vascular states were represented. Five hundred million candidate

amplitude and phase pairs were generated to ensure sufficient coverage across all possible combinations. Using the standard method of calculating impedance amplitude and phase using the FFT we can rearrange each equation to solve for the pressure amplitude and phase harmonics. By applying the inverse FFT we can obtain the time-resolved central pressure waveform. Each candidate set of impedance values was then used in this workflow along with the flow amplitude and phase calculated from the decomposed echocardiographic flow waveforms to obtain all-candidate central pressure signals. Using the well-validated generalized transfer function[36] this central pressure waveform was then converted into the corresponding brachial pressure waveform. Domain bounding criteria were applied to this signal to reduce the number of solutions to only those that were patient-specific and displayed a set of physiologic characteristics present in all human pressure waveforms.

Domain bounding criteria were broken down into patient-specific and knowledge-based criteria. First candidate waveforms were filtered with the patient-specific criteria of the measured brachial blood pressure set to a tolerance of +/- 2.5 mmHg. Physiologic knowledge-based criteria consisted of (1) all pressure waveforms must decrease after the end of the systolic portion of the cardiac cycle, (2) a peak pressure could not occur after the end of systole, (3) the difference between start pressure and minimum pressure must be less than 1 mmHg, (4) the first local maximum after peak pressure if one exists can be no greater than 3 mmHg above the first local minimum after peak pressure, (5) the first local pressure maximum must also be the global pressure maximum, and (6) the maximum pressure must occur after the peak flow (Figure 2.1). If multiple waveforms

passed all criteria, median values were taken and used for analysis. All simulations were conducted using a custom Python code (Python 3.6).

2.2.6 Vascular Parameters

A set of vascular parameters derived from each type of impedance calculation were used to allow for additional comparisons of SBVI and non-invasively recorded methods. Metrics selected for the comparison were derived both from the frequency domain representation of impedance and the time domain-based central pressure waveforms. Characteristic impedance (Zc) was taken as the average of the impedance amplitudes at harmonics with frequency values between 2-10 Hz, excluding amplitude values that were greater than two standard deviations above the mean amplitude. Wave Intensity analysis (WIA) was also conducted to calculate the total forward and backward wave intensities. In short, WIA is an alternative method to Fourier-based impedance to understanding vascular hemodynamics. In contrast to traditional Fourier techniques examining blood pressure and flow as the summation of a set of sinusoidal waves, instead, the waves are seen as a set of successive wavefronts[30]. WIA allows for the examination of flux in energy per unit area of a vascular segment due to pressure waves originating from the LV or returning from the peripheral due to wave reflection. Hydraulic work or energy lost due to inefficiencies or mismatches between the LV and vascular system were also calculated. Finally, a sensitivity analysis was conducted where central pressure derived from the SphygmoCor rather than brachial pressure was used for patient-specific domain bounding criteria. This was done to assess the effect associated with using the generalized transfer function to convert brachial to central aortic pressure in AS patients.

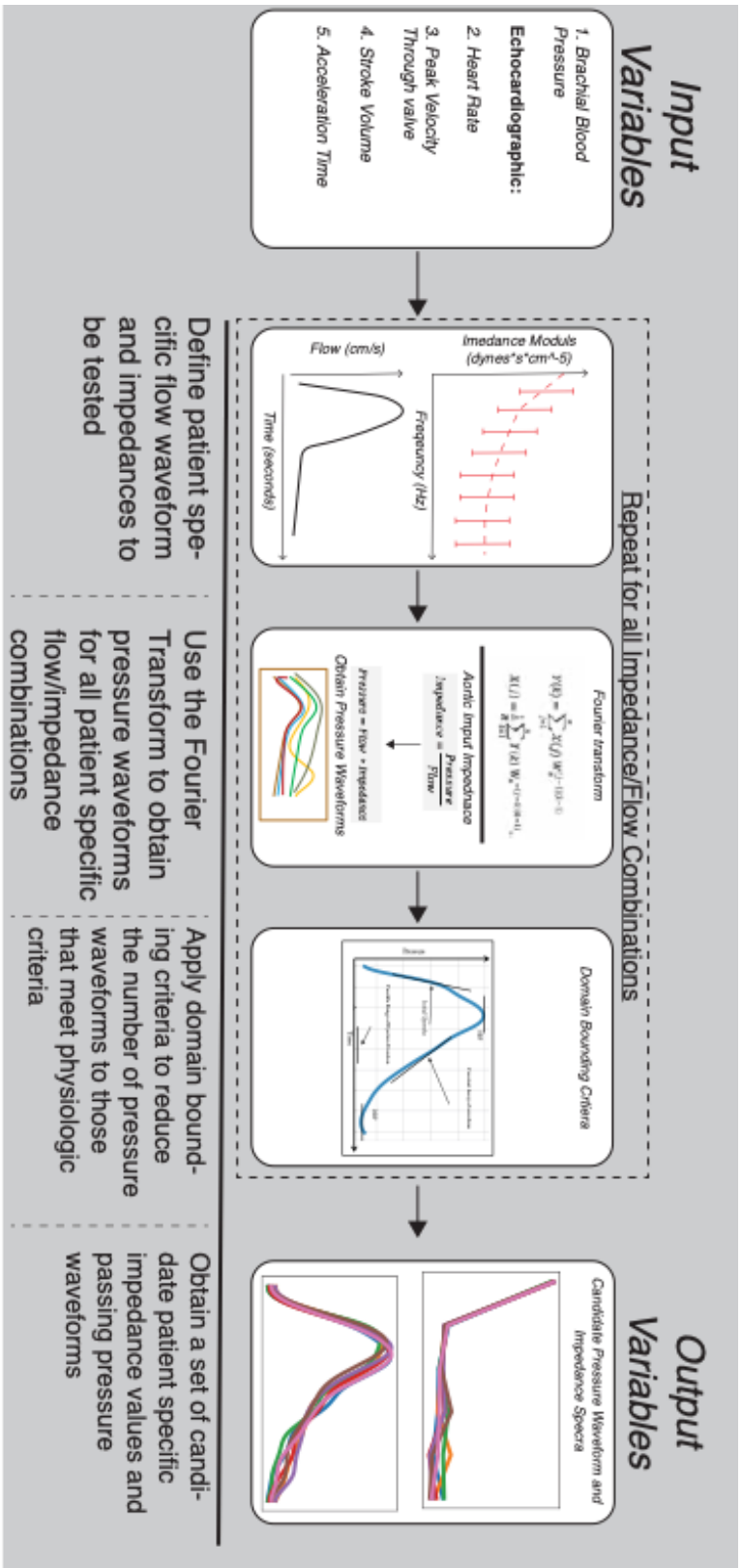

Figure 2.1 Impedance Simulation Workflow Diagram

2.2.7 Statistical Analysis

Continuous data were presented as means with standard deviations and categorical variables were presented as counts and percentages. Absolute differences in vascular parameters from each impedance calculation method were compared using measured impedance and SBVI techniques. Bland-Altman plots were used for visualization and to assess bias and limits of agreement. Differences between measurements were calculated as recorded minus simulated. Correlation coefficients for each set of metrics were also calculated. Point-by-point differences between central pressure waveforms derived from SBVI and recorded SphygmoCor central pressure waveforms were also calculated and compared.

2.3 Results

2.3.1 Cohort Characteristics

A total of 111 patients undergoing TAVR had sufficient echocardiographic and SphygmoCor data to complete both simulated and recorded vascular impedance measurements. The average age of the cohort was 73 (SD: 19), with 36% female, and 79% had hypertension at the time of baseline assessment. Overall hemodynamics were typical for patients with severe symptomatic AS. Group average AVA was 0.71 cm^2 (SD: 0.26), mean gradient 47 mmHg (SD: 16), and a peak velocity of 425 cm/s (SD: 79). From the initial generation of 500 million potential impedance values and resulting simulated central pressure waveforms a mean of 25 waveforms was generated for each case.

2.3.2 Central Pressure Waveforms

A visual comparison across all patients of central pressure waveforms between simulation and SphygmoCor showed overall good agreement (Appendix Figure 6.2). After alignment of central waveforms, point-by-point differences across all patients averaged 4.01 mmHg (CI: 3.9, 4.1 mmHg) with a small underestimation found with the simulation-based method. Similarly, sensitivity analysis using the central pressure from the SphygmoCor for the patient specific domain bounding decreased point-by-point waveform differences to 2.95 mmHg (CI: 2.16, 4.34 mmHg).

2.3.3 Vascular Parameters

Mean bias of the characteristic impedance, and steady hydraulic work indicated on average overestimation of simulation values compared to recorded values. Total forward and backward wave intensities were found on average to underestimate values. Similarly pulsatile hydraulic work was underestimated as well (Table 2.1). Visual inspection of Bland-Altman plots showed agreement between recorded and simulated measurements decreased as the measurement increased in magnitude. Correlation coefficients across these metrics showed a high degree of correlation (R^2 = 0.72 to 0.99) except for total backward wave intensity (R^2 = 0.4) (Appendix Figure 6.4 - Figure 6.6). The magnitude as a percentage of the 95% limits of agreement was large, relative to the standard deviation of the recorded metric (Table 2.2), for several of the parameters. As a percentage of the standard deviation the larger limit of agreement was 2 times the standard deviation for characteristic impedance, 1.05 times the total forward wave intensity, 2.5 times the total backward wave intensity, 0.2 times the steady hydraulic work, and 1.0 times the pulsatile

hydraulic work. Poor agreement was also seen in raw impedance amplitude values, except for the 0^{th} harmonic which displayed a maximum limit of agreement of only 0.25 times the standard deviation. High correlation between recorded and simulated values were seen in all amplitude harmonics except for the 3^{rd} harmonic. (Appendix Figure 6.3, Table 6.1).

2.4 Discussion

In this study, we sought to develop and validate a novel method of determining vascular input impedance using only echocardiographic data and standard clinical brachial blood pressure. The primary finding of this study was that simulation based vascular impedance can measure metrics of vascular function similarly to those measured non-invasively. Excellent agreement was seen in simulation and measured central pressure waveforms. With respect to impedance metrics high correlation was found between recorded and simulated metrics for characteristic impedance, hydraulic work, and forward wave intensity metrics. However, the 95% limits of agreement were large for most of the parameters, and a small degree of bias was also associated with each metric. For prediction, correlation is more important than Bland-Altman agreement, however in other contexts, it may not be valid to substitute the simulated for the actual metrics. The measurement of vascular impedance is not new but the technique itself has been sparsely used in the AS space. The majority of investigations have been limited to acute post-TAVR studies with longitudinal studies nonexistent. Due to the need for repeated pressure and flow measurements and the traditionally invasive nature to capture this data, the longitudinal progression of impedance in the general population has also been

limited. With the adoption of echocardiography for flow measurements, larger-scale population-based studies of impedance became possible. For example use of vascular impedance in the Framingham Heart Study allowed for the broad population-level understanding of ventricular-vascular coupling and potential risk factors for cardiovascular disease[43–45]. However, these studies have required long follow-up and specialized equipment.

Measurement of impedance in AS patients has presented further challenges due to the blood flow jet produced by the narrowing AV. Narrowing of the valve creates a venturi effect causing a pressure decrease near the valve along with an increase in jet velocity as is traditionally measured by continuous wave echocardiography. In the case of invasive assessment, this creates the need to pay special attention to the catheter position for pressure and flow measurements[46,47].

Clinically, AS presents significant challenges as no pharmacological therapies have been shown to be effective, and treatment is limited to AVR as the disease progresses to its severe form. This paradigm of "watchful waiting" creates the need for novel metrics to better track the disease course. Vascular afterload has been an aspect of disease progression that in the past has been either ignored or taken as simple systolic blood pressure. However, the dynamic time varying nature of the coupling of the LV and the AV requires techniques such as vascular impedance to be fully characterized. Our simulation-based method attempted to overcome measurement hurdles of the past and

create a platform to allow for larger more detailed investigations of impedance in AS patients.

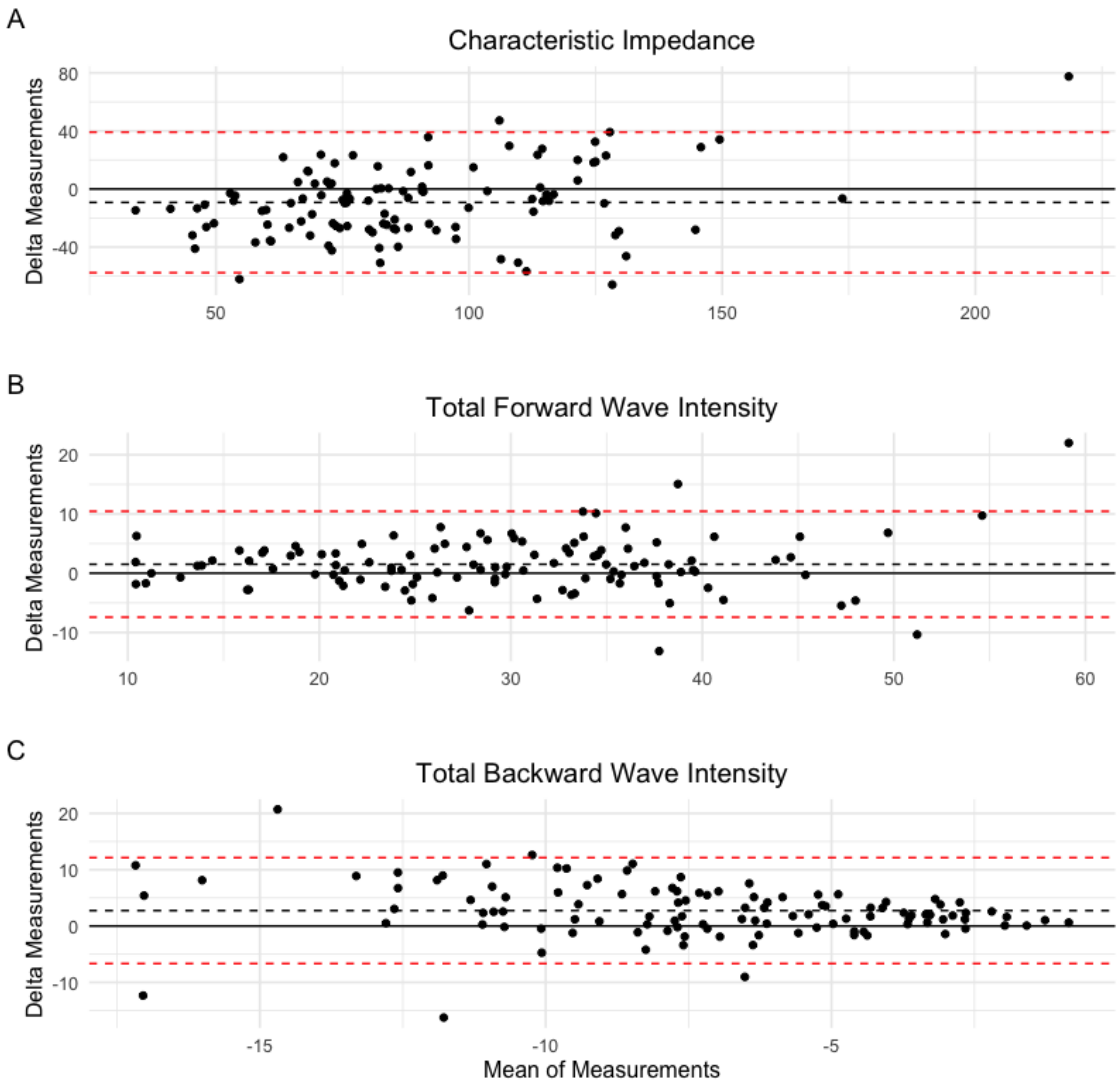

Figure 2.2 Bland-Altman plots showing characteristic impedance (dynes/cm^3), total forward and backward wave intensity (W*m^{-2}*s^{-1}*1e4) values. The black dashed line indicates the overall mean value and dashed red lines the 95% limits of agreement. The delta of the measurements was taken as recorded minus simulated.

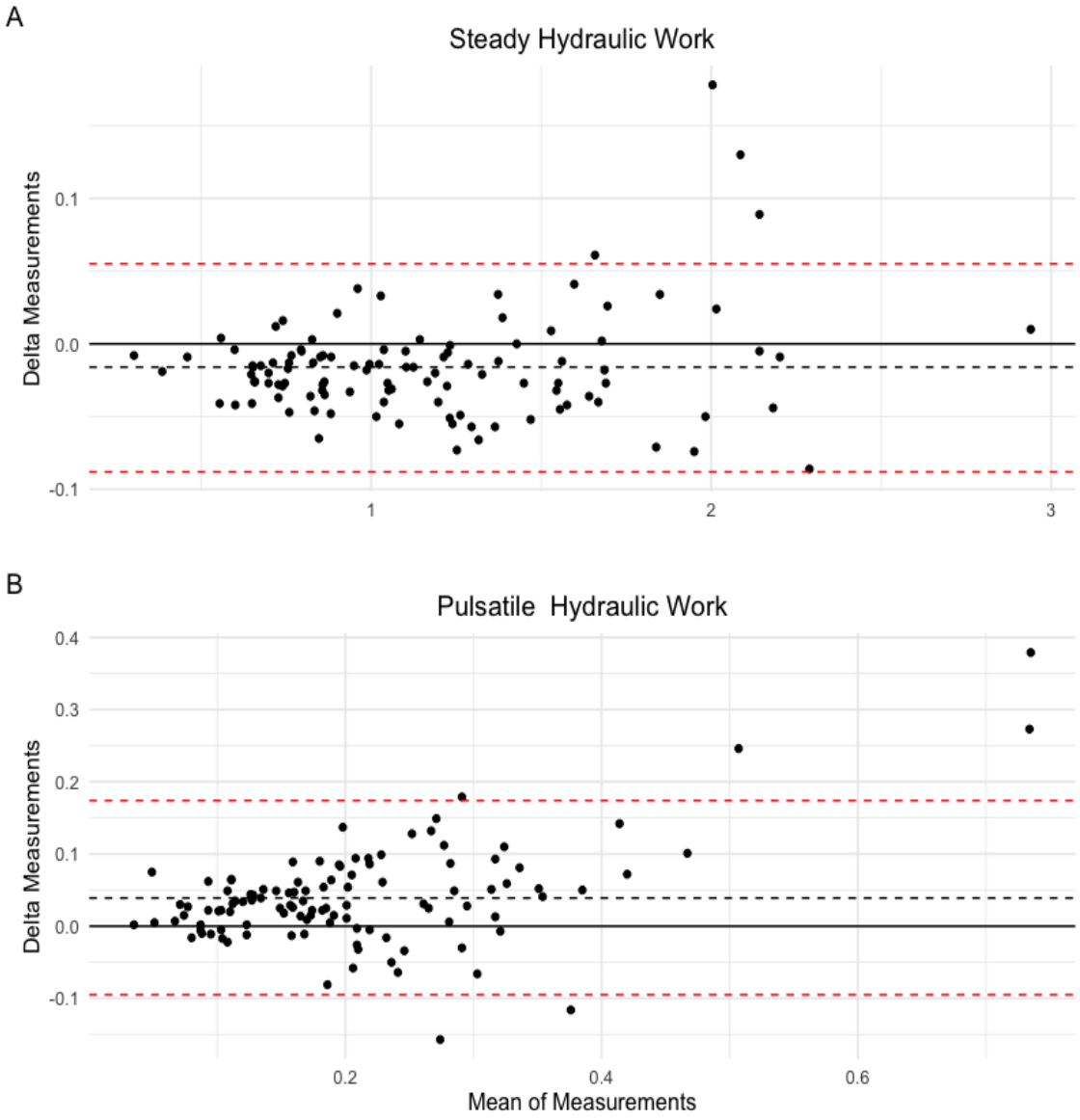

Figure 2.3 Bland-Altman plots steady and pulsatile hydraulic work (watts). The black dashed line indicates the overall mean value and dashed red lines the 95% limits of agreement. The delta of the measurements were taken as recorded minus simulated.

Table 2.1 Pre-TAVR baseline demographic and hemodynamic variables

Characteristic	Baseline, N = 111[1]
Demographics	
Age (yrs)	73 (19)
Sex	
Male	25 (64%)
Female	14 (36%)
Body Mass Index	29.1 (5.7)
Hypertension	31 (79%)
Hemodynamics	
Systolic Blood Pressure (mmHg)	138 (21)
Diastolic Blood Pressure (mmHg)	75 (13)
Heart Rate (bpm)	75 (12)
Mean Gradeint (mmHg)	47 (16)
Peak Aortic Velocity (cm/s)	425 (79)
Aortic Valve Area (cm^2)	0.71 (0.26)
Dimentionless Index	1.37 (12.27)
Stroke Volume (ml)	74 (27)
Ejection Duration (s)	0.336 (0.032)
Acceleration Time (s)	0.119 (0.022)
AVACT/ED Ratio	0.36 (0.06)

[1] Mean (SD); n (%)

Table 2.2 Comparison table of vascular parameters calculated from non-invasively recorded and simulated methods for determination of vascular impedance.

Metrics N = 111	*Recorded (Mean±SD)*	*Simulated (Mean±SD)*	*Correlation Coefficient*	*Mean Bias*	*95% Limits of Agreement*	*Maximum Limit of Agreement as a Percentage of SD*
			Frequency Domain Parameters			
Characteristic Impedance (dynes/cm^3)	84 (36)	93 (28)	0.72	-9.2	-57.7, 39.2	206
			Total Wave Intensity Analysis Parameters			
*Forward (Watts*meters^{-2}*seconds^{-1}*1e4)*	30 (11)	29 (10)	0.91	1.5	-7.4, 10.5	105
*Backward (Watts*meters^{-2}*seconds^{-1}*1e4)*	-5.9 (3.8)	-8.7 (4.8)	0.40	2.7	-6.7, 12.1	252
			Hydraulic work			
Steady (Watts)	1.16 (0.49)	1.17 (0.48)	0.99	-0.02	-0.09, 0.06	18.8
Pulsatile (Watts)	0.23 (0.14)	0.19 (0.10)	0.88	0.04	-0.1, 0.2	200

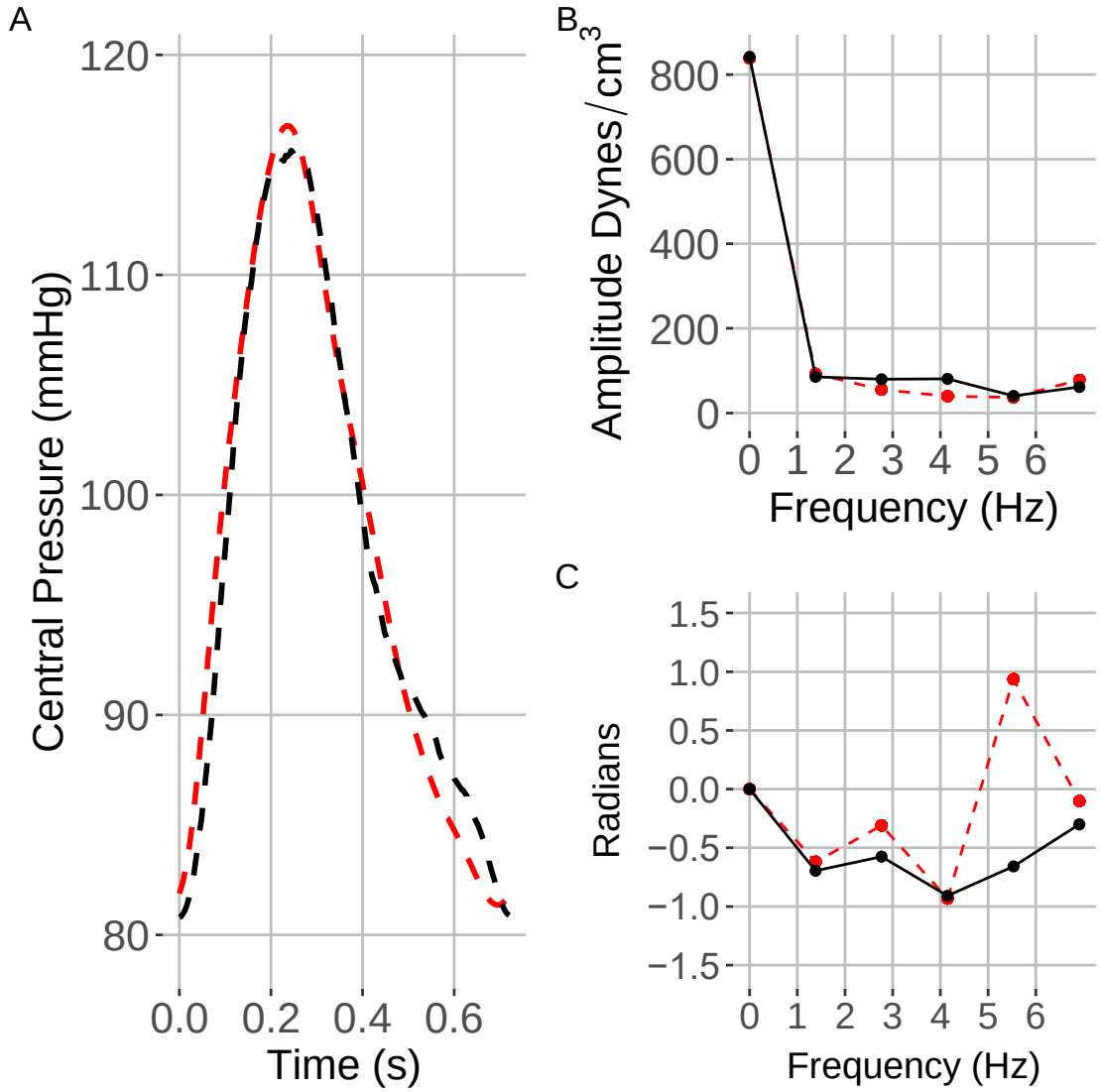

Figure 2.4 Example set of central pressure wave and impedance data is shown comparing measured and simulated values. Panel A shows a comparison of non-invasively measured central pressure (dashed red), simulation based central pressure waveforms that passed all domain bounding criteria (blue), and signal averaged median value (dashed black). Panel B and C similarly show impedance amplitude and phase for the corresponding waveforms found in panel A.

2.4.1 Input Data Measurement Error

Given the simulation-based nature of our method, measurement error is limited to the input variables of the flow data and temporal distance between flow and pressure-based data capture. Prior work has shown that over the course of a standard clinical echocardiographic evaluation systolic blood pressure can decrease as much as 12.4 mmHg[48]. This presents a logistical challenge, as without accurate measurements, errors will filter down within the analysis. To address this issue, we attempted to collect all pressure and flow data as close in time as possible to eliminate the chance of discordance and obtain as accurate measurements as possible.

An additional source of error is the generalized transfer function used in both the simulation method and SphygmoCor device which we used for comparison of measured and simulation based central pressure waveforms. Sensitivity analysis showed a small decrease in point-by-point waveform error when using central pressure only for patient specific calibration. While this analysis does not remove the need for the generalized transfer function, by using the central aortic pressure measured non-invasively, it did not require an additional transformation within the simulation framework. While this did reduce the error associated with point-by-point differences. The benefit was relatively small given brachial pressure is nearly always measured clinically. Given the relatively small decrease of 0.53 mmHg in point-by-point waveform difference this may indicate that the use of the transfer function, while introducing some error, has limited effect on overall waveform morphology.

2.4.2 Waveform Comparison

Point-by-point comparisons of waveforms showed good agreement with only a 3.5 mmHg underestimation of central pressure relative to non-invasive measurement. As part of an invasive study of impedance in AS patients Yotti et al showed when measuring pressure using two different types of catheters, one of which was a high sensitivity pressure flow Combowire, that differences up to 15 mmHg could be found[47]. However, morphological features of central pressure waveforms between devices showed little difference. A similar effect was seen with a visual inspection of our method in an example patient (Figure 2). This would suggest that while our simulation-based method does underestimate central pressure by a small amount this is similar to other invasive methods. Importantly like non-invasive studies our simulation method maintains morphologic features as seen in the comparison of recorded and simulated central pressure waveforms across all subjects (Appendix Figure 6.2). Furthermore, similar results have also been found when comparing the SphygmoCor device, used in this validation study, to invasive catheter-based measurements. In these studies the mean differences in absolute value were found to be as large as 4.6 mmHg[49] but with a strong correlation between central systolic and pulse pressure[49].

2.4.3 Impedance Spectrums

Due to the lack of scatter around the mean bias line, quantification of limits of agreement are not possible in the 0^{st} through 3^{rd} amplitude harmonics. However high degrees of correlation were seen in all but the 3^{rd} harmonic. Given the known increase in noise with increasing harmonic, this finding is not surprising. Furthermore, most of the total

impedance amplitude values are found in the first 2 or 3 harmonics with higher frequency values lumped together and taken as the characteristic impedance. Most of the impedance spectrum values are found in this low-frequency range are the driving features of central pressure waveform morphology. One prior validation study that compared invasive to non-invasive techniques identified a tendency toward underestimation of impedance[50]. Despite this underestimation, high correlation between the invasive and non-invasive techniques were seen like our study. This may be of particular importance when it comes to the clinical application of these techniques. While absolute differences in values were seen, high correlation among the simulation and recorded values may still allow for impedance-based variables to be used in prediction models. Finally given the non-intuitive meaning of these variables their clinical application is limited. Metrics derived from parts of this spectrum have been shown to be more clinically relevant such as wave intensity or hydraulic work[28,32,35].

2.4.4 Characteristic Impedance

Limited prior literature exists on validation studies comparing methods of calculating impedance, and none in the AS population. Despite this Kelly el at[50] examined invasive to non-invasive calculation of impedance in patients undergoing left heart catheterization for coronary artery disease. While comparisons of impedance metrics across studies is challenging given differences in how and which impedance metrics are calculated we were able to compare characteristic impedance values. We found our own limits of agreement ranging from -57 to 39 dynes/cm^3 where Kelly et al found approximately -75 to 52 dynes/cm^5. To directly compare the two studies differences in how blood flow was

measured needs to be considered. In our study we used linear blood flow from echocardiographic data, whereas Kelly at el used similar echocardiographic data and then measured the valve area and multiplied the two to obtain volumetric flow. Converting one unit to the other would require a known aortic valve area for each patient, but if we take an assumed value for AS patients of 0.8 cm^2 we obtain volumetric flow-based limits of agreement in our study of -71 to 48 dynes/cm^5. Displaying similar results to those found in this prior study.

2.4.5 Hydraulic Work and Total Wave Intensity

Simulated steady and hydraulic work showed high degrees of correlation to measured values, but poor agreement with respect to limits of agreement as a percentage of standard deviation. Furthermore, a tendency for values at the extremes were shown to have a greater degree of bias. In contrast steady hydraulic work displayed excellent agreement by both correlation coefficient and limits of agreement as a percentage of standard deviation. This agreement was most likely due to the fact that the primary components in the calculation of steady hydraulic work are mean flow and mean pressure. Given the tight agreement between the measured and simulated central pressure waveforms and the use of the same flow data good agreement is not surprising.

Total wave intensity showed better agreement as measured by the correlation coefficient in the forward versus backward direction. Backward wave intensity relies upon accurate separation of the pressure wave into forward and backward components with the use of characteristic impedance. Similarly, in the time domain, this can be thought of as the

acceleration time of the flow waveform, which is the point at which the pressure waveform is not yet affected by wave reflection effects. There is some debate as to whether calculation in the time or frequency domain is best for the determination of the characteristic impedance [51]. In our analysis we chose to use the frequency domain-based calculation as the flow data for the measured and simulation-based methods were the same. Thus, any differences in any downstream calculations that required the use of characteristic impedance could be attributed to differences in the method used. Correlation between characteristic impedance measured and recorded were similar despite the underestimation in the simulation-based data. This leads to the potential conclusion that while there was not good agreement between the total backward wave intensities any differences are most likely due to differences in how characteristic impedance was determined and ultimately the forward to backward separation point. However, in the time domain, the acceleration time differences are on the order of 20 ms indicating that trying to determine a difference this small may be more noise than signal. This is especially evident when, as with many echocardiographic-based measurements, the acceleration time is hand drawn and some inherent error is present in a person-to-person measurement. Taken together this might suggest that while total backward wave intensity may be a high noise metric, that signal may be present provided that the same measurement technique is used.

2.4.6 Limitations

As with any study, there are limitations to this validation. Some data has shown poor agreement between SphygmoCor and invasive measurements in AS patients, but these

studies examined only absolute systolic and diastolic values and not waveform morphology[52]. This would also suggest that any differences in AS patients are not due to any inherent issues with the method but rather the use of the generalized transfer function in AS patients. However, in our sensitivity analysis using central rather than brachial pressure from the SphygmoCor, without the need for the generalized transfer function, we found similar agreement in correlation of impedance metrics supporting the conclusion that the generalized transfer function does not add a significant amount of error. The development of an AS-specific generalized transfer function would further increase the accuracy of our simulation-based method. Simultaneous non-invasive capture of pressure and flow data is difficult. We attempted to reduce temporal mismatch as much as possible however, differences between the measured pressure and flow data may have caused errors in downstream impedance measurements in both measured and simulated results.

2.5 Conclusion

Simulation-based vascular impedance has the potential to allow for greater exploration of the effect of impedance on AS patients. Given the limited data required for our method, we believe it to be well positioned for use in large-scale retrospective studies to further explore both the acute and long-term effects of vascular changes over the course of AS.

2.6 Contributions

All authors contributed to the design, interpretation, and revision of the manuscript. JB drafted the manuscript. JYB, GVF, JMH, MM, BW and ERE contributed to subsequent revisions.

Chapter 3 Longitudinal Metrics of Vascular Function and Time to Aortic Valve Replacement

---

Brown JY, Terrin N, Kent DK, Wessler BW, Edelman ER. To be submitted to Journal of the American College of Cardiology

3.1 Introduction

Aortic stenosis (AS) is one of the most common forms of valvular heart disease worldwide. While AS primarily affects those over the age of 65, due to the aging baby boomer population in the United States it is estimated that there will be nearly 5 million individuals with AS by 2030 [5]. The progressive stenosis of the Aortic Valve due to the increased deposition of calcium and fibrosis[53] is often seen as the primary source of increased myocardial afterload. However, it is increasingly being recognized that the vascular system may also be a significant contributor to the total afterload imposed on the left ventricle[32,54,55].

Due to the progressive nature of the disease and the current lack of medical therapies available for slowing or halting progression, timing of Aortic Valve Replacement (AVR) is key. Normally echocardiographic analysis along with patient reported symptoms are used for disease tracking and procedural decision making[21]. However, research into the longitudinal contribution of the vascular system to disease progression and ultimately AVR has been lacking.

The gold standard for complete assessment of pressure flow relationships in the vascular system as well as vascular function is vascular impedance. In the past invasive pressure and flow measurement were the standard for assessment, however this limited longitudinal measurement. Non-invasive methods utilizing echocardiography and non-invasive central pressure measurement devices have been developed. But these require large long term prospective cohort studies along with expensive and specialized

equipment. Advancements now allow frequency domain based vascular impedance to be simulated on a patient specific basis, using standard clinical echocardiographic data and a simple brachial blood pressure measurement. By applying these techniques to a large retrospective cohort, we can now describe how vascular afterload changes over time for patients with AS and how metrics of vascular impedance effect time to AVR.

To better understand the effect that vascular impedance has on time to AVR and if increased vascular stiffness leads to earlier need for AVR, we examined a cohort of AS patients followed at Tufts Medical Center (Boston, MA). We evaluated association between metrics derived from the frequency domain representation of vascular impedance and time to AVR.

3.2 Methods

3.2.1 Study Population

All patients undergoing echocardiographic evaluation at the Tufts Medical Center (TMC) from 2006 to 2021 were screened for an indication of AS at any point in time. AS was defined from clinical echocardiographic reports as having a peak aortic valve velocity of greater than 2.5 m/s, a mean aortic valve gradient of 20 mmHg or greater, an aortic valve area of less than 1.5 cm^2 or a record of an aortic valve replacement (AVR). For patients identified as having any of these indications, all available echocardiographic data was obtained from the echocardiographic laboratory database (IntelliSpace Cardiovascular, Phillips). Corresponding clinical data was obtained from the TMC electronic medical record via the Tufts Research Data warehouse. For each echocardiographic encounter AS

severity was defined as either mild, moderate, or severe using the European Association of Cardiovascular Imaging and the American Society of Echocardiography[13] (EACI/ASE) recommendations. This was based on peak aortic valve velocity, mean aortic valve gradient, aortic valve area, and dimensionless index. If an echocardiographic encounter was found to have discordant criteria for severity, the more severe class was chosen. A limited number of echocardiographic exams had AS severity determined by a board-certified cardiologist. While these labels integrate additional data not found in the numerical values obtained during the exam, these labels were used for comparison against EACI/ASE derived guidelines. Patients were then filtered by including only those who had at least two echocardiographic evaluations. Finally, to facilitate determination of both baseline AS severity and data for impedance simulations, a minimum number of echocardiographic variables were required to be present (Appendix Table 6.3, Table 6.4). If any of these variables were missing for a patient during their longitudinal follow up, only the missing echocardiographic encounters where this data was found was removed. This study was reviewed and approved by the Tufts Institutional Review Board (STUDY00000157).

3.2.2 Aortic Input Impedance Simulation

Aortic input impedance simulations were conducted with the method validated from our prior validation study (see Chapter 2). In short, data obtained from each echocardiographic encounter was inputted into the simulation model. Data required for input was systolic blood pressure, diastolic blood pressure, heart rate, peak aortic valve velocity, stroke volume, and acceleration time. Since acceleration time was not available

in this dataset, a previously built linear regression sub-model used to model acceleration time and used as input for the simulation method. (Appendix 6.4.1). Primary outputs from the simulation used for calculation of vascular function parameters were the frequency domain-based amplitude, magnitude, and phase, central pressure, and linear velocity flow waveforms.

3.2.3 Vascular Parameters

Three vascular parameters derived from the impedance simulations were calculated. Characteristic impedance (Zc), or overall vascular stiffness in the absence of wave reflection, was calculated as the mean amplitude value of the frequency domain harmonics ranging from 2 to 10 Hz, excluding any values 3 times greater than the mean[51]. Wave Intensity Analysis (WIA) was used to quantify the afterload in the presence of wave reflection. Total forward and backward wave intensity was calculated as the product of the derivative of the central pressure and the velocity waveforms[30].

3.2.4 Statistical Analysis

The primary endpoint of this study was time from index echocardiographic evaluation until AVR. Baseline demographic, clinical, hemodynamic, and vascular parameters were summarized with median and interquartile ranges stratified by baseline AS severity. Categorical variables were summarized as counts and percentages. Kaplan-Meier curves were generated for time to AVR stratified by baseline AS severity. To assess any differences in the cohort between those with and without all data needed for simulations, rates of AVR between those groups were compared.

Two separate multivariable cox proportion hazard regression models were fitted. First a model that included only data at baseline was fitted to model the association between vascular parameters and time to AVR stratified by baseline AS severity. That is, different baseline hazard functions were estimated for each of the three severity groups, but the hazard ratios for the vascular parameters were assumed to be equal across groups. A second model was then fitted that included all vascular parameters as time varying covariates plus age and left ventricular ejection fraction (LVEF). The three primary vascular parameters of interest were characteristic impedance, total forward and backward wave intensity. All continuous variables were scaled to their standard deviation. Variables included for adjustment were age, sex and LVEF dichotomized as above or below 50%. LVEF was chosen for adjustment due to its inclusions in treatment guidelines as a factor to consider in addition to AS severity when making a recommendations for AVR[12]. The Bonferroni correction was used to adjust for multiple comparisons of each of the vascular parameters entered within model. A p-value of 0.017 was considered significant. The proportional hazard assumption was assessed with Schoenfeld residuals and the linearity assumption with martingale residuals. To test for any interaction between baseline AS severity and the vascular parameters, a further model was fit with interaction terms.

Finally, a sensitivity analysis was conducted where any patients who underwent SAVR were removed. This was done to assess time to AVR as a surrogate for time to symptoms. Under current AHA/ACC recommendations only those with symptoms should be offered either a SAVR or TAVR. Those patients without symptoms and specifically those being

considered for another cardiac surgery such as coronary artery bypass graft could also be offered a SAVR concurrently. While we did not have access to symptomatic state of patients, by removing those that underwent SAVR, this sensitivity analysis was intended to estimate time to symptoms with the time to AVR endpoint. All statistical analysis were conducted in R 4.1.2[56] and RStudio[57].

3.3 Results

3.3.1 Study Population

11,028 echocardiographic encounters recorded from 4,050 patients were used as an initial screen and a minimum indication of AS or AVR during evaluation at TMC. Some 1,540 patients across 2,392 encounters had some indication of AS or underwent AVR during follow up and had sufficient data to run the impedance simulations and met simulation convergence criteria (Figure 3.1). A total of 297 (19%) patients in the cohort underwent AVR. Stratified by baseline severity those in the severe group has the highest rate of AVR followed by moderate and then mild AS (Table 3.2). Across all strata the median time to AVR was 3.63 years (95% CI: 3.27, 4.55 years). Median time to AVR for the severe strata was the shortest followed by moderate then mild (severe: 1.14, moderate: 5.68, mild: 6.72 years).

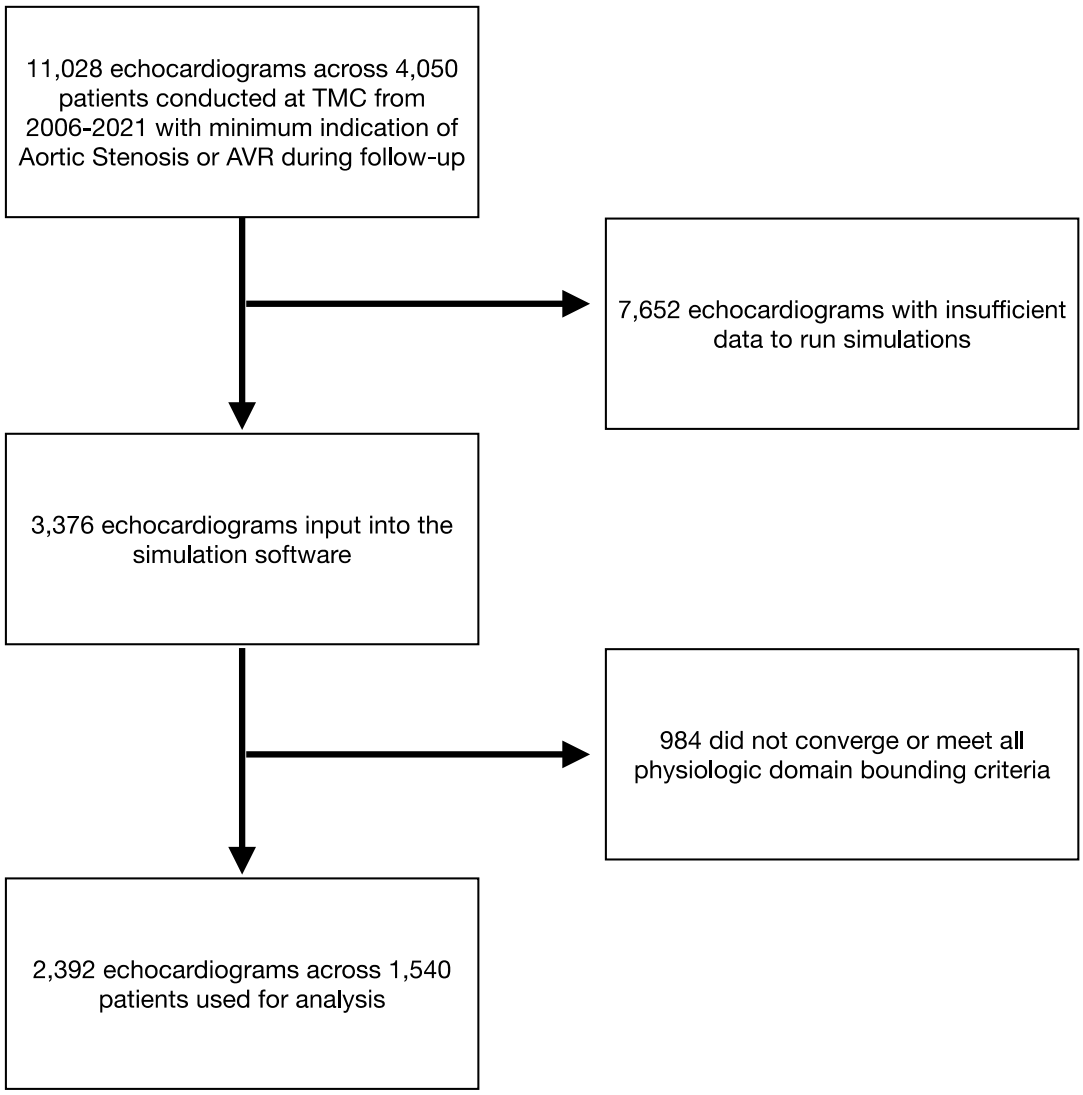

Figure 3.1 Flow diagram of patients and echocardiographic encounters screened and included in the analysis.

3.3.2 Baseline Cohort Characteristics

Baseline demographic characteristics across strata were similar with respect to body mass index, rates of hypertension, cardiovascular disease, diabetes, and cerebrovascular disease. Median age was lowest in the mild group (median: 66 IQR: 56, 76 years) and increased with each stratum. Distribution of male and female subjects were similar in

moderate (43% Female) and severe (41% Female) strata with a slightly lower rate of female subjects seen in the mild group (32% Female). The cohort as a whole was 77% white. Hemodynamic metrics were all consistent with the assigned baseline AS severity label. Clinically labeled severity was higher than guideline-based severity (Table 6.7). Of note that an increasing percentage of patients within each stratum of AS severity had ejection fractions that were less than 50% (mild: 27%, moderate: 31%, severe: 39%). Similar rates of mitral regurgitation were seen across all groups, with a larger percentage of severe AS patients having trace to mild mitral regurgitation (Table 3.1).

3.3.3 Baseline Vascular Parameters

Baseline characteristic impedance decreased with each increasing baseline severity strata (mild: 129 IQR: 108, 161, moderate: 106 IQR: 84,133, severe: 85 IQR: 68, 111 [dynes*sec/cm^3]). Similarly total forward wave intensity increased as well (mild: 9 IQR: 7, 14, moderate: 14 IQR: 10,19, severe: 20 IQR: 15, 26 [$W*m^{-2}*s^{-1}$ *1e4]). Backward wave intensity decreased across strata (mild: -4.9 IQR: -6.7, -3.3, moderate: -6.3 IQR: -8.3, -4.6, severe: -6.6 IQR: -9.3, -4.8 [$W*m^{-2}*s^{-1}$ *1e4]), but due to the fact that the directionality of these waves travels from the periphery back to the LV a more negative value indicates a larger magnitude reflected wave.

Table 3.1 Baseline Cohort Characteristics stratified by AS severity at index echocardiographic encounter

Variable	Mild, N = 531[1]	Moderate, N = 486[1]	Severe, N = 523[1]
Age	66 (56, 76)	71 (61, 79)	76 (65, 83)
Sex			
M	214 (68%)	267 (57%)	309 (59%)
F	99 (32%)	200 (43%)	213 (41%)
Body Mass Index	27 (24, 32)	28 (25, 33)	28 (25, 34)
Systolic BP (mmHg)	122 (111, 134)	124 (111, 136)	124 (111, 138)
Diatolic BP (mmHg)	72 (63, 80)	70 (60, 79)	69 (60, 78)
Hypertension	325 (61%)	300 (62%)	332 (63%)
Peak Aortic Valve Velocity (cm/s)	189 (145, 223)	251 (218, 289)	354 (292, 412)
Mean Aortic Valve Gradient (mmHg)	7 (4, 10)	13 (10, 18)	28 (19, 39)
Stroke Volume (ml)	74 (62, 91)	65 (54, 78)	59 (47, 71)
Aortic Valve Area (cm^2)	2.15 (1.83, 2.68)	1.31 (1.17, 1.46)	0.78 (0.65, 0.94)
AVAi (cm^2)	1.23 (1.01, 1.47)	0.75 (0.66, 0.82)	0.45 (0.35, 0.52)
Dimentionless Index	0.62 (0.52, 0.75)	0.40 (0.34, 0.46)	0.25 (0.20, 0.30)
Ejection Fraction			
<50%	141 (27%)	151 (31%)	205 (39%)
>50%	390 (73%)	335 (69%)	318 (61%)
Cardiovascular Disease	146 (76%)	326 (71%)	423 (81%)
Diabetes	62 (32%)	189 (41%)	216 (41%)
Cerebrovascular Disease	44 (23%)	110 (24%)	137 (26%)
Procedure Type			
SAVR	9 (1.7%)	29 (6.0%)	66 (13%)
TAVR	14 (2.6%)	43 (8.8%)	137 (26%)
No AVR	508 (96%)	414 (85%)	320 (61%)
Mitral Regurgitation			
None	63 (12%)	57 (12%)	50 (9.6%)
Trace/Mild	404 (76%)	342 (70%)	369 (71%)
Moderate/Severe	64 (12%)	87 (18%)	104 (20%)
Aortic Regurgitation			
None	284 (53%)	200 (41%)	165 (32%)
Trace/Mild	178 (34%)	225 (46%)	265 (51%)
Moderate/Severe	69 (13%)	61 (13%)	93 (18%)
Characteristic Impedance (dyne*sec/cm^3)	129 (108, 161)	106 (84, 133)	85 (68, 111)
Total Forward Wave Reflection (W*m^−2*s^−1*1e4)	9 (7, 14)	14 (10, 19)	20 (15, 26)
Total Backward Wave Reflection (W*m^−2*s^−1*1e4)	-4.9 (-6.7, -3.3)	-6.3 (-8.3, -4.6)	-6.6 (-9.3, -4.8)

[1] Median (IQR); n (%)

Table 3.2 Rates of Aortic Valve Replacement Stratified by Baseline Aortic Stenosis Severity

	Event		
	No AVR	AVR	Total
Baseline AS Severity			
Mild	508 (96%)	23 (4.3%)	531 (100%)
Moderate	414 (85%)	72 (15%)	486 (100%)
Severe	321 (61%)	202 (39%)	523 (100%)
Total	1,243 (81%)	297 (19%)	1,540 (100%)

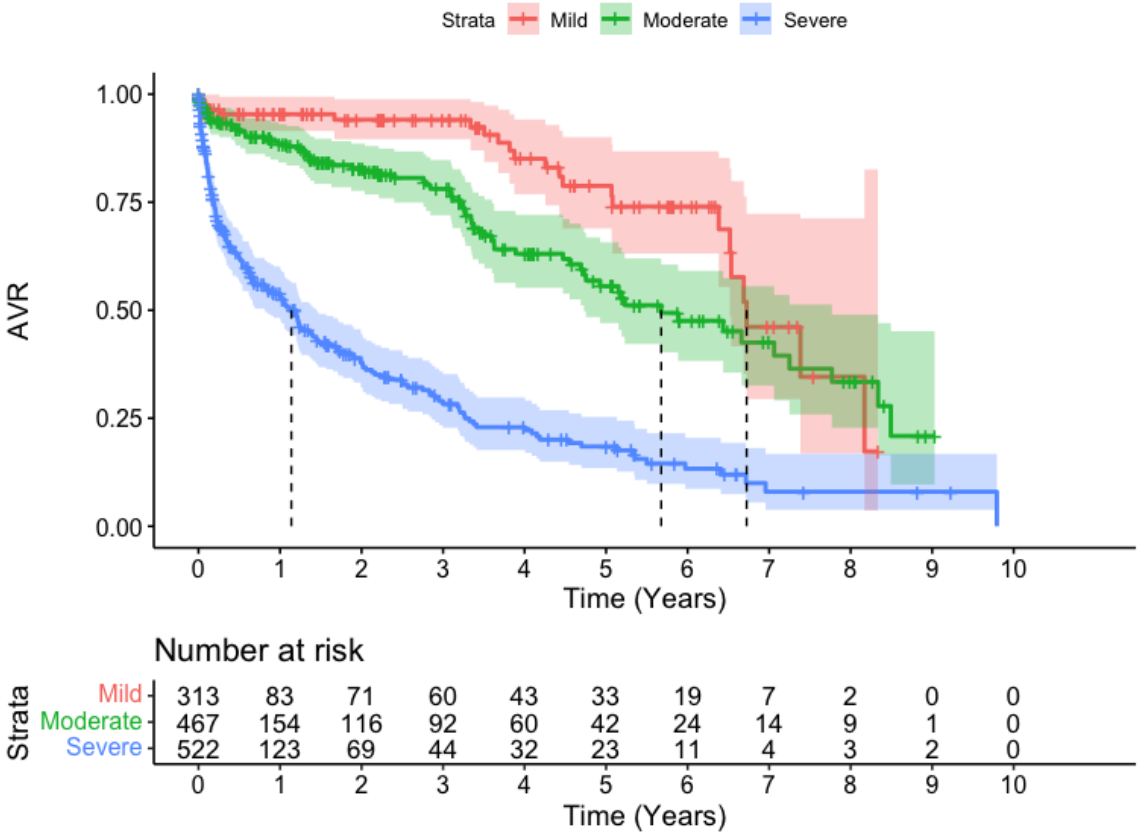

Figure 3.2 Time to Aortic Valve Replacement Curves Stratified by Baseline AS Severity

3.3.4 Trends Over Time

Peak velocity and mean gradient increased in all groups from index to either last recorded echocardiogram or prior to AVR. Aortic valve area decreased in each stratum. These changes were consistent with the known clinical course of AS in the absence of AVR (Table 3.3). Characteristic impedance on average increased over time in the mild and severe groups but decreased in the moderate group. Forward wave intensity increased in all strata with the moderate group displaying the greatest increase. Backward wave intensity increased in magnitude in mild and moderate but not severe groups (Table 3.4).

3.3.5 Missing Data

Event rates in the analytic cohort compared to those with either insufficient data to run the simulations, or simulations that did not converge, were found to be similar for mild and moderate severities. There were differences in rates of AVR for the severe group with almost double the rate of AVR in the analytic cohort compared to those with insufficient or failed simulation data (39% vs. 19%) (Appendix Table 6.5). The highest rates of missingness were found in body surface area, systolic and diastolic blood pressure, and heart rate. All other variables had missingness below 20% and were all variables obtained during the echocardiographic evaluation rather prior to the exam (Appendix Table 6.6). The greatest combination of missing variables was body surface area, and blood pressure. From a temporal perspective the highest rates of missingness were clustered from 2006-2012 and then a second cluster of missing blood pressure values from 2017 to 2021 (Appendix Figure 6.7).

Table 3.3 Change in hemodynamic metrics from index to last recorded echocardiogram

Characteristic	Mild, N = 531[1]	Moderate, N = 486[1]	Severe, N = 523[1]
Peak Velocity (cm/s)	20 (-10, 56)	21 (-10, 68)	20 (-19, 51)
Mean Gradient (mmHg)	2 (-1, 8)	3 (-1, 9)	4 (-2, 9)
Aortic Valve Area (cm^2)	-0.44 (-0.74, -0.06)	-0.15 (-0.35, 0.17)	0.01 (-0.15, 0.15)

[1] Median (IQR)

Table 3.4 Change in impedance metrics from index to last recorded echocardiogram. Note that the difference in sample size for each group is due to some subjects only having a single timepoint prior to AVR that met all impedance modeling convergence criteria

Characteristic	Mild, N = 115[1]	Moderate, N = 198[1]	Severe, N = 193[1]
Characterstic Impedance [dynes*sec/cm3]	2.13 (-26.27, 26.68)	-1.45 (-24.03, 18.47)	0.93 (-22.98, 24.98)
Total Forward Wave Intensity [W*m-2*s-1 *1e4]	1.10 (-1.99, 5.69)	1.35 (-2.45, 5.62)	0.74 (-4.37, 7.78)
Total Backward Wave Intensity [W*m-2*s-1 *1e4]	-0.60 (-1.93, 1.45)	-0.04 (-1.91, 1.67)	0.02 (-2.18, 2.65)

[1] Median (IQR)

3.3.6 Multivariable Cox Regression Models

Cox models that included only baseline information displayed strong associations between vascular parameters and time to AVR, with increased hazard for increased increases in hazard were seen with larger magnitude wave intensity (Forward wave intensity HR: 1.74 95% CI: 1.47, 2.06, Backward wave intensity HR: 1.23 95% CI: 1.05, 1.44), and a decrease in hazard with increasing characteristic impedance (HR: 0.56 95% CI: 0.47, 0.67). values of forward and backward wave intensities. In the model with baseline vascular parameters, this association was found both at the p=0.05 and p=0.017

when using the Bonferroni correction for multiple testing (Table 3.5). In models with vascular parameters modeled as time-varying similar direction of association but with attenuated hazard ratios were seen compared with baseline only models. (Forward wave intensity HR: 1.07 95% CI: 1.06, 1.09, Backward wave intensity HR: 1.08 95% CI: 1.06, 1.11), and a decrease in hazard with increasing characteristic impedance (HR: 0.98 95% CI: 0.98, 0.98) (Table 3.6). Ejection fraction was ultimately stratified on in both models to address violations in the proportion hazard assumption (Appendix Figure 6.8, Figure 6.9, Figure 6.10, Figure 6.11). After the addition of an interaction term between baseline AS severity and vascular parameters, only characteristic impedance was found to be significant in the severe strata. No significant interactions were found with the time varying vascular parameters. (Appendix Table 6.8, Table 6.9). Sensitivity analysis that removed subjects who underwent a SAVR displayed similar results in models both with and without time-varying impedance metrics (Appendix Table 6.10, Table 6.11).

3.4 Discussion

In this study we utilized a simulation method to calculate parameters of vascular function encompassing both overall vascular stiffness along with wave reflection effects for patients with AS. As initially hypothesized increased vascular impedance, defined as higher forward and backward wave intensities, was associated with a greater hazard of AVR.

Table 3.5 Cox regression model results with baseline vascular impedance metrics.

Characteristic	HR[1,2]	SE[2]	95% CI[2]
Age	1.17*	0.065	1.03, 1.33
Sex			
M	1.00	—	—
F	0.74*	0.126	0.58, 0.95
Characteristic Impedance	0.56**	0.091	0.47, 0.67
Total Forward Wave Intensity	1.74**	0.086	1.47, 2.06
Total Backward Wave Intenisty	1.23**	0.079	1.05, 1.44

*All continuous variables scaled to their SD
[1] *p<0.05; **p<0.017
[2] HR = Hazard Ratio, SE = Standard Error, CI = Confidence Interval

Table 3.6 Cox regression model results with time varying vascular impedance metrics.

Characteristic	HR[1,2]	SE[2]	95% CI[2]
Age	1.00	0.003	1.00, 1.01
Sex			
M	1.00	—	—
F	0.72**	0.075	0.62, 0.83
Characteristic Impedance	0.98**	0.001	0.98, 0.98
Total Forward Wave Intensity	1.07**	0.005	1.06, 1.09
Total Backward Wave Intenisty	1.08**	0.012	1.06, 1.11

*All continuous variables scaled to their SD
[1] *p<0.05; **p<0.017
[2] HR = Hazard Ratio, SE = Standard Error, CI = Confidence Interval

In sensitivity analysis designed to estimate time to AVR as emergence of symptoms, increased forward and backward wave intensities in both baseline and time-vary models were associated with time to symptoms. To our knowledge this is the first study to

examine the longitudinal impact of vascular function on progression to symptomatic severe AS requiring AVR.

3.4.1 Assessment of Vascular Function

Wave intensity parameters have not been well studied in patients with AS. A major reason for this evidence gap is that the technique to delineate forward and backward pressure wave intensity components was only developed in the last 10 years[30]. Much of the focus on this technique has centered on coronary pathology. The limited AS literature has mainly focused on pre/post-TAVR studies. These have found significant increases in wave intensity parameters after the unloading of the valve[32,58]. Our data show that as baseline AS severity increases so does forward and backward wave intensity parameters. This suggests that from a baseline perspective, as the valve motion becomes more limited due to calcific deposits, the increased force and reduced cross sectional area results in a more intense forward traveling pressure wave. More interestingly this brings up the potential for modifiable factors that may change the course of the disease. While many pharmacological treatments have failed to slow the progression of calcium deposition, a pharmacological that can effect ventricular function and vascular tone may be able to reduced total afterload.

When looking at change from baseline state with standard echocardiographic parameters we saw a continuing worsening of severity. With only aortic valve area displaying a slowing of change in the severe strata. This is reflective of a biological limit of area reduction before symptoms present and patients undergo AVR. In contrast the change

seen in forward wave intensity parameters increase in the mild and moderate group as a more intense forward wave is required to maintain adequate profusion to the distal organs. The increase in magnitude of the backward traveling wave follows given the reflection of this wave and already very stiff arterial system. Taken together we see that change in wave intensity parameters is more indicative of overall system response to the load imposed not just by the stiffening valve but also the vascular system. We can see this highlighted in trend of backward wave intensity change in the mild and moderate but not severe groups. While wave intensity is a function of both the LV and vasculature the characteristic impedance is a mediator of the later state. The lack of change in characteristic impedance, most likely due to advance age of this strata, doesn't allow for changes over time in wave intensity unless modified by LV function. This trend might suggest that at this end stage the vascular state has reached its limit of adaption and either further compensation from the LV is needed or symptoms emerge.

Results from the time-to-event models further support this by displaying a significant effect of both the forward and backward wave intensities increasing the hazard of an AVR. Interestingly a reduced effect was seen in the time-vary models. These results suggested two different but interrelated mechanisms. First is that AS is a dynamic disease process that occurs over long periods of time. Our results show that at baseline, hazard of an AVR, and possibly symptoms, are increased for those with greater wave intensity values, and lower characteristics impedances. But over time the association of these parameters with AVR becomes weaker. This may indicate that other compensatory mechanisms compensate of the increased load thus reducing the need for greater wave

intensities. Second is that our total follows up time did not exceed 10 years in any of the strata. Given the known decade scale that changes in vascular function are typically seen little vascular remodeling may have taken place. This suggests that the vascular state patients "start with" as the aortic valve begins stiffening sets patients on different pathways of compensation as valve obstruction becomes critical. Identifying those with increased wave intensity parameters at baseline and thus a greater hazard of need for an AVR would benefit from closer monitoring via echocardiography or symptom reporting.

3.4.2 Markers of Disease Progression

The study of AS over the past 60 years has attempted to identify markers of progression. More rapid progression has variably been related to clinical and echocardiography-based hemodynamic parameters. Several large multi-center studies have shown widely varying rates of disease progression using echocardiographic metrics for stratification of disease severity[20,59]. In both of our cox models, we saw statistically significant results that translated into in increased hazard of AVR with larger wave intensities values. Using our technique during the following or watchful waiting period of AS might provide greater insight into patients who are likely to progress more rapidly.

3.4.3 Hemodynamic and Vascular Function Parameters

Newer metrics proposed to quantify the hemodynamic burden from AS have previously focused on the LV, e.g. global longitude strain[60]. As AS is now increasingly recognized as a disease of two loads – that which is imposed by the stenotic valve and the arterial system – AS metrics should describe both the ventricular and vascular systems. One

recently proposed metric is valvuloarterial impedance (Z_{va}) which describes the total load on the LV[61,62] though does not integrate the pulsatile effects of the cardiovascular system. The lack of integration of this critical, pulsatile, component of the cardiovascular system may be a reason for the poor performance of this metric in the long-term mortality and preoperative studies[63,64].

The majority of studies looking at both the steady and pulsatile components of vascular function in AS have focused on changes in pre to post-AVR. The vast majority of which have been done in TAVR patients[32], with only one study by Chirinos et al examining the relationship between vascular function and a patient centered outcome. Specifically using the six minute walk test and change in Kansas City Cardiomyopathy Questionnaire (KCCQ) score[35] as outcomes. However, these studies have been extremely limited with very small sample sizes (<38 patients). These studies limited sample size have largely been a result of need for either invasive catheterization to capture pressure and flow data, or specialized non-invasive equipment. In contrast we utilized a non-invasive method that only requires data that is currently captured as part of the clinical workflow. Use of our method further allowed for a large-scale longitudinal analysis given the vast amount of clinical echocardiographic data already available on AS patients. It however should be noted that longitudinal studies of vascular impedance with direct non-invasive central pressure measurements via tonometry and flow via echocardiography have been conducted in the general population. One of the largest being the Asklepios Study which examined metrics of vascular function over a 10-year period in healthy middle-aged adults. Despite the large sample size (N=2,026) the oldest strata only encompassed those

who were 58 years of age on average at baseline[42]. This is almost a full 10 years younger than our mild AS strata and free of disease at baseline. Thus, making it hard to directly translate and compare these results into our population.

3.4.4 Longitudinal Changes in Vascular Function for AS Patients

While little data exists on changes in vascular function over time in the AS population some similarities can be found in studies of impedance in the general population. Characteristic impedance or arterial stiffness in the absence of wave reflection decreases with increasing AS severity or as a proxy increasing age. This is consistent directionally with the Asklepios study[65]. From a physiologic standpoint this represents the overall stiffening of the arterial system as we age. Interestingly a leveling-off effect has been in the 5th and 6th decades of life in healthily individuals. In contrast, patients within our cohort continued and even decreased their characteristic impedance to a degree. But change over the course of follow up within each of our severity strata varied widely. However, the median value of characteristic impedance changes within each stratum was small compared to the absolute value of this measure. This would suggest that while some patients do have large changes in characteristic impedance, most patients' impedance changes little given the less than decade time scale patients are followed with AS. In particular we saw this in our own data.

3.4.5 Under treatment of AS

There are other important observations from these data. Perhaps most striking is the low overall treatment rate for patients with moderate and severe AS. This is a concerning

observation given the known high mortality associated with untreated AS. These data are consistent with a recent report from another health system in severe AS patients, but we extend these results to the moderate AS group as well. Even after 17 years of follow up only 48% had AVR despite a significant mortality benefit in those that were treated[66]. In our data we similarly saw lower rates of AVR than might be expected. However, we did not have access to mortality data in those that did not undergo AVR to assess the mortally in our cohort. These results highlight a significant concern in the undertreatment in those with AS despite the known poor mortality in the absence of treatment.

A further point is that under current AHA/ACC class 1 recommendations, AVR is only indicated for patients with symptoms. Hence, in our study AVR may considered a surrogate marker of symptoms. In our sensitivity analysis that removed patients with a potential for early indication for AVR, not connected to symptoms, we saw similar results to our main analysis. This may suggest that total forward and backward wave intensity parameters can be a marker of symptoms prior to presentation. Symptoms are highly subjective and transient in nature. Given the importance of symptom presentation in AS, earlier identification based on quantitative metrics would be a significant step in early identification and treatment of AS.

3.4.6 Limitations

Several limitations are present in our study. Firstly, we did not have patient reported symptomatic status. Symptoms are a key, but often subjective and variable when it comes to recommendation for AVR. Given the large size of our data full chart extraction was

not feasible to obtain this information. Secondly, the simulation method is just that, a simulation. While patient specific data is inputted, error in data collection may have occurred that would in turn effect simulation output. Finally, the simulation method was designed with only clinically obtained data in mind; not all data was available at all timepoints. This might have caused bias in that those with a more comprehensive set of echocardiographic data compared to those with a more limited set of data. This was seen most notably in the severe AS stratum where the rate of AVR among those with data to run the simulations were almost double those without, but less so in the mild and moderate strata. Finally, bias may have been introduced due to selection bias in the mild AS group. It may have been more likely that those with moderate and severe AS were having echocardiographic exams primarily for their AS. In contrast those with mild AS, maybe have been identified not due to their AS but coincidentally due to an echocardiographic exam for a separate clinical indication. Additionally, most of this group was censor after the first year and was not followed at TMC thereafter. These factors may have distorted the results given the long follow-up time in the small number of mild patients seen and followed at TMC.

3.5 Conclusion

In this study we examined the longitudinal association between vascular function and time to aortic valve replacement. Vascular parameters were seen to increase with AS severity. Furthermore, small but statistically significant increase in hazard was seen in models with vascular parameters modeled as time-varying. This method and these finding

present a potential new biomarker for further investigation into tracking of progression of AS and identifying earlier trigger point for intervention.

3.6 Contributions

JYB designed the study, created the dataset, conducted the analysis, and drafted the manuscript. NT contribution to data analysis and manuscript revisions. DK, BW and ERE contributed to data interpretation and manuscript revisions.

Chapter 4 Association Between Metrics of Vascular Function and Post-Transcatheter Aortic Valve Replacement Outcomes

---

Brown JY, Terrin N, Kent DK, Wessler BW, Edelman ER. To be submitted to Journal of the American College of Cardiology.

4.1 Introduction

Aortic Stenosis (AS) is one of the most common types of valvular heart disease in the western world[5]. While AS has historically been viewed as a disease of the valve, there is increasing recognition that the resistance the left ventricle (LV) must overcome to allow forward blood flow is important to understanding post-aortic valve replacement (AVR) outcomes[32,34]. These resistances have several components, namely the calcified stenotic valve and the vasculature. We are able with echocardiography and left heart catheterization to quantify the obstructions imposed by the valve; however, the vascular resistance or impedance has been less defined. The fact that this complex impedance is not yet fully defined may help explain why, despite the revolutionary nature of the Transcatheter Aortic Valve Replacement (TAVR), up to one-third of patients report no improvement in quality of life (QOL) or are dead at one year[23,24]. It may be that a valve replacement without consideration of the load imposed by the vasculature, limits full procedural benefit.

Traditional methods to investigate the contribution of vascular impedance to cardiac afterload and ventricular vascular coupling have normally relied on the frequency rather than time domain-based analysis[27]. Frequency domain-based techniques to measure vascular impedance take the approach of viewing all blood pressure and flow signals as a summation of a set of infinite sinusoidal waves. Each of these waves can then be quantified by their frequency, amplitude, and phase. Furthermore, these can then be used to calculate vascular parameters that not only integrate traditional metrics of vascular

state such as systemic vascular resistance, but additional metrics that take into account the pulsatile components of the vascular systems.

However, methods such as these rely on technically challenging and invasive measurements taken from left heart catheterization of simultaneous pressure and flow signals at the central aortic position[32,33,67]. Non-invasive methods have been developed to measure impedance but require expensive equipment to non-invasively measure central aortic pressure[42,51]. This makes prospective evaluation challenging for both research and potential clinical use and would further burden an already busy clinical workflow. Newer simulation-based methods have been developed and validated to take advantage of clinically available retrospective echocardiographic data. By using these tools and large clinical datasets we are now able to comprehensively investigate how vascular state may affect post-TAVR clinical outcomes with precision from non-invasive metrics.

To better understand the contribution of vascular impedance to post-TAVR outcomes, we used data from patients who underwent TAVR in the Placement of AoRTic TraNscathetER Valves II (PARTNERS II) trial to calculate vascular impedance pre-TAVR. We then built a predictive model to explore the association and incremental contribution of vascular impedance to the prediction of a binary composite mortality and quality of life outcome at one-year post-TAVR. Finally, we externally validated our model in a contemporary real-world setting of patients undergoing TAVR at a tertiary medical center (Tufts Medical Center, Boston, MA).

4.2 Methods

4.2.1 Study Population

Patients who underwent TAVR as part of the PARTNERS II trial or patients enrolled as part of the corresponding continued access registry were included for analysis in the model derivation set. An external validation set was created from patients who underwent TAVR at Tufts Medical Center (TMC) between 2012 - 2021. Demographic, echocardiographic, and clinical data were extracted from the Tufts Research Datawarehouse. Outcome data for the external validation set was obtained from the Society of Thoracic Surgeons/Transcatheter Valves (STS/TVT) registry data at TMC.

4.2.2 Primary Outcome

The primary outcome was a binary composite metric of mortality and QOL measured at one-year post-TAVR. QOL was assessed via the Kansas City Cardiomyopathy Questionnaire (KCCQ). A poor outcome was defined as a KCCQ less than 60, a drop in KCCQ by more than 10 points from pre to post-TAVR, or death. This validated endpoint was chosen as it allows for the integration of both survival and QOL benefits from the procedure. [68–70]

4.2.3 Aortic Input Impedance Simulation

A novel simulation-based method was used to calculate impedance from echocardiographic data. When both pressure and flow waveforms are available at the same time impedance can be calculated as the ratio of their Fourier harmonics and presented as amplitude and phase. In this work, blood flow waveforms were extrapolated

from echocardiographic information (Appendix 6.2.1). Candidate central pressure waveforms were obtained by solving the standard impedance equation for pressure as a function of impedance and flow. Using this form, we then applied the inverse Fourier transform to obtain all possible time-resolved pressure waveforms. Five hundred million combinations of physiologic and pathophysiologic impedance spectra were generated and the ratio of all impedance combination to flow harmonics were taken. The inverse FFT was applied, and all possible time-resolved central aortic pressure waveforms were generated. A set of clinically derived domain bounding criteria were applied to reduce the number of pressure waveforms until convergence was achieved. This resulted in a set of patient-specific pressure waveforms and impedance amplitude and phase spectra. Convergence was determined with a set of domain bounding criteria consisting of patient-specific systolic and diastolic blood pressure at the time of echocardiographic evaluation. Additional knowledge-based criteria included information consistent with all human central pressure waveforms such as initial upstroke and pressure decay during the diastolic phase. A full description of the simulation method and validation can be found in Chapter 2.

4.2.4 Vascular Impedance Parameters

A set of vascular impedance parameters were extracted and calculated from the impedance simulation for use as variables in modeling. Frequency domain-based amplitude values for the zero through third harmonics were extracted. Characteristic impedance was calculated as the mean amplitude value of the harmonics from 2 to 10 Hz, excluding any values three times greater than the median[51]. Wave Intensity Analysis

(WIA) was also applied to all patient-specific pressure and flow waveforms that "passed" (met the domain-bounding criteria) to calculate the total forward and backward wave intensities. WIA is an alternative method to frequency domain techniques used to assess vascular hemodynamics. In contrast to traditional frequency domain techniques that view blood pressure and flow as the sum of a set of sinusoidal waves, in WIA the waves are seen as a set of successive wavefronts[30]. WIA allows for the examination of flux in energy per unit area or a cross-section of a vascular segment. Blood pressure waves are either seen as originating antegrade from the LV or returning retrograde from the periphery with wave reflection. Each forward and backward component can be further broken down into compression and expansion. The compression component in the forward case qualifies the pressure generated by the LV. The forward expansion wave component represents the slowing of the pressure wave by the LV in late systole as well as integrating downstream ventricular-vascular coupling factors[71]. Hydraulic work was calculated as a measure of arterial efficiencies, or the energy generated by the LV that is lost in arterial inefficiencies or mismatches[72]. Finally, the reflection coefficient was taken as the ratio of the peak backward pressure wave to the peak forward pressure wave. The reflection coefficient was dichotomized at a value of 0.65 based on prior literature indicating that this is a predictive marker of outcome post-TAVR[73,74]. For each patient-specific set of passing waveforms the median value was taken for all calculated vascular parameters and used for analysis.

4.3 Statistical Analysis

Continuous data was presented as means with standard deviations and categorical variables as counts and percentages. The association between baseline metrics and the outcome was estimated with odds ratios. All continuous variables were scaled to their standard deviation. Demographic, hemodynamic, and impedance metrics were compared between the derivation and validated datasets at baseline. Multivariable logistic regression models were used to assess the association between a poor outcome post-TAVR at one year and metrics of vascular impedance. Two separate models were used for comparison. First, a model containing only the Society of Thoracic Surgeons (STS) risk score was fitted. The STS risk score is an adult cardiac surgery risk model designed to predict a range of outcomes. For those undergoing TAVR, the 30-day risk of mortality outcome was used. The STS risk score was used as all baseline characteristics we had access to were included in this score. This score was also calculated for all patients undergoing TAVR and represents an easy to obtain value that has been well validated[75,76].

A second model that included both the STS risk score and impedance metrics was fit for comparison. Variable selection for the impedance metrics was conducted in two parts. First, a univariate screen was performed and all variables with p-values less than 0.05 were included. Second, any additional variables that did not meet this criterion, but prior studies had indicated may have an association, were also included. If multicollinearity was found between variables, expert opinion was used to determine which variables to include. To correct for multiple testing, the Bonferroni correction was used for the

candidate impedance parameters to include in the model. P-values less than 0.005 were considered significant. Logistic regression modeling assumptions were assessed for multicollinearity using variance inflation factor, outliers with Pearson residuals, and log-odds plots for linearity. To address model overfitting uniform shrinkage via bootstrap, resampling was applied for use with external model validation. Model discrimination was assessed via the area under the receiver operating curve (AUC) and the differences between models compared with the Delong test for comparisons of ROC curves.

Each model was then externally validated on patients who underwent TAVR at TMC. Percentage change in discrimination was calculated as [(Validation AUC-0.5) - (Derivation AUC-0.5)/(Derivation AUC-0.5)*100]. Calibration was assessed visually with calibration plots and quantitively by calibration slope. Harrell's E statistics was also calculated which represents the prediction error for each individual patient by using a lowess-estimated probability as a proxy for observed outcome rate. Emax and E90 were calculated as the maximum or 90% absolute difference in predicted and loess-calibrated probabilities[77]. Finally, each models coefficients and intercepts were recalibrated for the external validation set.

To determine the minimum detectable effect, a power analysis was conducted for both derivation and validation datasets prior to running simulations. Within the derivation dataset 2,710 patients had sufficient data to run the simulations. Using an adjusted alpha of 0.005 to correct for multiple testing of the 10 potential impedance values to be included in modeling, we would be able to detect an odds ratio per standard deviation of

1.18 at 80% power, or an odds ratio per standard deviation of 1.2 at 90% power. In the validation datasets given, the 842 patients with required data and the same adjusted alpha, we were able to detect an odds ratio of 1.39 at 80% power, or 1.44 at 90% power. All impedance simulations were conducted using a custom Python code (Python 3.6) and all statistical analyses were conducted using R 4.1.2[56] and RStudio[57].

4.4 Results

4.4.1 Study Population

Of the total 4,716 patients within the PARTNERS II trial, 2,710 patients who underwent TAVR had sufficient data to run the impedance simulations. Of those 1,798 TAVR patients had at least 1 waveform that met all domain bounding convergence criteria and outcome data available. A total of 690 TAVR patients produced no usable waveforms. The primary reason for exclusion was insufficient data to run the simulation and specifically lack of acceleration time (89%) as recorded on the echocardiogram. In 17% of patients there was no recording of stroke volume. When stratified by the primary outcome, rates of missing data were similar between the two groups. In the external validation set of patients who underwent TAVR at TMC, 840 were initially screened. Among those 337 had sufficient data to run the simulations, with 329 meeting all domain bounding criteria, however, only 318 patients had complete quality of life and mortality data available. The frequency of missingness within the validation set without necessary data to run the simulations was highest for heart rate (27%), blood pressure (17%), and AVA (10%). As acceleration time was not available within the validation dataset, a linear

regression sub-model was built using the derivation set and applied to the validation set (Appendix 6.4.1).

4.4.2 Cohort Characterization and Outcomes

Baseline clinical, hemodynamic, and impedance metrics are shown for both the derivation and validation cohorts in Table 4.1. Patients in the validation cohort were 3 years older on average (Derivation: 82 (8) vs. Validation: 79 (9) years). There was a larger percentage of male subjects in the derivation cohort compared to the validation. Both cohorts were overwhelmingly white. Baseline KCCQ score was similar in both groups (Derivation: 46 (23) vs. Validation: 49 (26)), however baseline STS Risk Score was notably higher in the derivation cohort (Derivation: 7.2 (4.7) vs. Validation: 5.1 (6.9) %). Hemodynamic metrics in both groups were indicative of patients with severe AS. While differences were seen in peak aortic valve velocity, aortic valve area, and left ventricle ejection fraction, these differences were not clinically significant. Differences were seen across a range of vascular impedance parameters. A tendency was seen for larger magnitude forward wave intensities and greater pulsatile work in the derivation cohort. Backward wave intensities were similar in both cohorts. The percent of patients in the derivation cohort with reflection coefficients below 0.65 was more than 4 times that of the validation cohort. The overall event rate in the derivation cohort was 26% and 30% in the validation cohort.

Table 4.1 Baseline demographic and clinical characteristics in both the derivation and external validation cohorts.

Characteristic	Derivation, N = 1,798[1]	External Validation, N = 432[1]	p-value[2]
Demographics			
Age (yrs)	82 (8)	79 (9)	<0.001
Sex			0.001
M	1,079 (60%)	223 (52%)	
F	719 (40%)	209 (48%)	
Race			<0.001
White	1,630 (94%)	386 (97%)	
Black	46 (2.7%)	3 (0.8%)	
Hispanic	32 (1.8%)	0 (0%)	
Asian	17 (1.0%)	7 (1.8%)	
Other	8 (0.5%)	0 (0%)	
BMI	27.9 (6.3)	30.2 (27.2)	0.13
Diabetes	666 (37%)	166 (38%)	0.6
Coronary Arterty Diease	1,393 (77%)	361 (84%)	0.006
Hypertension	1,648 (92%)	311 (72%)	<0.001
STS Risk Score	8.5 (4.7)	7.4 (6.9)	0.002
Baseline KCCQ Score	47 (23)	49 (26)	0.15
Hemodynamics			
Systolic Blood Pressure (mmHg)	128 (20)	129 (20)	0.4
Diastolic Blood Pressure (mmHg)	67 (12)	70 (13)	<0.001
Peak Aortic Valve Velocity (cm/s)	423 (67)	387 (72)	<0.001
Aortic Valve Area (cm^2)	0.71 (0.26)	0.77 (0.25)	<0.001
Left Ventricle Ejection Fraction (%)	51 (13)	55 (14)	<0.001
Impedance			
Characteristic Impedance (dyne*sec/cm^3)	94 (32)	89 (28)	0.001
Total Forward Wave Intensity (W*m^−2*s^−1*1e4)	28 (10)	24 (10)	<0.001
Total Backward Wave Intensity (W*m^−2*s^−1*1e4)	-7.6 (3.9)	-8.3 (4.3)	0.004
Cumulative Foward Wave Compression Intensity (W*m^−2*s^−1*1e4)	18 (6)	16 (6)	<0.001
Cumulative Foward Wave Expansion Intensity (W*m^−2*s^−1*1e4)	10.4 (4.2)	8.5 (4.0)	<0.001
Cumulative Backward Wave Compression Intensity (W*m^−2*s^−1*1e4)	-5.46 (3.02)	-6.24 (3.27)	<0.001
Cumulative Backward Wave Expansion Intensity (W*m^−2*s^−1*1e4)	-2.19 (1.55)	-2.07 (1.60)	0.2
0th Harmonic Amplitude (dyne*s*cm^-3)	1,023 (289)	1,252 (399)	<0.001
1st Harmonic Amplitude (dyne*s*cm^-3)	158 (57)	167 (61)	0.005
2nd Harmonic Amplitude (dyne*s*cm^-3)	135 (59)	133 (55)	0.5
3rd Harmonic Amplitude (dyne*s*cm^-3)	105 (58)	110 (55)	0.12
Steady Hydraulic Work (W)	1.04 (0.35)	0.98 (0.30)	<0.001
Pulsatile Hydraulic Work (W)	0.18 (0.09)	0.15 (0.08)	<0.001
Reflection Coefficent < 0.65	430 (24%)	24 (5.6%)	<0.001

[1] Mean (SD); n (%)
[2] Welch Two Sample t-test; Pearson's Chi-squared test; Fisher's exact test

4.4.3 Initial Variable Screen

Initial screen for univariable association between baseline characteristics and poor outcome in the derivation cohort can be seen in Table 4.2. Age, Sex, Body Mass Index, New York Heart Association Class (NYHA), STS Risk Score, baseline KCCQ score, acceleration time, mean gradient, peak aortic valve velocity, stroke volume and stroke

volume index, and EF were found to be significant. Impedance metrics found to be significant on initial screen were all forward wave intensity metrics, reflection coefficient <= 0.65, 0^{th} harmonic amplitude, steady and pulsatile hydraulic work.

4.4.4 Modeling Results

After the initial screen for impedance parameters for inclusion total forward wave intensity, forward compression wave, forward expansion wave, pulsatile hydraulic work, steady hydraulic work, 0^{th} amplitude harmonic, and reflection coefficient below 0.65 were included. As characteristic impedance is a well-known metric of overall vascular stiffness in the absence of wave reflection, this parameter was included. The variance inflation factors indicated significant co-linearity in wave intensity metrics (Total Forward Wave Intensity: 455, Forward Compression Wave: 189, Forward Expansion Wave: 76). Since the total forward wave intensity is the integral of the forward compression and expansion wave components, the total forward wave intensity coefficient was removed. Additionally significant correlation was found between forward expansion and compression wave variables (Appendix Figure 6.15). From a physiologic standpoint the compression wave is normally larger as this represent the initial wave propagated from the LV down the arterial tree. For this reason, the compression wave was kept in the model and expansion wave dropped. Finally, from a physiologic perspective, since the back wave reflection effects contribute to the total afterload that the LV must overcome, the backward compression and expansion variables were added to the final model. In the STS-based model STS risk score was associated with poor outcomes at 1 year (OR: 1.53 CI: 1.38-1.69).

Table 4.2 Univariable Associations of Poor Outcome in the Derivation Cohort. Odds ratios are per 1 standard deviation differences for each continuous variable.

Characteristic	OR[1,2]	SE[2]	95% CI[2]
Demographics			
Age (years)	1.14*	0.056	1.02, 1.28
Sex			
F	1.00	—	—
M	0.67**	0.112	0.54, 0.84
Race			
White	1.00	—	—
Black	1.36	0.320	0.71, 2.51
Hispanic	0.52	0.490	0.18, 1.25
Asian	1.17	0.535	0.37, 3.18
Other	0.40	1.07	0.02, 2.27
Body Mass Index	0.84**	0.057	0.75, 0.94
Diabetes			
Yes	1.00	—	—
No	0.89	0.112	0.72, 1.11
Hypertension			
Yes	1.00	—	—
No	1.02	0.194	0.70, 1.51
Coronary Artery Disease			
Yes	1.00	—	—
No	1.15	0.131	0.90, 1.50
NYHA			
2	1.00	—	—
3	1.89**	0.200	1.29, 2.83
4	2.60**	0.208	1.75, 3.96
STS Risk Score	1.53**	0.052	1.38, 1.69
Baseline KCCQ Score	0.67**	0.058	0.59, 0.75
Hemodynamics			
Systolic Blood Pressure (mmHg)	0.90	0.054	0.81, 1.00
Diastolic Blood Pressure (mmHg)	0.97	0.054	0.87, 1.08
Heart Rate (BPM)	0.94	0.054	0.84, 1.04
Acceleration Time (ms)	0.88*	0.054	0.79, 0.98
Mean Gradient (mmHg)	0.78**	0.057	0.70, 0.87
Peak Velocity (cm/s)	0.78**	0.055	0.70, 0.87
Stroke Volume (ml)	0.81**	0.056	0.72, 0.90
Stroke Volume Index (ml/m^2)	0.79**	0.056	0.71, 0.88
Ejection Fraction (%)	0.74**	0.063	0.66, 0.84
Aortic Valve Area (cm^2)	1.00	0.054	0.90, 1.11
Indexed AVA (cm^2/m^2)	0.98	0.054	0.88, 1.09
Impedance			
Characteristic Impedance (dynes*sec/cm^3)	0.95	0.054	0.85, 1.05
Total Forward Wave Intensity (W*m^−2*s^−1*1e4)	0.82**	0.056	0.73, 0.91
Forward Compression Wave (W*m^−2*s^−1*1e4)	0.83**	0.056	0.74, 0.93
Forward Expansion Wave (W*m^−2*s^−1*1e4)	0.79**	0.057	0.70, 0.88
Total Backward Wave Intensity (W*m^−2*s^−1*1e4)	0.99	0.053	0.90, 1.11
Backward Compression Wave (W*m^−2*s^−1*1e4)	0.97	0.053	0.88, 1.08
Backward Expansion Wave (W*m^−2*s^−1*1e4)	1.05	0.055	0.95, 1.18
Pulsatile Hydraulic Work (Watts)	0.78**	0.058	0.70, 0.88
Steady Hydraulic Work (Watts)	0.79**	0.057	0.70, 0.88
0th Harmonic Amplitude (dyne*s*cm^-3)	1.25**	0.052	1.13, 1.39
1st Harmonic Amplitude (dyne*s*cm^-3)	1.05	0.053	0.95, 1.17
2nd Harmonic Amplitude (dyne*s*cm^-3)	0.95	0.055	0.85, 1.05
3rd Harmonic Amplitude (dyne*s*cm^-3)	1.00	0.054	0.90, 1.11
Reflection Coefficent <= 0.65			
Yes	1.00	—	—
No	0.71*	0.132	0.54, 0.91

[1] *p<0.05; **p<0.005

[2] OR = Odds Ratio, SE = Standard Error, CI = Confidence Interval

After inclusion of vascular parameters, the 0^{th} amplitude harmonic (OR: 1.24 CI: 1.06-1.45) were associated with poor outcome at 1 year but only at the p=0.05 level. After correction for multiple testing only STS risk score was associated with poor outcome. Discrimination was not statistically significant better in the STS + Impedance model (AUC: 0.66 vs. 0.65 p = 0.17) compared to the STS-only model (Figure 4.1). Discrimination in the external validation dataset for the STS risk-based model and impedance model was 0.65 and 0.64 respectively. This resulted in a 12.5% increase and a 7.1% decrease in model discrimination between derivation and external validation set. Both models showed moderate calibration-in-the-large, or agreement between observed and predicted risk. With the STS risk-only model having a predicted mean outcome probability of 26.3% compared to the actual mean outcome rate of 26.0%. For the impedance-based model, the mean predicted probability was 27.8%. Recalibration of both the intercept and slope for each model did result in better overall calibration for each model (STS: original slope: 1.33, recalibrated: 1.0 vs. impedance: original slope: 1.10, recalibrated: 1.0). Both Emax and E90 found similar error rates between predicted and actual outcomes in both models (STS: Emax: 0.23, recalibrated: 0.24 vs. impedance: Emax: 0.23, recalibrated: 0.20) (Table 4.4).

4.5 Discussion

The current study examined the association and prediction between vascular impedance and one-year post-TAVR patient-centered outcomes. Here we show that after correction for multiple testing none of the impedance based vascular parameters were associated with poor outcomes post-TAVR. This model was found to poorly discriminate between

those that did and did not have a poor outcome both within the derivation dataset as well as the external validation dataset. Furthermore, addition of impedance metrics did not substantially improve discrimination over a model with only STS risk score. Calibration was moderate but better in the impedance-based model both before and after recalibration of both the intercept and slope of both models.

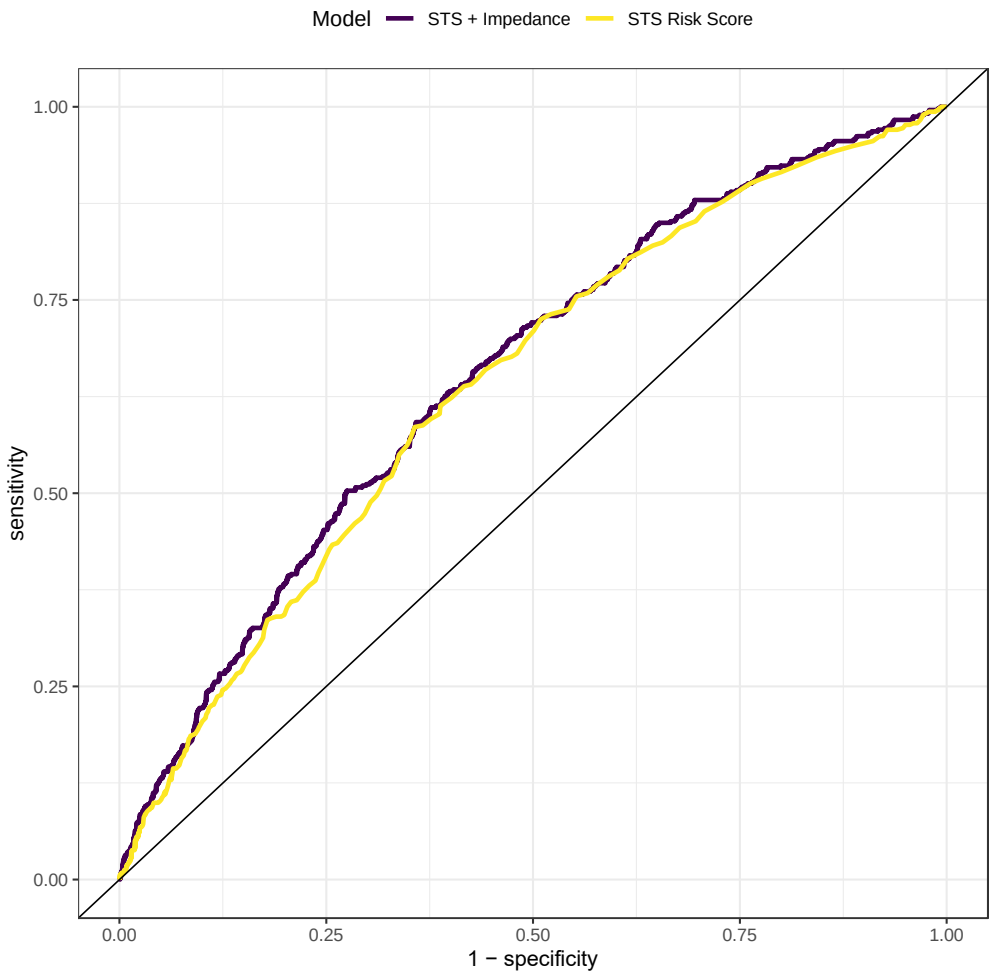

Figure 4.1 ROC curve displays a comparison of the STS risk-only model and the impedance-based model in the derivation cohort. Similar performance is seen in both models with the impedance-based model displaying slightly better overall performance (STS AUC = 0.64 vs. Impedance AUC = 0.66)

Table 4.3 Logistic Regression Modeling Results

	STS Risk			STS Risk + Impedance		
Predictor	**OR[1,2]**	**SE[2]**	**95% CI[2]**	**OR[1,2]**	**SE[2]**	**95% CI[2]**
(Intercept)	0.16**	0.115	0.13, 0.20	0.10**	0.389	0.05, 0.22
STS Risk Score	1.53**	0.052	1.38, 1.69	1.50**	0.054	1.35, 1.67
Characteristic Impedance				1.00	0.111	0.80, 1.24
Forward Compression Wave				1.06	0.114	0.84, 1.32
Backward Compression Wave				1.00	0.082	0.85, 1.17
Backward Expansion Wave				1.02	0.068	0.89, 1.17
Pulsatile Hydraulic Work				0.83	0.156	0.61, 1.13
Steady Hydraulic Work				0.98	0.102	0.80, 1.19
0th Harmonic Amplitude				1.24*	0.081	1.06, 1.45
Reflection Coefficent <= 0.65				0.96	0.194	0.65, 1.40

[1] *p<0.05; **p<0.005

[2] OR = Odds Ratio, SE = Standard Error, CI = Confidence Interval

Table 4.4 Summary of Area Under the Curve/Slope Results

Model	AUC		% Change in AUC	Calibration Slope	E90 Original	E90 Recalibrated	EMax Original	EMax Recalibrated
	Original	External Validation						
STS Risk Score	0.64	0.66	12.5	1.33	0.16	0.06	0.23	0.24
STS + Impedance	0.66	0.64	-7.1	1.10	0.16	0.05	0.23	0.20

4.5.1 Prediction Models in TAVR

Prediction models for TAVR have by in large focused on clinical outcomes such as in-hospital, 30 days, or 1-year mortality. Fewer studies have tried to predict patient-centered

outcomes post-TAVR with largely moderate results using standard clinical or hemodynamic variables. Even in models trained on large, randomized control trial[23,78] or real-world registry-based[24] datasets, predictive performance has fallen short of the performance needed to inform clinical decision making. These models largely have shown moderate discrimination with good calibration thus falling short of being able to inform us of patients unlikely to benefit from TAVR. Instead of using a standard set of clinical variables, we assessed the use of a novel biomarker. Vascular impedance can be described using a range of metrics with each quantifying a different part of the vascular system and response to LV pulsation. Global metrics of vascular stiffness such as pulse wave velocity, augmentation index, and cardio ankle vascular index have been used in many studies in the past but only describe individual components of vascular function. No single metric can fully quantify the dynamic nature of the ventricular-vascular coupling thus the need for a range of techniques such as WIA, hydraulic work, and of course clinical factors. While commercial devices exist to measure global metrics of stiffness[79], they put an additional burden on an already busy clinical workflow, and their clinical value has still yet to be fully realized. However, in our study despite the addition of a range of these metrics derived from a novel method we did not find any substantial improvement in prediction.

As TAVR becomes poised to become the method of choice for AVR, patient selection will continue to be key to optimizing outcomes. However transformative this technology has been, approximately 1/3 of patients still derive no benefit from the procedure[23]. The lack of high-quality prediction models with good performance indicates the need for a

new set of clinical biomarkers to assess clinical state. Especially as the use of TAVR moves into lower surgical risk classes, and less severe classes of AS, such as the EXPAND TAVR II Pivotal Trial in moderate symptomatic AS patients, better metrics and models are needed to inform expected procedural benefit and help set patient expectations. A recent systemic review identified that even if restricted to the highest-risk class of TAVR patients, a range of prediction models showed large differences in event rates in different populations for the same outcome[25]. Furthermore, it was also found that none of these models were able to identify patients who were not likely to benefit from a TAVR.

4.5.2 Vascular Function in AS Models

While the integration of metrics of vascular function in AS models has been examined in the past due to the difficult nature of capturing and processing this data, or the additional commercial equipment required, sample sizes of these studies have been limited. Additionally, each study may use a different set of metrics to quantify the same physiologic phenomena or different types of devices[80]. Furthermore, many of these studies have found contradictory results. Yotti et al [32] looked at 23 patients undergoing TAVR and found a significant increase in vascular load post-TAVR. Yet only stroke volume index was predictive of post-TAVR functional class as measured using the NYHA classifications. In contrast, Pagolatou et al [67] examining 33 TAVR patients found a decrease in vascular load pre to post-TAVR. Few studies have specifically modeled metrics of vascular impedance pre-TAVR against QOL post-TAVR. Chirinos et al[35] did a study of 33 patients undergoing surgical aortic valve replacement (SAVR) and found as a

secondary endpoint that reflection wave transit time was positively associated with the 6-minute walk distance post-SAVR. In addition, reflection wave magnitude was a significant predictor of post-SAVR quality of life improvements with those with higher reflection wave magnitudes, having lower improvement as measured by KCCQ score. Indeed, in our own derivation cohort using the same reflection coefficient metric, we found that having a reflection coefficient less than 0.65 was initially associated with better post-TAVR outcomes. However, despite inclusion of many of these metrics we did not find statistically significant associations after correction for multiple testing or in our models' ability to predict poor post-TAVR outcomes over STS risk score alone.

During our initial variable screen, we found a significant but inverse association between forward compression and expansion waves after the addition of vascular impedance metrics. After correction for multiple testing this association was no longer significant. Furthermore, in our final model we found a reversal of the forward compression wave compared to that of the initial variable screen. After incremental addition of each variable to our final model in order of odds ratio strength on initial screen, after the addition of pulsatile hydraulic work did the odds ratio reverse direction (Appendix Table 6.14). A potential reason for this was the high degree of correlation between these two variables (Appendix Figure 6.15).

4.5.3 Model Performance

Performance of other published TAVR models vary widely however most models attempting to predict 1-year post-TAVR mortality are in the range of 0.68-0.83[25] as

measured by AUC. However, if restricted to mortality or QOL performance drops to between 0.64-0.66[25]. Our own models showed a similar level of performance both in internal and external validation. Notably, the STS risk score seems to perform well despite it was initially intended to predict 30-day in-hospital mortality. While calibration was moderate in the STS risk model, good calibration was found in the impedance-based model. Other published models did not report the E90 or Emax, however, our impedance-based model showed only minor improvement in E90 over the STS risk-based model. From the clinical perspective, despite no change in discrimination, improvement in model calibration can be particularly important. With improved model calibration we are able to better inform patients of their probability of a poor outcome post-TAVR.

The only other QOL-based model known to us that has been externally validated in a real-world dataset was validated in the STS/TVT registry which showed moderate discrimination with an AUC of 0.639, but poor calibration with a slope of 0.7759. Using the same definition in our own models with the addition of the impedance parameters we saw a small improvement calibration when impedance measures were included (Table 4.4). It should be noted that the modest discrimination seen in these, and our own models may be due to the relative case mix differences seen between the RCT data used to train the model data used for validation.

4.5.4 Limitations

There are limitations to this work. First, the impedance simulations themselves, while having been validated, are only as good as the input data used to run them. The derivation dataset consisted of a high-quality randomized control trial ensuring the best input

parameters, however, the validation dataset used real-world echocardiographic examinations, which presumably are associated with more measurement variability. Differences in “matched” inputs, such as blood pressure taken at the start of an exam and hemodynamic measurements taken at the end, may have caused errors that resulted in simulation that did not fully converge. While “matching” was probably better in an RCT setting due to strict protocols, this might not be true in everyday clinical practice. Furthermore, our derivation dataset was comprised of a randomized control trial with a narrower inclusion criterion than the "real world" validation set that for example included multivalve disease patients excluded from the RCT. These patients may have also additional comorbid conditions that may have effect external validation. The PARTNERS II dataset consisted of high and intermediate-risk patients with devices that are no longer used for TAVR. Thus, while the impedance-based metrics would not change as they were all taken pre-AVR, outcome rates may not be the same. This is especially relevant when it comes to cohorts with STS risk score lower than 4%. Finally, given the large number of variables that can be used to describe impedance of the vascular system our study may have been under powered to detect an effect. Our univariable screen did find that almost all impedance-based parameters were associated with our primary outcome. These points together may suggest that further explorations of these variables may yield better metrics to predict post-TAVR QOL outcomes.

4.6 Conclusions

We explored the use of a novel metric for the prediction of post-TAVR outcomes. Given the lack of models that perform adequately in prediction of QOL outcomes, the

exploration of novel metrics may lead to better models to aid in setting patient expectations. While the addition of impedance metrics in the prediction setting did not substantially improve model discrimination over the STS risk score only, overall results were on par with other published TAVR prediction models. However, the addition of impedance in external validation did show minor benefit in calibration. Due to the difficulty in predicting post-TAVR QOL outcomes with traditional clinical data, studies examining new and novel variables to better quantify clinical, hemodynamic, and vascular state may provide additional predictive value.

4.7 Contributions

JYB designed the study, conducted the analysis, and drafted the manuscript. NT contribution to data analysis and manuscript revisions. DK, BW and ERE contributed to data interpretation and manuscript revisions.

Chapter 5 Discussion

5.1 Summary

In these series of studies, we developed and validated a simulation-based method to calculate vascular impedance using only clinically available echocardiographic data. We then used this method to study the effect of vascular function on two aspects of AS. First, we examined the longitudinal contribution of vascular function to time to AVR and second the incremental contribution of vascular parameters to the prediction of post-TAVR outcomes. To the best of our knowledge these studies represent the largest analysis of vascular function in the AS population to date.

5.2 Non-Invasive Evaluation of Impedance

The use of impedance to quantify vascular function dates back to the late 1940's[81,82]. However, its use in the AS population has been limited due to a range of factors. Most critically is the lack of easy access to pressure and flow data required for its calculation. Normally left heart catheterization would be required to obtain this data. More recent introduction of advance imaging modalities such as magnetic resonance imaging allows for less invasive methods of determination of blood flow. Similarly, the introduction of non-invasive central pressure measurement devices allows for the assessment of central pressure without catheterization. But there are drawbacks to these methods. First, is the need for specialized equipment and training required for their use. Second, is their need for prospective evaluation as neither are collected as routine standard of care for AS patients. With the simulation-based method we developed, large scale evaluation of the AS population is possible as only limited clinically available data is needed.

Comparison of the simulated central pressure waveforms when compared with the error associated with high quality invasive studies showed low error compared to reference[32]. Additionally, while bias seen in several of the vascular parameters simulated, correlation across most of these parameters was excellent. This is of particular importance when it comes to the use of these methods in prediction where high correlation between simulated values and references means that both values can add the same potential predictive information.

5.3 Change in Impedance at Scale

While many studies have looked at the longitudinal change in vascular parameters over time, most of these have been in the healthy population. Tracking change during the progression of AS has not been conducted before. For the most part this has been due to the lack of tools to easily obtain impedance data in this population and the long disease progression making evaluation difficult. Within our cohort we saw hemodynamic progression of AS consistent with prior studies. Notably we saw a non-linear effect in the progression of AS with the most significant changes in hemodynamic parameters occurring in patients entering the cohort with mild and moderate AS. This is most likely a ceiling effect where patients are either offered AVR, and thus no further progression can occur. This effect was not seen in the change in impedance parameters over time with differing amounts of change across each baseline AS severity group. A possible explanation for this is that vascular function does not track with AS severity but individually to a patient's physiology. If true, then "typing" each patient's vascular state

and response to the LV's compensation in the face of increased AV stiffening may lead to greater insights into early alerting for presentation of symptoms.

Our time-to-event analysis, using both baseline and time-varying impedance showed a significant effect with increases in forward and backward wave intensities conferring increased hazard of AVR. This was prominent in the baseline model and less so in the time varying model. A potential physiologic explanation for this is that as afterload in AS increases and the LV compensates, a more intense forward and in turn reflected wave is generated. This is done to maintain adequate distal organ profusion. But ultimately this leads to increased progression, earlier symptoms, and the need for AVR. Most interestingly, was the stronger associations we found in the baseline models. A potential implication here is that each patient has their own trajectory and compensation pathway. This leads to an overall lower effect of impedance as time goes on, as all patients become more LV limited. However, this presents the opportunity to identify patients that will require closer monitoring or earlier intervention.

5.4 Impedance and Treatment of AS

Despite the long history of AVR as the only but extremely effective treatment for AS, predicting time to intervention or optimizing QOL outcomes rather than mortality is still lacking. TAVR has opened AVR to a new large pool of patients and is expanding and even overtaking the traditional SAVR as the preferred method for AVR[37]. The minimally invasive nature of TAVR promises shorter hospitalization times and recovery. But in a large minority of patients, good quality of life outcomes are still lacking. Analyses of pre-

procedural predictors and models developed to predict poor outcomes have yet to identify which predictors are most important[25]. Vascular parameters are a possibly overlooked predictor, as the idea that AS is a disease of multiple resistances in series gains traction. Indeed secondary analyses of large RCT data such as the PARTNER I trial showed significantly lower mortality in those with hypertension and high systemic arterial compliance compared with those that were normotensive[26]. Furthermore, small scale studies that examined the change in vascular parameters[32,33,35] pre to post-TAVR indicated that significant stiffening in the downstream vasculature post-TAVR. One small scale study did find that a more stiffened vasculature, as measured by reflection coefficient at baseline, led to less improvement in post-TAVR KCCQ scores. This metric was included in our own models, but after adjustment and comparison against models with only STS Risk score present, we did not find a significant association. Nor did we find that a model with added WIA metrics and characteristic impedance adds significant predictive value over a model with just the STS risk score included. These results might suggest that at the point of needing a TAVR, the overall effect of vascular function is overtaken by the load imposed by the valve. Rather than downstream impedance solely contributing to poor outcomes post-TAVR, additional clinical factors are at play. These results additionally reinforce our findings from our longitudinal analysis in that changes in vascular function occur over decades. Ultimately, we may need to consider more intensive tracking earlier in the disease process to identify those patients in whom vascular function plays a larger role in progression and outcomes.

5.5 Future Directions

These studies and results lead to several potential additional lines of research. First is an expansion of the data used into different cohorts. While high quality RCT data was used to examine how pre-TAVR impedance may predict post-TAVR QOL outcomes, the PARTNER II trial was conducted in high and intermediate risk subjects. With younger and lower risk patients now enrolled in ongoing trials, investigation of the effect of vascular function should be studied in these population. Younger patients will have more compliant vascular systems hence the effects we saw in higher risk patients may not apply to this younger group. In a similar line, further expanding the assessment of impedance into younger and more mild AS severities is required. Population studies in healthy individuals have shown significant change in vascular parameters in the 3rd, 4th, and 5th decades of life. The AS population followed and seen at TMC was for the most part older. Earlier studies of vascular function in this cohort may yield predictive markers that are associated with greater long-term effect when it comes to time to AVR or presentation of symptoms. Finally, critical to the current treatment recommendations in AS is the ascertainment of symptomatic status. This was not available to us in the longitudinal dataset we created. Attempting to see if vascular function is associated with the rate of AS progression or time to symptomatic status would give further insight into the physiologic mechanisms and predictors that can help define the optimal points for intervention during the progression of AS.

Chapter 6 Appendix

6.1 Calculation of Wave Separation and Wave Intensity Analysis

a. Forward pressure waveform component [dyne/cm^2]:

$(pressure\ waveform) + (characteristic\ impedance) *$

$(flow\ waveform)$, where pressure is in dyne/cm^2, characteristic impedance is in dyne*sec/cm^3, and flow is in cm/sec

b. Backward pressure waveform component [dyne/cm^2]:

$(pressure\ waveform) - (characteristic\ impedance) *$

$(flow\ waveform)$, where pressure is in dyne/cm^2, characteristic impedance is in dyne*sec/cm^3, and flow is in cm/sec

c. Forward flow waveform component [cm/s]:

$\frac{forward\ pressure\ waveform\ component}{characteristic\ impedance}$, where forward pressure is in dyne/cm^2 and impedance is in dyne*sec/cm^3.

d. Backward flow waveform component [cm/s]:

$\frac{backward\ pressure\ waveform\ component}{characteristic\ impedance}$, where backward pressure is in dyne/cm^2 and impedance is in dyne*sec/cm^3.

e. Forward wave intensity [W*m^−2*s^−2]:

$\frac{d}{dt}(forward\ pressure\ waveform\ component) *$

$\frac{d}{dt}(forward\ flow\ waveform\ component) * \frac{1}{1000}$, where forward pressure is in dyne/cm^2 and forward flow is in cm/sec.

f. Backward wave intensity [W*m^−2*s^−2]:

$\frac{d}{dt}(backward\ pressure\ waveform\ component) *$

$\frac{d}{dt}(backward\ flow\ waveform\ component) * \frac{1}{1000}$, where backward pressure is in dyne/cm^2 and backward flow is in cm/sec.

g. Total forward cumulative wave intensity [W*m^−2*s^−1*1e4]:

$\frac{1}{10^4}\int_{t_0}^{t_n}(forward\ wave\ intensity)dt$, where forward wave intensity is in [W*m^−2*s^−2] and the integral is taken from the start time to the end time of the forward wave.

h. Total backward cumulative wave intensity [W*m^−2*s^−1*1e4]:

$\frac{1}{10^4}\int_{t_0}^{t_n}(backward\ wave\ intensity)dt$, where backward wave intensity is in [W*m^−2*s^−2] and the integral is taken from the start time to the end time of the backward wave.

i. Forward compression cumulative wave intensity [W*m^−2*s^−1*1e4]:

$\frac{1}{10^4}\int_{t_0}^{t_{separation}}(forward\ wave\ intensity)dt$, where forward wave intensity is in [W*m^−2*s^−2] and the integral is taken from the start time to the end time of the forward compression wave (i.e. where it transitions to an expansion wave).

j. Backward compression cumulative wave intensity [W*m^−2*s^−1*1e4]:

$\frac{1}{10^4}\int_{t_0}^{t_{separation}}(backward\ wave\ intensity)dt$, where backward wave intensity is in [W*m^−2*s^−2] and the integral is taken from the start time

to the end time of the backward compression wave (i.e. where it transitions to an expansion wave).

k. Forward expansion cumulative wave intensity [W*m^−2*s^−1*1e4]: $\frac{1}{10^4}\int_{t_{separation}}^{t_n}(forward\ wave\ intensity)dt$, where forward wave intensity is in [W*m^−2*s^−2] and the integral is taken from the start of the forward expansion wave to the end time of the wave.

l. Backward expansion cumulative wave intensity [W*m^−2*s^−1*1e4]: $\frac{1}{10^4}\int_{t_{separation}}^{t_n}(backward\ wave\ intensity)dt$, where backward wave intensity is in [W*m^−2*s^−2] and the integral is taken from the start of the backward expansion wave to the end time of the wave.

m. Peak forward compression wave intensity [W*m^−2*s^−2*1e6]: $\max(forward\ compression\ wave\ intensity) * \frac{1}{10^6}$, where forward compression wave intensity is in [W*m^−2*s^−2].

n. Peak backward compression wave intensity [W*m^−2*s^−2*1e6]: $\min(backward\ compression\ wave\ intensity) * \frac{1}{10^6}$, where backward compression wave intensity is in [W*m^−2*s^−2].

o. Peak forward expansion wave intensity [W*m^−2*s^−2*1e6]: $\max(forward\ expansion\ wave\ intensity) * \frac{1}{10^6}$, where forward expansion wave intensity is in [W*m^−2*s^−2].

p. Peak backward expansion wave intensity [W*m^−2*s^−2*1e6]: $\min(backward\ expansion\ wave\ intensity) * \frac{1}{10^6}$, where backward expansion wave intensity is in [W*m^−2*s^−2].

q. Reflection Coefficient [unitless]: $\max(backward\ pressure\ wave)$ / $\max\ (forward\ pressure\ wave)$

6.2 Clinical Validation of Non-Invasive Simulation Based Determination of Vascular Impedance in Patients Undergoing Transcatheter Aortic Valve Replacement

6.2.1 Ejection Duration Optimization Algorithm

To obtain the patient flow velocity frequency spectrum, the patient time domain flow velocity waveform is first constructed. This is done in three steps using 5 required parameters: heart period, sample rate, maximum flow velocity, and input ejection duration and optional acceleration time. The units of the flow velocity waveform are cm/sec.

1. A parabola (2^{nd}-degree polynomial) is created to model the flow velocity waveform during the ejection period. The width of this parabola is given by the input ejection duration and the peak is given by the max flow velocity. If acceleration time is provided, the peak of the parabola is placed at the acceleration time. If acceleration time is not specified, the peak of the parabola is placed exactly in the center of the input ejection duration. The sample rate is used to determine time on the x-axis.

2. A vector of zeros is used to model the absence of flow from the end of the input ejection duration to the end of the heart period. The parabola is concatenated with this vector to create the complete flow velocity waveform.
3. The flow waveform is smoothed using 5^{th} order B-spline interpolation to avoid the Gibbs phenomenon. This smoothing results in a slightly widened ejection duration and shifts time of peak velocity.

While the heart period, sample rate, and maximum flow velocity are required program input variables, the input ejection duration, which is the ejection duration used to initially construct the flow velocity waveform, is obtained from stroke volume (SV) as explained below. The input ejection duration is different from the ED (which is the ejection duration of the smoothed flow velocity waveform and therefore the actual patient ejection duration) due to the smoothing process described above – i.e. after the velocity waveform is smoothed, its ED is wider than the ejection duration that was used in its initial construction. Because of this, the processes described below are meant to obtain input ejection durations that will result in smoothed waveforms with ED values that match patient values.

Determination of input ejection duration:

1. Stroke Volume: The program will compute the input ejection duration from the given patient SV using an optimization process.
    a. A vector of 20 potential input ejection duration values is generated; it consists of values between 0.2 and 0.4 in increments of 0.01

b. For each input ejection duration, a flow velocity waveform is constructed via the above method including smoothing.

c. The velocity time integral of each generated flow velocity waveform is computed and the SV that is closest in value to the patient SV is determined.

d. The input ejection duration that gave rise to this closest SV is then stored and used to construct the flow velocity waveform that will be used for the patient.

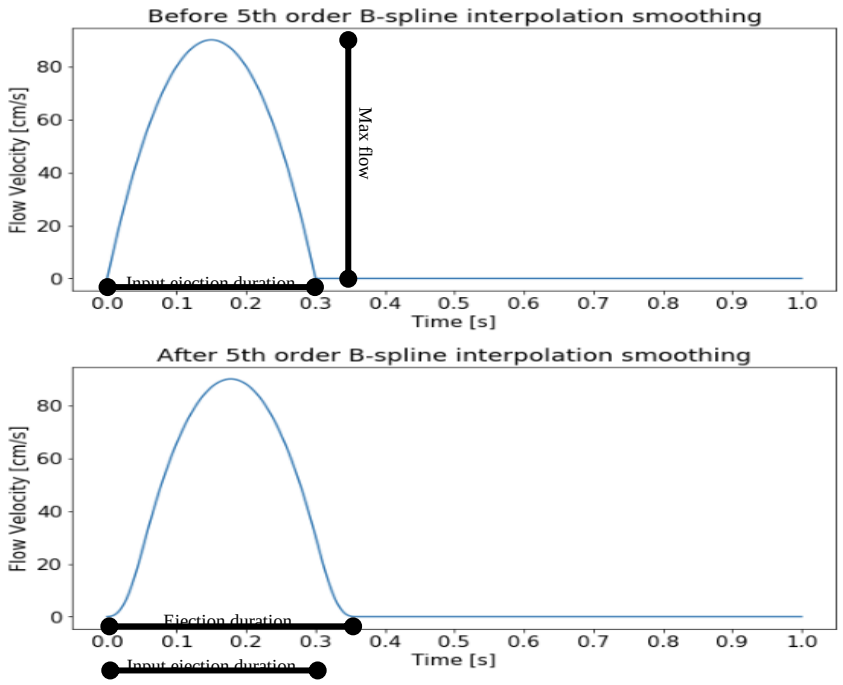

Figure 6.1 Figure depicting the flow waveform before and after 5th order B-spline interpolation smoothing. Note that the ejection duration of the waveform after smoothing is somewhat increased compared to the input ejection duration prior to smoothing.

6.2.2 Tables and Figure

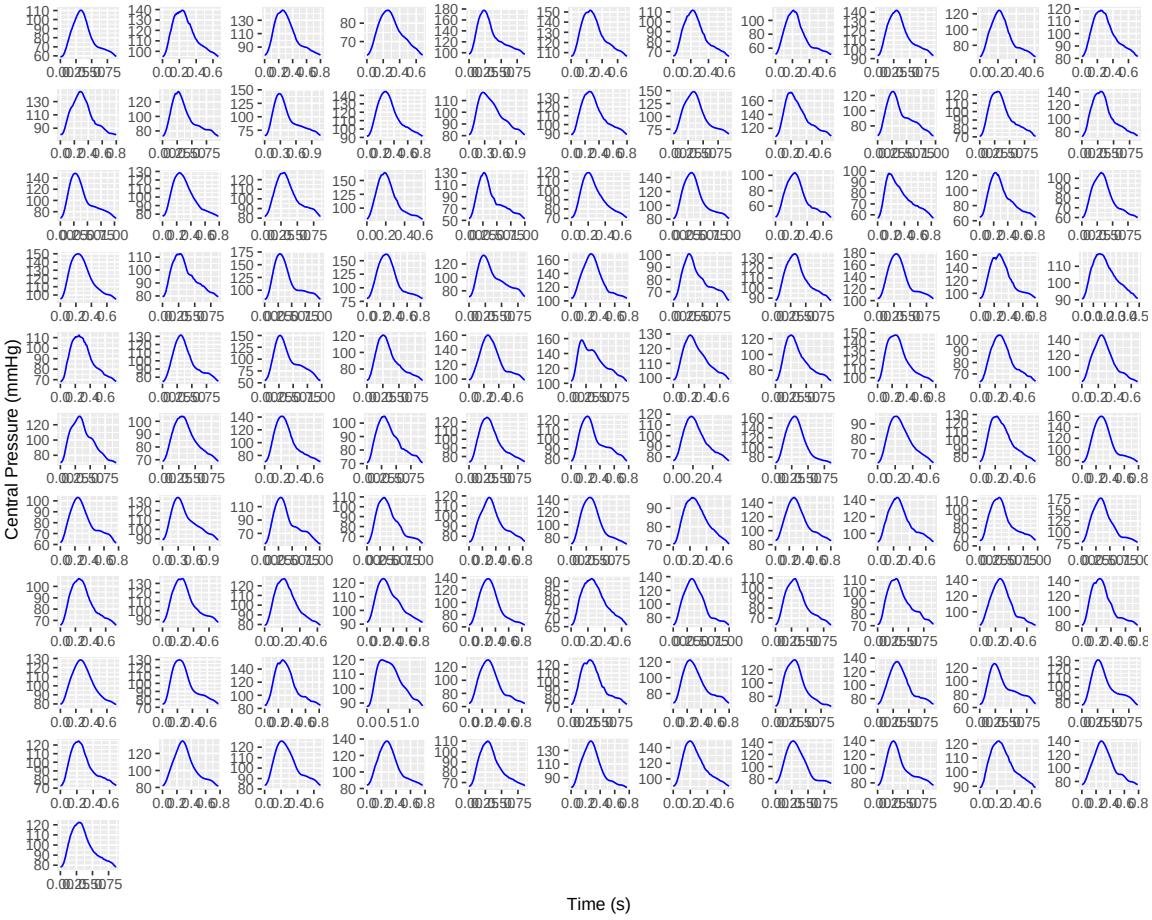

Figure 6.2 Full set comparison of non-invasive central pressure measured via the SphygmoCor XCEL device (Red) and aortic central pressure generated from simulated data (Blue). Overall waveform morphology concordance between measured and simulated data was good as measured by point-by-point differences. A tendency toward underestimation of aortic central pressure from simulated results.

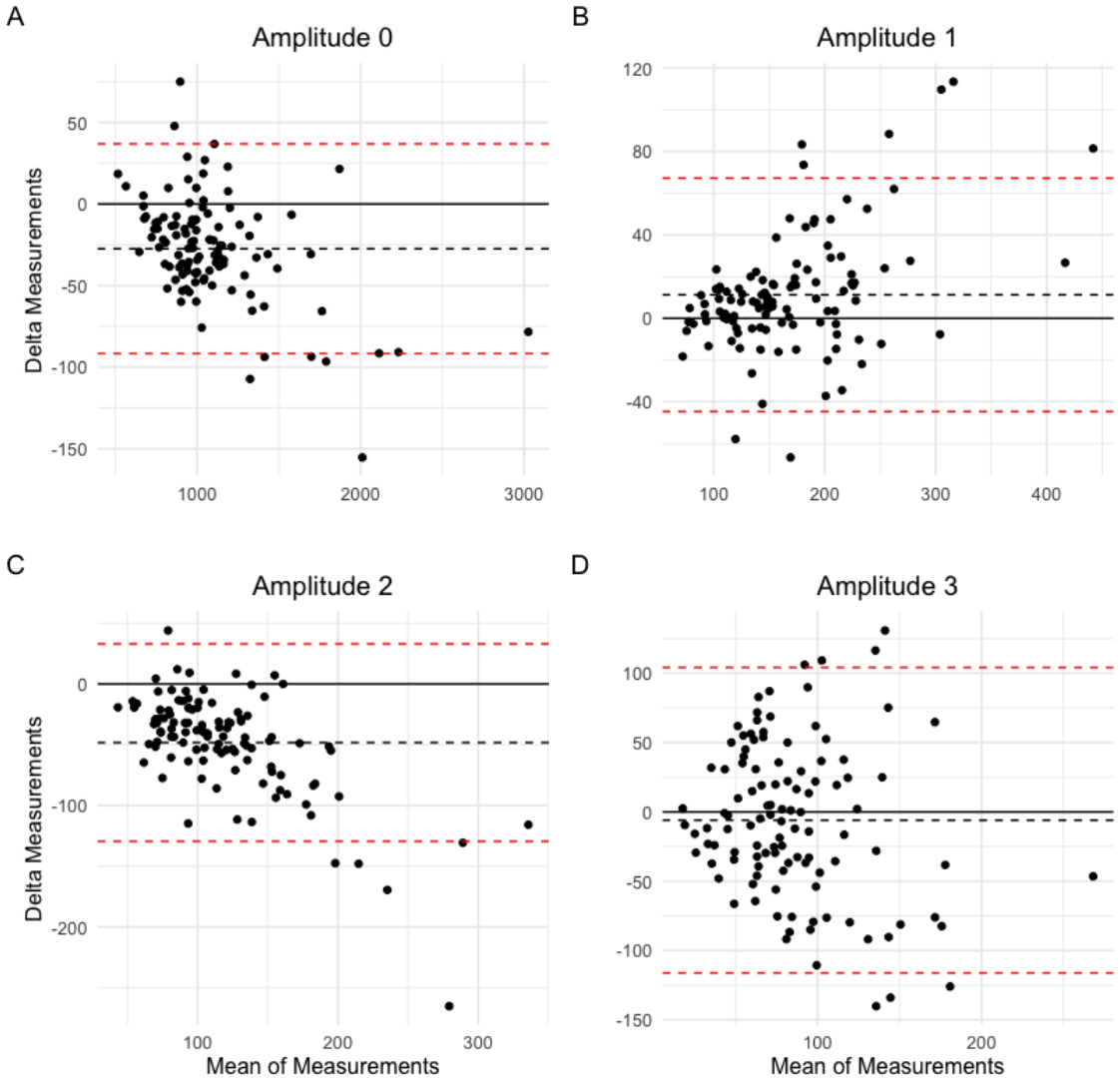

Figure 6.3 Bland-Altman plots showing the mean of the measurements on the x-axis and differences in measurements on the y-axis. Raw harmonic amplitude values from the 0^{th} to 3^{rd} harmonic are shown. Units for all amplitude values are dynes/cm^3. The black dashed line indicates the overall mean value and dashed red lines the 95% limits of agreement. Due to spread of values at higher values and non-random scatter around mean bias line limits of agreement cannot be used to fully assess agreement.

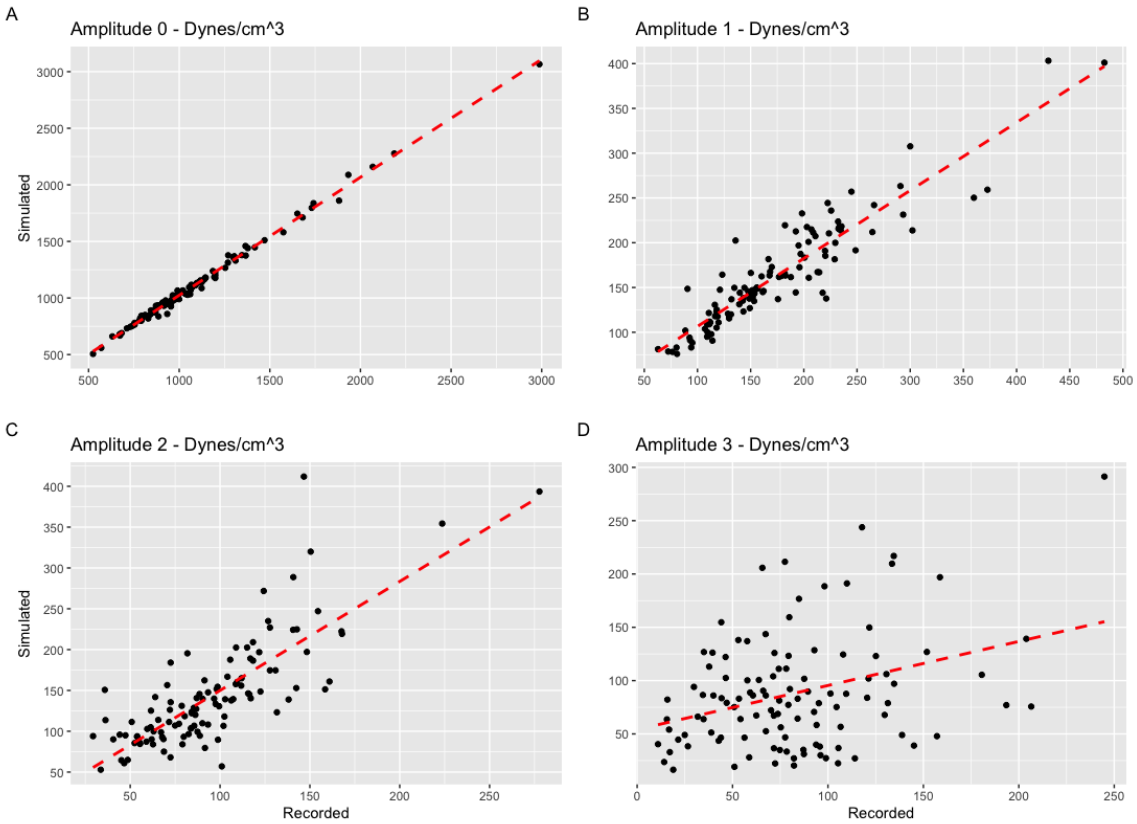

Figure 6.4 Scatter plots comparing recorded and simulated impedance amplitude values. Red dashed line represents the best fit line.

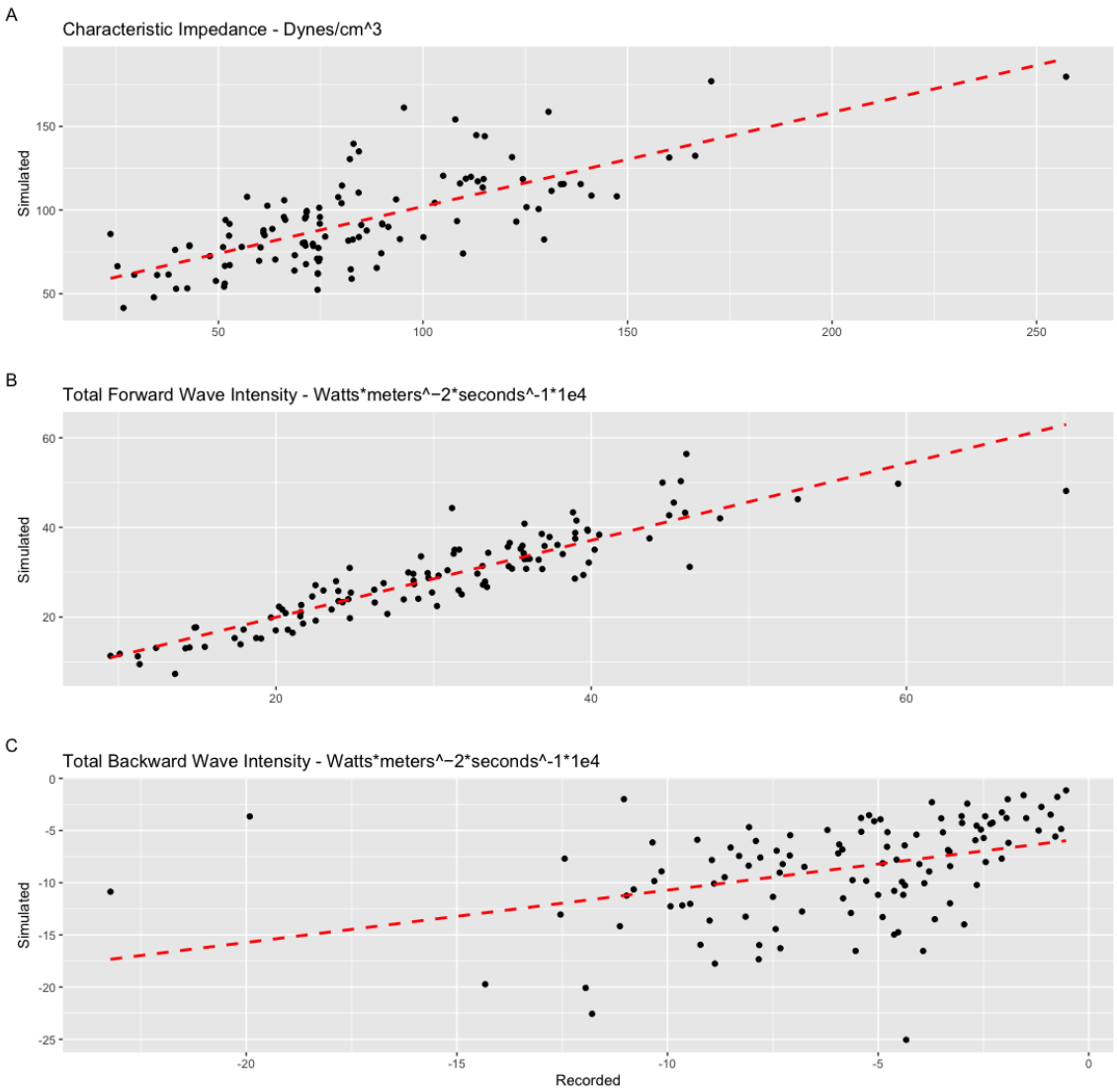

Figure 6.5 Scatter plot comparing recorded and simulated vascular parameters of characteristic impedance, and total forward and backward wave intensities. Red dashed line represents the best fit line.

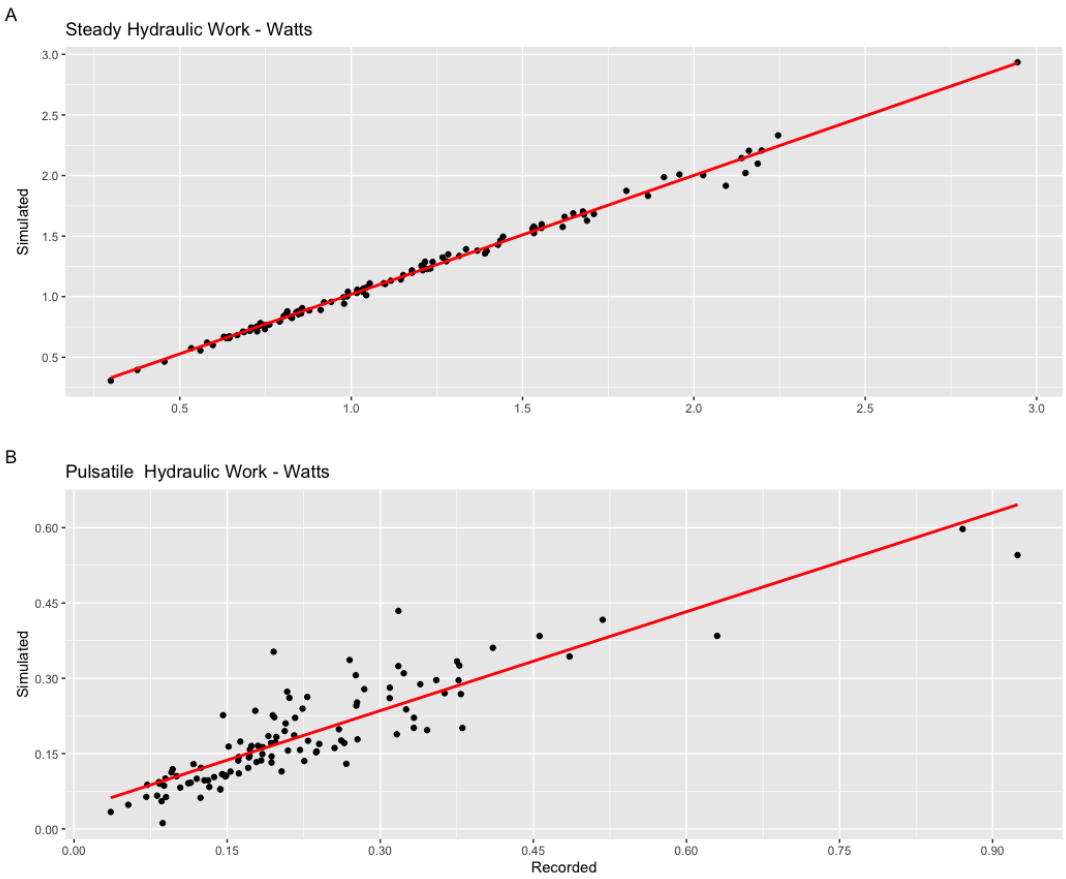

Figure 6.6 Scatter plot comparing recorded and simulated steady and pulsatile hydraulic work. Red dashed line represents the best fit line.

Table 6.1 Comparison table of frequency domain based vascular parameters calculated from non-invasive and simulated methods for determination of vascular impedance.

Metrics N = 111	*Recorded (Mean±SD)*	*Simulated (Mean±SD)*	*Correlation Coefficient*	*Mean Bias*	*95% Limits of Agreement*	*Maximum Limit of Agreement as a Percentage of SD*
			Frequency Domain Parameters			
0^{th} Amplitude Harmonic (dynes/cm^3)	1073 (352)	1100 (368)	0.99	-27.4	-91.6, 36.9	25
1^{st} Amplitude Harmonic (dynes/cm^3)	174 (71)	163 (59)	0.92	11.3	-44.7, 67.2	113
2^{nd} Amplitude Harmonic (dynes/cm^3)	95 (39)	143 (65)	0.80	-48.2	-129.5, 33.0	199
3^{rd} Amplitude Harmonic (dynes/cm^3)	82 (39)	88 (53)	0.34	-6.02	-116.2, 104.2	219

Table 6.2 Summary of vascular function metrics from sensitivity analysis using central instead of brachial blood pressure

Metrics N = 102	*Recorded (Mean±SD)*	*Simulated (Mean±SD)*	*Correlation Coefficient*	*Mean Bias*	*95% Limits of Agreement*	*Maximum Limit of Agreement as a Percentage of SD*
		Frequency Domain Parameters				
0^{th} Amplitude Harmonic (dynes/cm^3)	1056 (310)	1061 (320)	0.99	-5.7	-62.3, 50.8	19.4
1^{st} Amplitude Harmonic (dynes/cm^3)	168 (69)	147 (58)	0.97	22.2	-12.6, 56.9	98
2^{nd} Amplitude Harmonic (dynes/cm^3)	93 (39)	135 (63)	0.83	-40.8	-110.9, 29.3	176
Characteristic Impedance (dynes/cm^3)	82 (45)	88 (27)	0.73	-4.6	-52.8, 44.6	196
		Total Wave Intensity Analysis Parameters				
*Forward (W*m^{-2}*s^{-1}*1e4)*	29 (10)	26 (10)	0.95	3.3	-3.6, 9.1	91
*Backward (W*m^{-2}*s^{-1}*1e4)*	-5.5 (3.3)	-7.7 (4.1)	0.51	2.2	-5.4, 9.6	234
		Hydraulic work				
Steady (Watts)	1.16 (0.49)	1.15 (0.48)	0.99	0.01	-0.06, 0.08	16
Pulsatile (Watts)	0.22 (0.12)	0.17 (0.10)	0.91	0.05	-0.6, 0.15	6

6.3 Longitudinal Metrics of Vascular Function and Time to Aortic Valve Replacement

6.3.1 Tables and Figures

Table 6.3 List Input Variables Required for Input Impedance Simulation

Systolic Blood Pressure (mmHg)
Diastolic Blood Pressure (mmHg)
Heart Rate (beats/min)
Peak Aortic Valve Velocity (cm/s)
Stroke Volume (ml)
Aortic Valve Area (cm^2)
Acceleration Time (s)

Table 6.4 List of Variables Required for Acceleration Time Sub-Model

Systolic Blood Pressure (mmHg)
Diastolic Blood Pressure (mmHg)
Heart Rate (beats/min)
Peak Aortic Valve Velocity (cm/s)
Mean Aortic Valve Gradient (mmHg)
Aortic Valve Area (cm^2)
Dimensionless Index
Stroke Volume Index (ml/m^2)
Aortic Valve Velocity Time Integral (cm)

Table 6.5 Rates of AVR in those subjects with either insufficient data or failed to converge during impedance simulation

	Event		
	No AVR	AVR	Total
Baseline AS Severity			
No AS	551 (93%)	41 (6.9%)	592 (100%)
Mild	1,048 (95%)	57 (5.2%)	1,105 (100%)
Moderate	739 (89%)	88 (11%)	827 (100%)
Severe	597 (81%)	138 (19%)	735 (100%)
Total	2,935 (90%)	324 (9.9%)	3,259 (100%)

Table 6.6 Number and rate of missing variables

Variables	Number Missing	Percent Missing
Body Surface Area	2468	60.9
Systolic BP	1704	42.1
Diastolic BP	1698	41.9
Heart Rate	1250	30.9
Aortic Valve Area	959	23.7
Dimensionless Index	847	20.9
Mean Gradient	713	17.6
AV Velocity Time Integral	668	16.5
Stroke Volume	430	10.6
Ejection Fraction	294	7.26
Peak Gradient	180	4.44
Peak Velocity	178	4.40

Table 6.7 Comparison of clinically read AS severity and guideline assigned values used for determination of baseline AS severity

	Guideline Based Severity				
	No AS	Mild	Moderate	Severe	Total
Clinical AS Finding					
(Missing)	0 (0%)	241 (52%)	118 (25%)	107 (23%)	466 (100%)
No AS	0 (0%)	0 (0%)	1 (100%)	0 (0%)	1 (100%)
AS Can't Be Excluded	0 (0%)	200 (71%)	71 (25%)	9 (3.2%)	280 (100%)
Mild	0 (0%)	83 (33%)	138 (55%)	29 (12%)	250 (100%)
Mild to Moderate	0 (0%)	4 (5.2%)	60 (78%)	13 (17%)	77 (100%)
Moderate	0 (0%)	3 (2.1%)	73 (51%)	67 (47%)	143 (100%)
Moderate to Severe	0 (0%)	0 (0%)	17 (21%)	65 (79%)	82 (100%)
Severe	0 (0%)	0 (0%)	8 (3.3%)	233 (97%)	241 (100%)
Total	0 (0%)	531 (34%)	486 (32%)	523 (34%)	1,540 (100%)

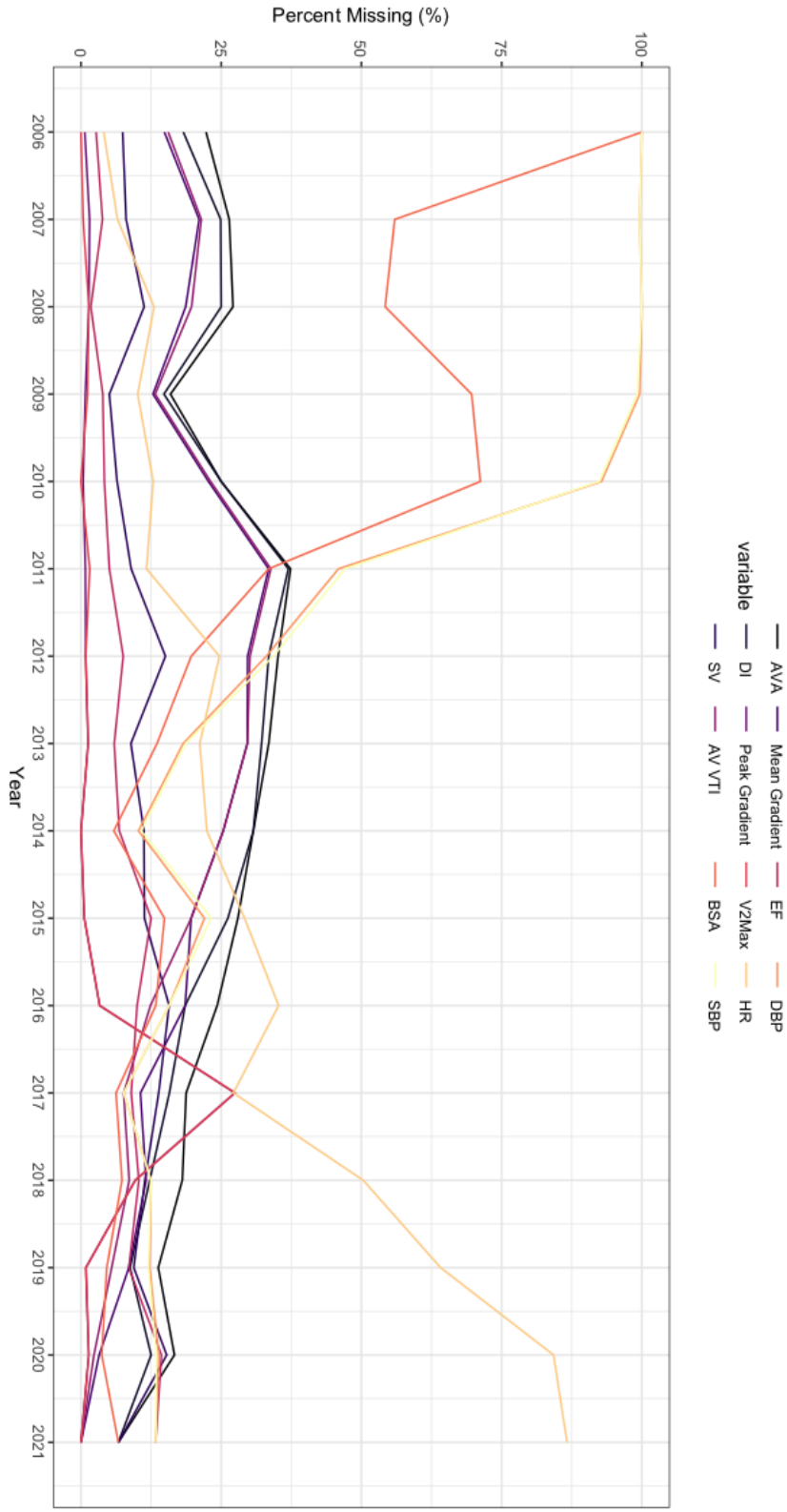

Figure 6.7 Rates of missingness over time by variable

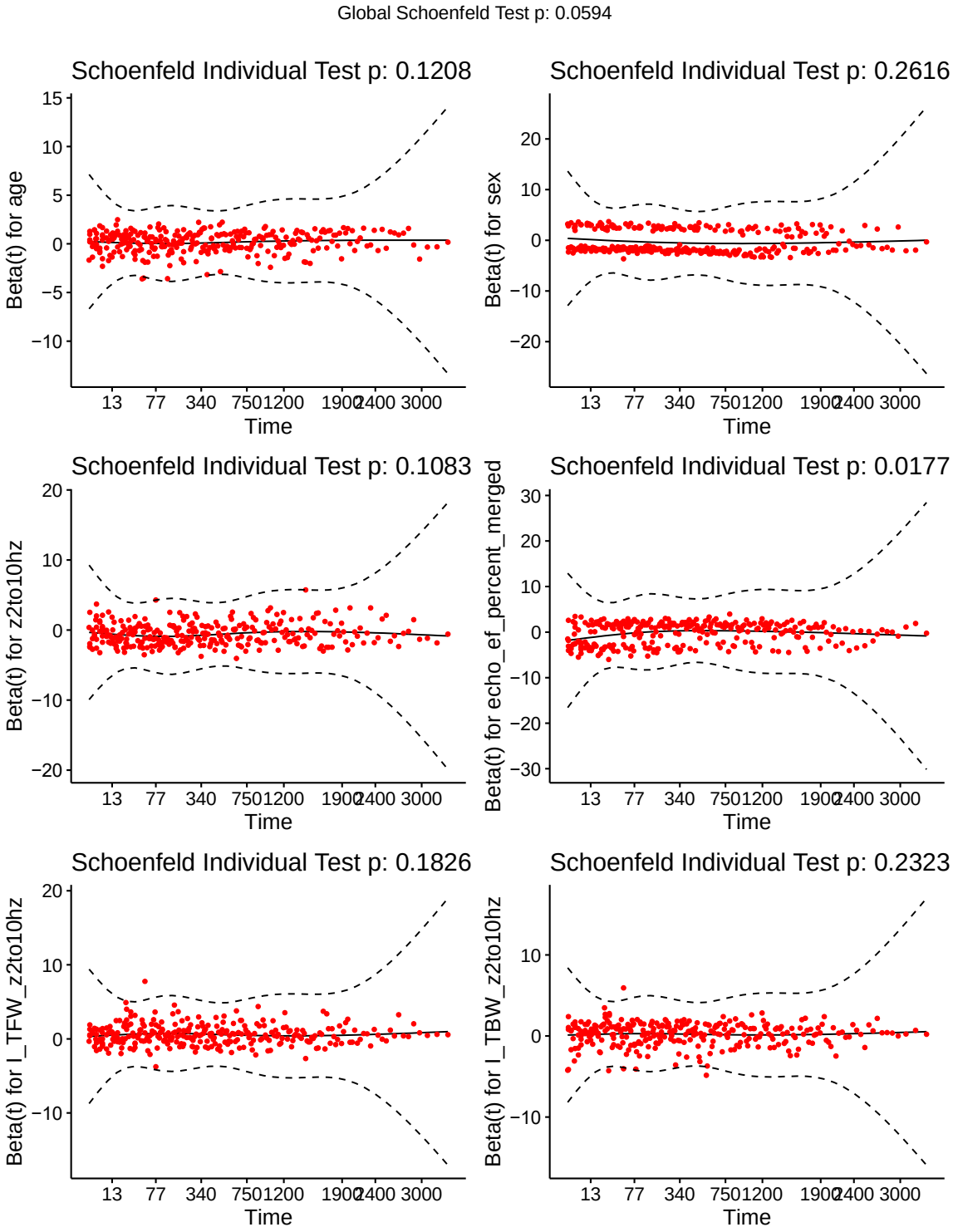

Figure 6.8 Schoenfeld Residual Plots for models with baseline impedance metrics prior to stratification by ejection fraction due to violation in proportional hazards assumption.

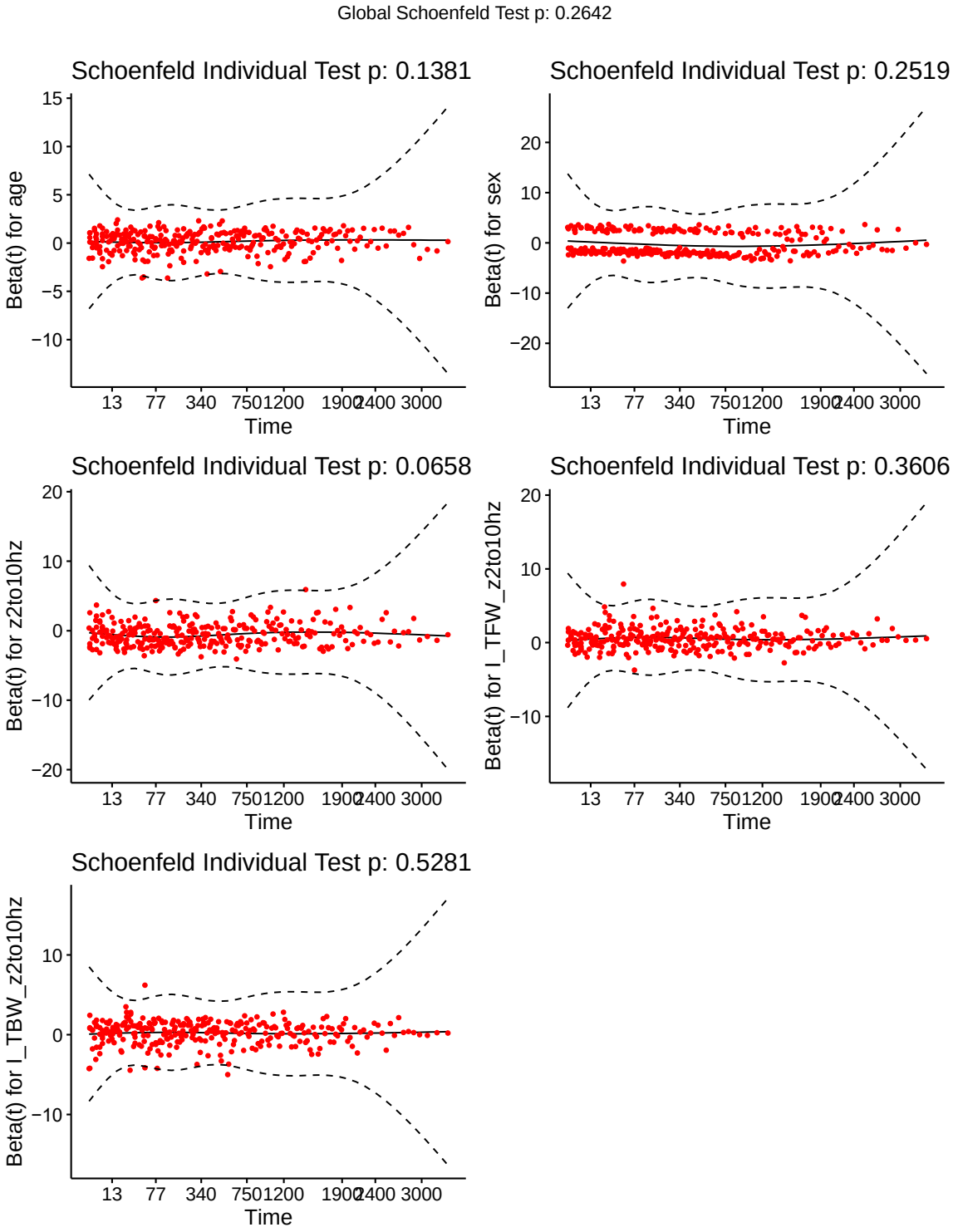

Figure 6.9 Schoenfeld Residual Plots for models with baseline impedance metrics after stratification by ejection fraction.

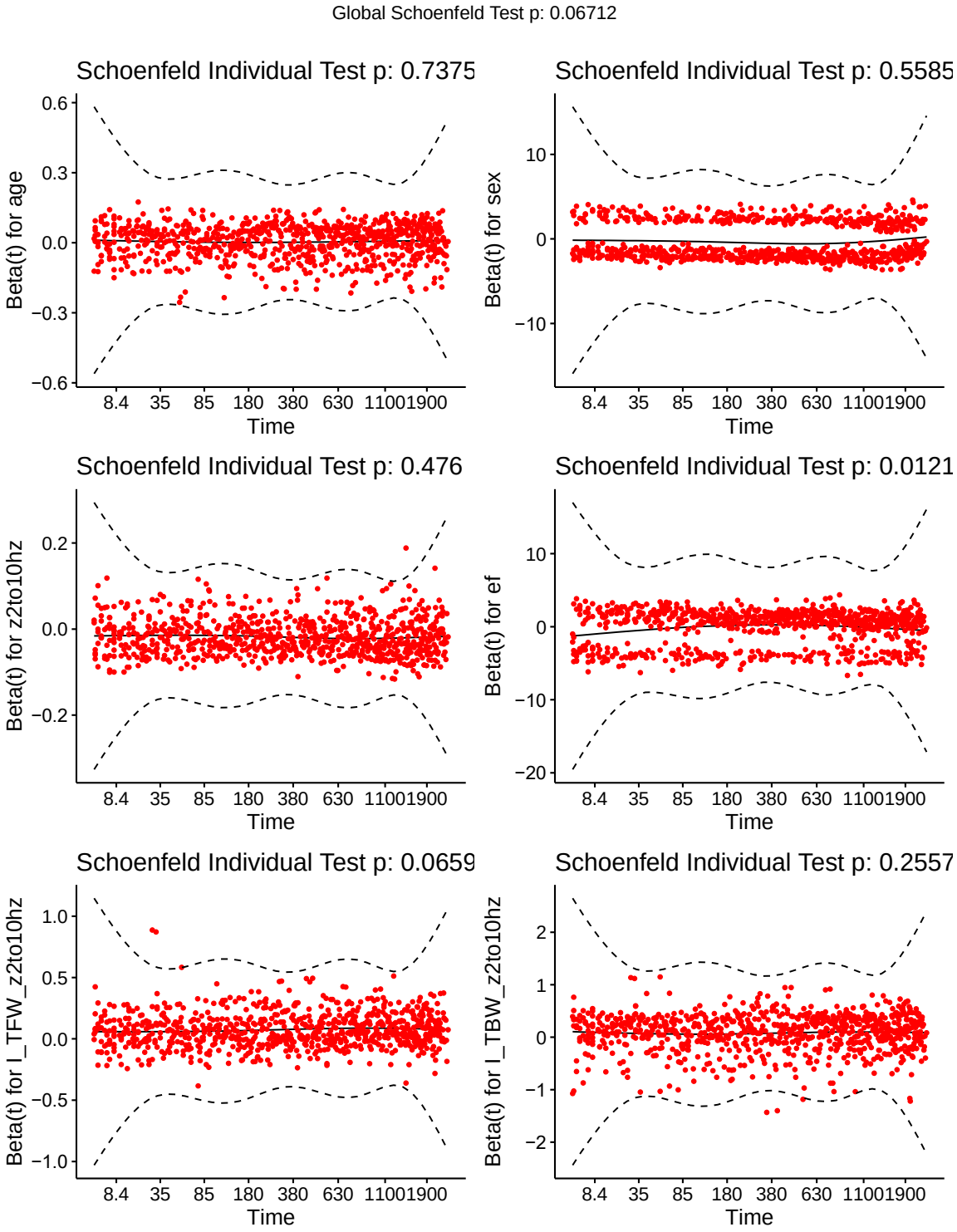

Figure 6.10 Schoenfeld Residual Plots for models with time-varying impedance metrics prior to stratification by ejection fraction due to violation in proportional hazards assumption.

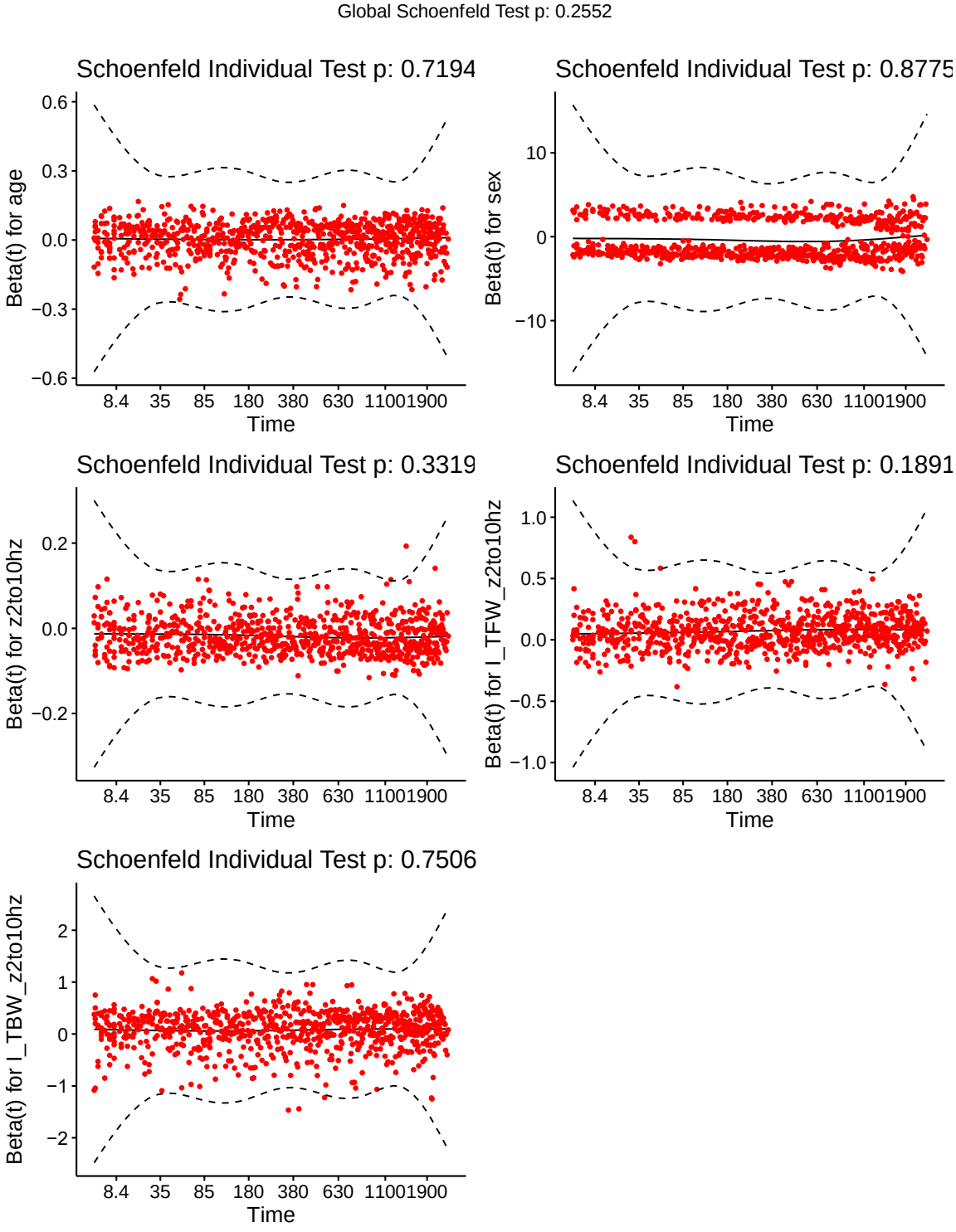

Figure 6.11 Schoenfeld Residual Plots for models with time-varying impedance metrics after stratification by ejection fraction.

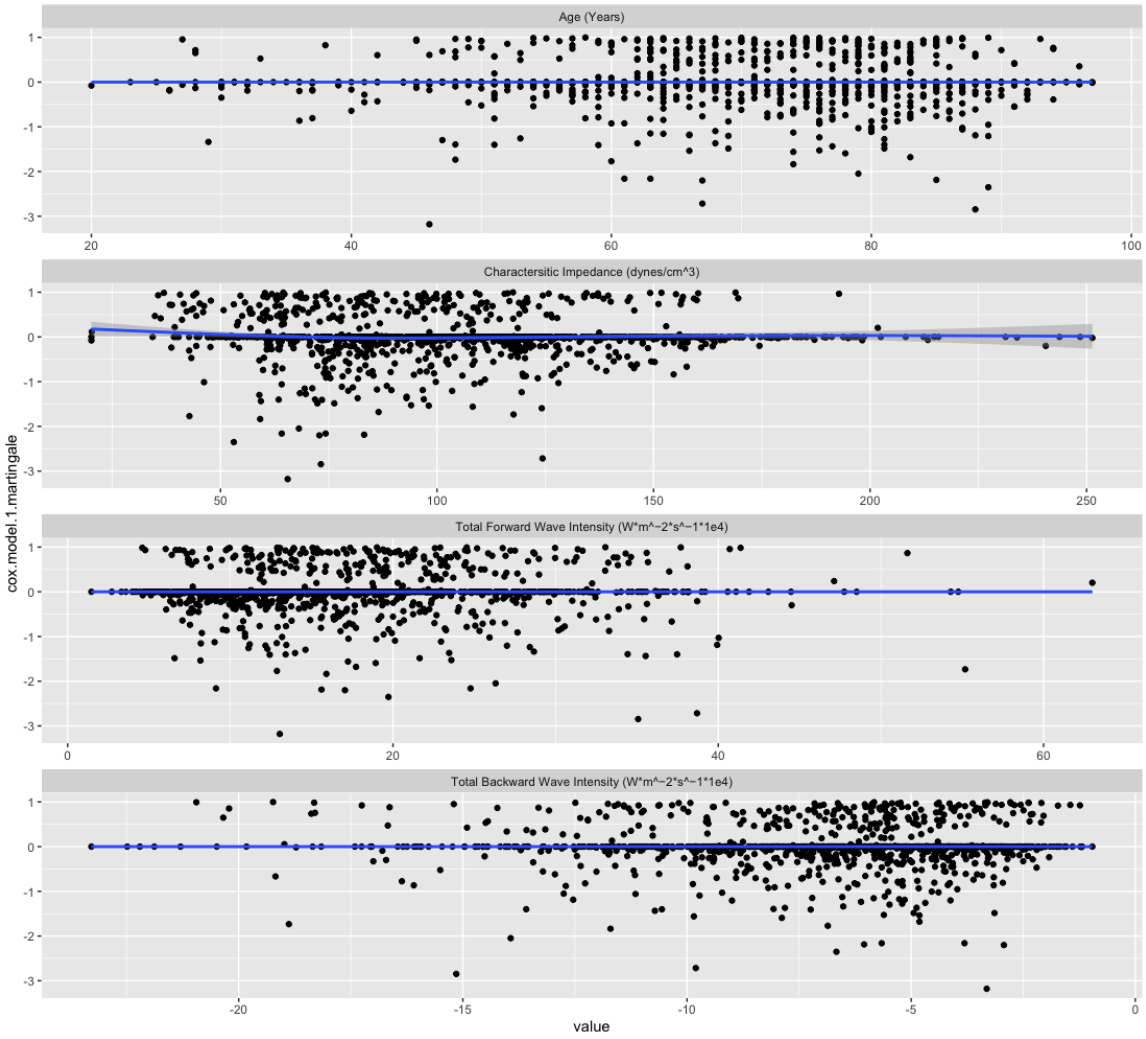

Figure 6.12 Martingale residuals for Cox Model with baseline impedance variables. The blue line represents a locally weighted scatterplot smoothing (LOESS) curve.

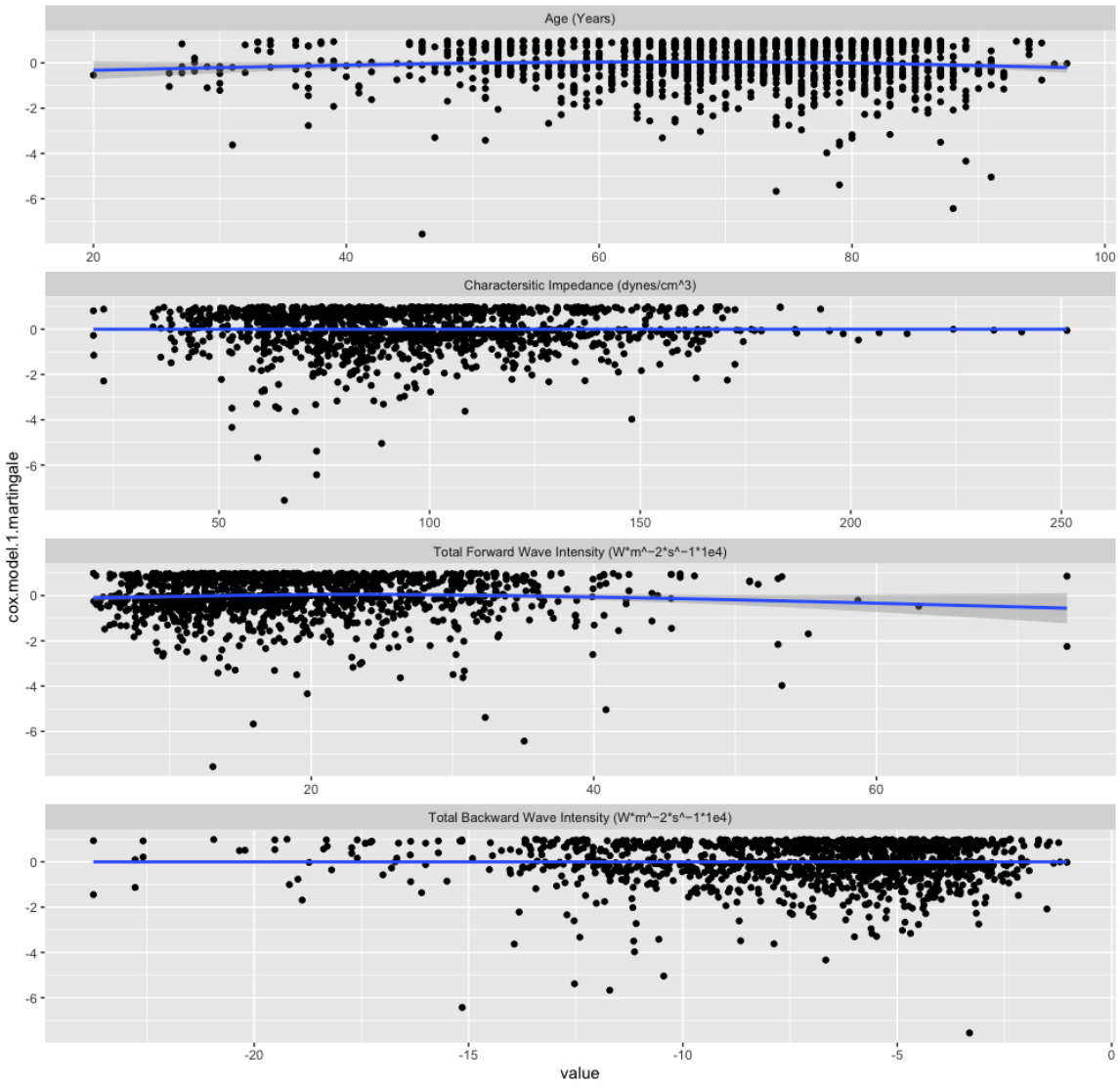

Figure 6.13 Martingale residuals for Cox Model with impedance variables included as time varying. The blue line represents a locally weighted scatterplot smoothing (LOESS) curve.

Table 6.8 Cox Regression Modeling with interaction between baseline AS severity strata without time varying vascular parameters

Characteristic	HR[1,2]	SE[2]	95% CI[2]
Age	1.18**	0.066	1.03, 1.34
Sex			
M	1.00	—	—
F	0.72**	0.126	0.56, 0.93
Characteristic Impedance	1.04	0.258	0.63, 1.73
Total Forward Wave Intensity	2.61	0.529	0.92, 7.35
Total Backward Wave Intenisty	1.97	0.429	0.85, 4.56
Characteristic Impedance * strata(baseline_as_severity)			
Characteristic Impedance * Moderate	0.52*	0.312	0.28, 0.95
Characteristic Impedance * Severe	0.47**	0.283	0.27, 0.82
Total Forward Wave Intensity * strata(baseline_as_severity)			
Total Forward Wave Intensity * Moderate	0.96	0.560	0.32, 2.88
Total Forward Wave Intensity * Severe	0.64	0.538	0.22, 1.83
Total Backward Wave Intenisty * strata(baseline_as_severity)			
Total Backward Wave Intenisty * Moderate	0.58	0.462	0.23, 1.44
Total Backward Wave Intenisty * Severe	0.63	0.438	0.27, 1.49

*All continuous variables scaled to their SD

[1] *p<0.05; **p<0.017

[2] HR = Hazard Ratio, SE = Standard Error, CI = Confidence Interval

Table 6.9. Cox Regression Modeling with interaction between baseline AS severity strata and time-varying vascular parameters

Characteristic	HR[1,2]	SE[2]	95% CI[2]
Age	1.00	0.003	1.00, 1.01
Sex			
M	1.00	—	—
F	0.71**	0.076	0.61, 0.82
Characteristic Impedance	0.99**	0.004	0.98, 1.00
Total Forward Wave Intensity	1.09**	0.029	1.03, 1.15
Total Backward Wave Intenisty	1.12*	0.053	1.01, 1.25
Characteristic Impedance * strata(baseline_as_severity)			
Characteristic Impedance * Moderate	0.99*	0.005	0.98, 1.00
Characteristic Impedance * Severe	1.00	0.004	0.99, 1.00
Total Forward Wave Intensity * strata(baseline_as_severity)			
Total Forward Wave Intensity * Moderate	1.03	0.031	0.97, 1.09
Total Forward Wave Intensity * Severe	0.98	0.030	0.92, 1.03
Total Backward Wave Intenisty * strata(baseline_as_severity)			
Total Backward Wave Intenisty * Moderate	0.99	0.057	0.89, 1.11
Total Backward Wave Intenisty * Severe	0.96	0.055	0.87, 1.07

*All continuous variables scaled to their SD

[1] *p<0.05; **p<0.017

[2] HR = Hazard Ratio, SE = Standard Error, CI = Confidence Interval

Table 6.10 Cox regression model results with baseline vascular impedance metrics in sensitivity analysis that removed SAVR patients. Due to violations of the proportional hazard's assumption on the characteristic impedance parameter an interaction term to define a set of time periods before 450 days, 450-1200 days, and after 1200 days were created as an interaction term.

Characteristic	HR[1,2]	SE[2]	95% CI[2]
Age	1.46**	0.092	1.22, 1.75
Sex			
M	1.00	—	—
F	0.77	0.157	0.57, 1.05
Characteristic Impedance	0.78	0.219	0.51, 1.20
Total Forward Wave Intensity	2.00**	0.116	1.59, 2.51
Total Backward Wave Intenisty	1.30**	0.099	1.07, 1.58
Characteristic Impedance * zc_period			
Characteristic Impedance * after 1200	0.79	0.288	0.45, 1.39
Characteristic Impedance * before 450	0.48**	0.250	0.29, 0.78

*All continuous variables scaled to their SD

[1] *p<0.05; **p<0.017

[2] HR = Hazard Ratio, SE = Standard Error, CI = Confidence Interval

Table 6.11 Cox regression model results with time varying vascular impedance metrics in sensitivity analysis that removed SAVR patients.

Characteristic	HR[1,2]	SE[2]	95% CI[2]
Age	1.02**	0.004	1.01, 1.03
Sex			
M	1.00	—	—
F	0.66**	0.097	0.55, 0.80
Characteristic Impedance	0.98**	0.002	0.98, 0.99
Total Forward Wave Intensity	1.07**	0.006	1.06, 1.09
Total Backward Wave Intenisty	1.08**	0.015	1.05, 1.11

*All continuous variables scaled to their SD

[1] *p<0.05; **p<0.017

[2] HR = Hazard Ratio, SE = Standard Error, CI = Confidence Interval

6.4 Association Between Metrics of Vascular Function and Post Transcatheter Aortic Valve Replacement Outcomes

6.4.1 Acceleration Time Linear Regression Sub Modeling

Due to the lack of acceleration time present in the clinical data used for external validation we created a predictive sub-model from other echocardiographic and demographic parameters present in the data. Two prior studies were identified that explored this, and the variables from these models were used as starting points[83,84]. Two separate datasets were used for modeling. First data was taken from the derivation dataset, the PARTNERS II trial. The second dataset used was a sample of 38 patients from Tufts Medical Center (Boston, MA) where the acceleration time was extracted manually from the echocardiographic images. Both forward and backward stepwise linear regression was used to model acceleration time. The initial "full model" with all variables included systolic and diastolic blood pressure, age, sex, peak aortic valve velocity, mean gradient, peak gradient, stoke volume, stroke volume index, aortic valve area, indexed aortic valve area, directionless index, and aortic valve velocity time integral (VTI). After stepwise selection the final model chosen included, systolic and diastolic blood pressure, mean and peak gradient, dimensionless index, aortic valve VTI, peak aortic valve velocity, heart rate and stroke volume index. Internal validation was via a bootstrap method to determine the range of R^2 values and model stability.

Model coefficients can be seen below along with a scatter plot displaying model fit between predicted acceleration time (x-axis) and measured acceleration times (y-axis). R^2 values with internal validation ranged from 0.313 to 0.397.

Table 6.12 Acceleration Time Sub-model cohort characteristics

Characteristic	**TMC**, N = 38[1]	**PARTNERS**, N = 3,983[1]
Age (Years)	79 (74, 83)	83 (78, 87)
Sex		
Female	17 (45%)	1,719 (43%)
Male	21 (55%)	2,264 (57%)
Body Surface Area (m^2)	2.01 (1.85, 2.09)	1.88 (1.71, 2.06)
Body Mass Index	27.7 (26.1, 29.8)	27.1 (24.0, 31.2)
Acceleration Time (s)	0.100 (0.080, 0.120)	0.120 (0.105, 0.136)
Ejection Duration (s)	0.34 (0.31, 0.36)	NA (NA, NA)
Heart Rate (BPM)	65 (59, 79)	71 (63, 80)
Systolic BP (mmHg)	131 (115, 153)	130 (117, 144)
Diastolic BP (mmHg)	71 (62, 80)	67 (60, 74)
Peak Aortic Velocity (cm/s)	366 (303, 432)	426 (392, 467)
Mean Aortic Velocity (cm/s)	262 (208, 302)	NA (NA, NA)
Mean Aortic Valve Gradient (mmHg)	33 (21, 42)	41 (34, 50)
Peak Aortic Valve Gradient (mmHg)	54 (37, 75)	73 (62, 87)
Stroke Volume (ml)	68 (62, 83)	69 (57, 82)
Stroke Volume Index (ml/m^2)	35 (29, 39)	37 (31, 44)
Aortic Valve Area (cm^2)	0.80 (0.64, 0.93)	0.68 (0.56, 0.81)
Aortic Valve Area Index (cm^2/m^2)	0.36 (0.32, 0.44)	0.37 (0.30, 0.43)
Dimentionless Index	0.24 (0.20, 0.30)	0.21 (0.17, 0.24)
AV VTI	88 (67, 101)	102 (89, 116)
LV Ejection Fraction (%)	60 (56, 64)	57 (46, 63)
LV Mass (g)	193 (159, 251)	NA (NA, NA)

[1] Median (IQR); n (%)

Table 6.13 Final Model Coefficients

	Coefficient	Standard Error	P-Value
(Intercept)	1.512E-01	1.174E-02	2E-16
SBP	-1.964E-04	1.908E-05	2E-16
DBP	6.381E-05	3.493E-05	0.06783
Heart Rate	9.241E-05	2.897E-05	0.00144
V2Max	-3.222E-04	4.625E-05	3.86E-12
Mean Gradient	-6.817E-04	1.022E-04	2.95E-11
Peak Gradient	5.513E-04	1.399E-04	8.26E-05
Aortic Valve Area	1.318E-02	3.141E-03	2.78E-05
Dimensionless Index	-8.667E-02	9.125E-03	2E-16
Stroke Volume Index	-1.413E-04	6.283E-05	0.02458
AV VTI	1.216E-03	4.111E-05	2E-16

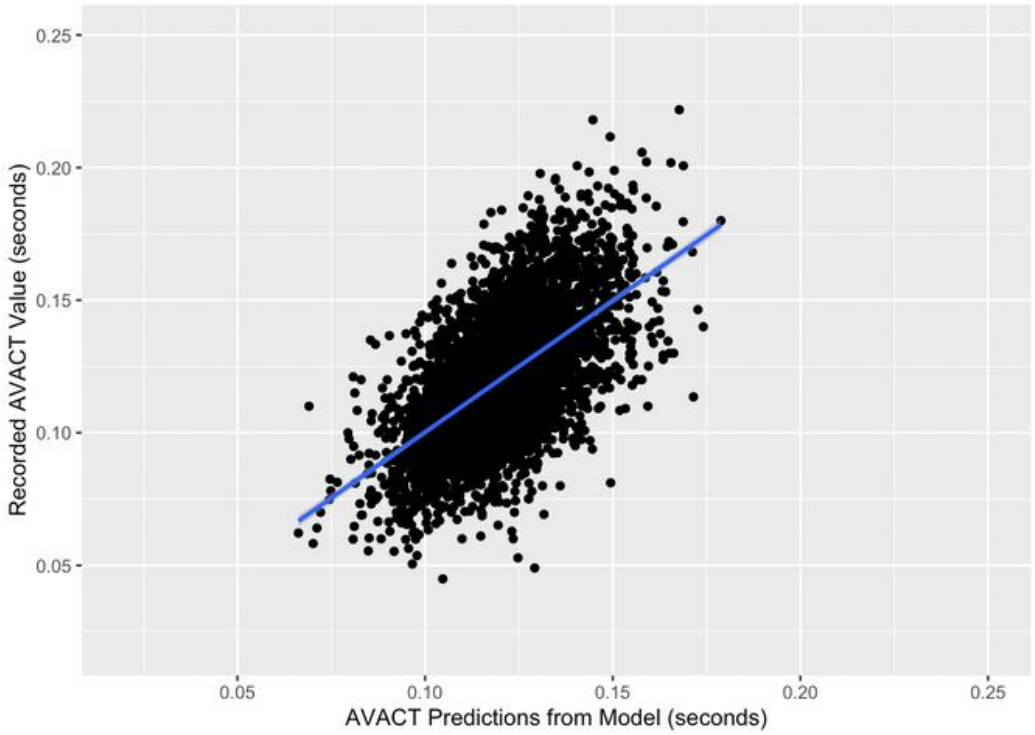

Figure 6.14 Figure of acceleration time submodule predictions versus acceleration time measured via an echocardiogram

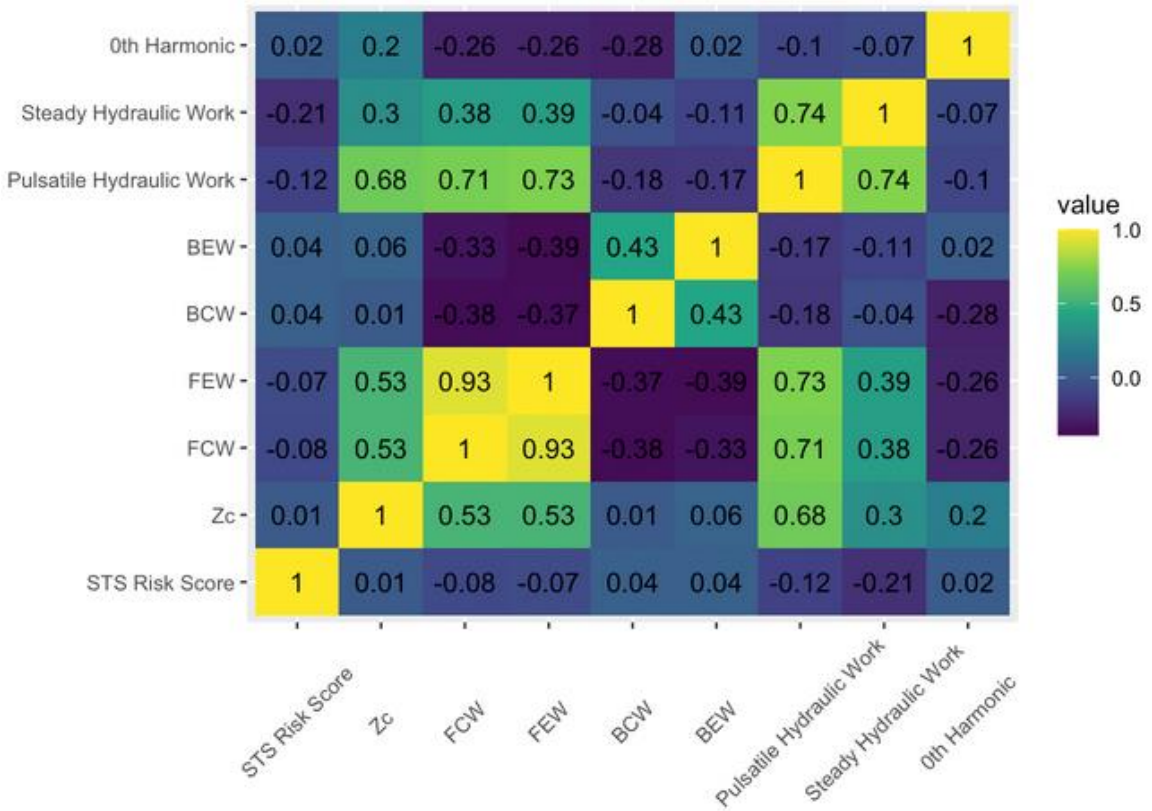

Figure 6.15 Correlation plot of variables initially selected for inclusion

Table 6.14 Sensitivity analysis of incremental addition of candidate variables to explore reversal of forward wave compression odds ratio direction from initial variable screen to final model. Odds ratio reverse occurred after the inclusion of the pulsatile work impedance variable

	Base		+0th Harmonic		+Pulsatile Work		+Steady Work		+Reflection Coef		+Zc		+BEW		+BCW	
Characteristic	**OR**[1,2]	**SE**[2]	**OR**[1,2]	**SE**[2]	**OR**[1,2]	**SE**[2]	**OR**[1,2]	**SE**[2]	**OR**[1,2]	**SE**[2]	**OR**[1,2]	**SE**[2]	**OR**[1,2]	**SE**[2]	**OR**[1,2]	**SE**[2]
STS Risk Score	1.51***	0.052	1.52***	0.052	1.50***	0.053	1.50***	0.054	1.50***	0.054	1.50***	0.054	1.50***	0.054	1.50***	0.054
Forward Compression Wave	0.86**	0.057	0.91	0.059	1.05	0.083	1.05	0.088	1.05	0.089	1.05	0.089	1.06	0.097	1.06	0.114
0th Harmonic			1.22***	0.055	1.24***	0.055	1.24***	0.055	1.24***	0.058	1.24**	0.069	1.24**	0.069	1.24**	0.081
Pulsatile Hydraulic Work					0.81*	0.084	0.83	0.120	0.83	0.123	0.83	0.151	0.83	0.151	0.83	0.156
Steady Hydraulic Work							0.98	0.090	0.98	0.092	0.98	0.098	0.98	0.098	0.98	0.102
Reflection Coefficent <= 0.65									0.97	0.164	0.97	0.179	0.95	0.189	0.96	0.194
Characteristic Impedance											1.00	0.099	1.00	0.101	1.00	0.111
Backward Expansion Wave													1.02	0.067	1.02	0.068
Backward Compression Wave															1.00	0.082

[1] *p<0.05; **p<0.01; ***p<0.001
[2] OR = Odds Ratio, SE = Standard Error

6.4.2 Tables and Figures

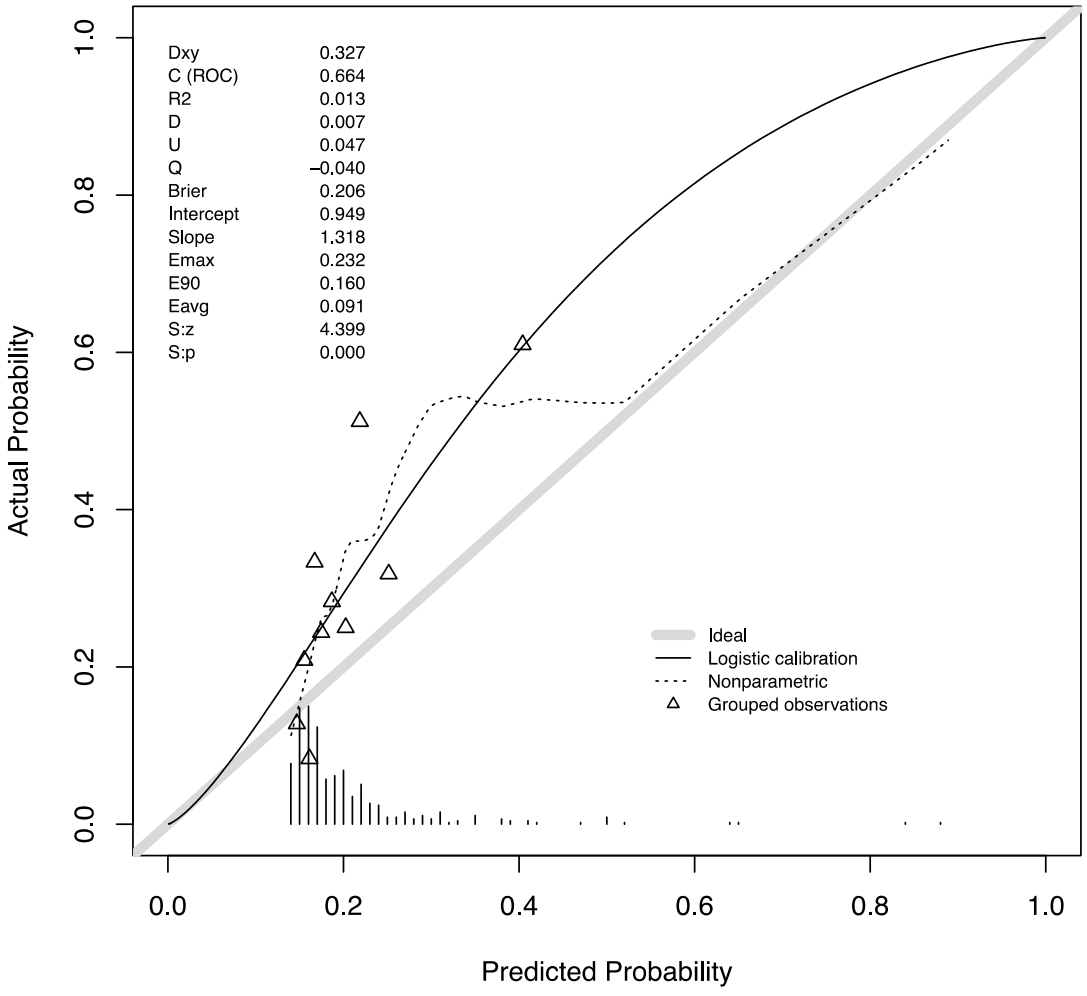

Figure 6.16 Calibration plot for STS risk score only model prior to model updating

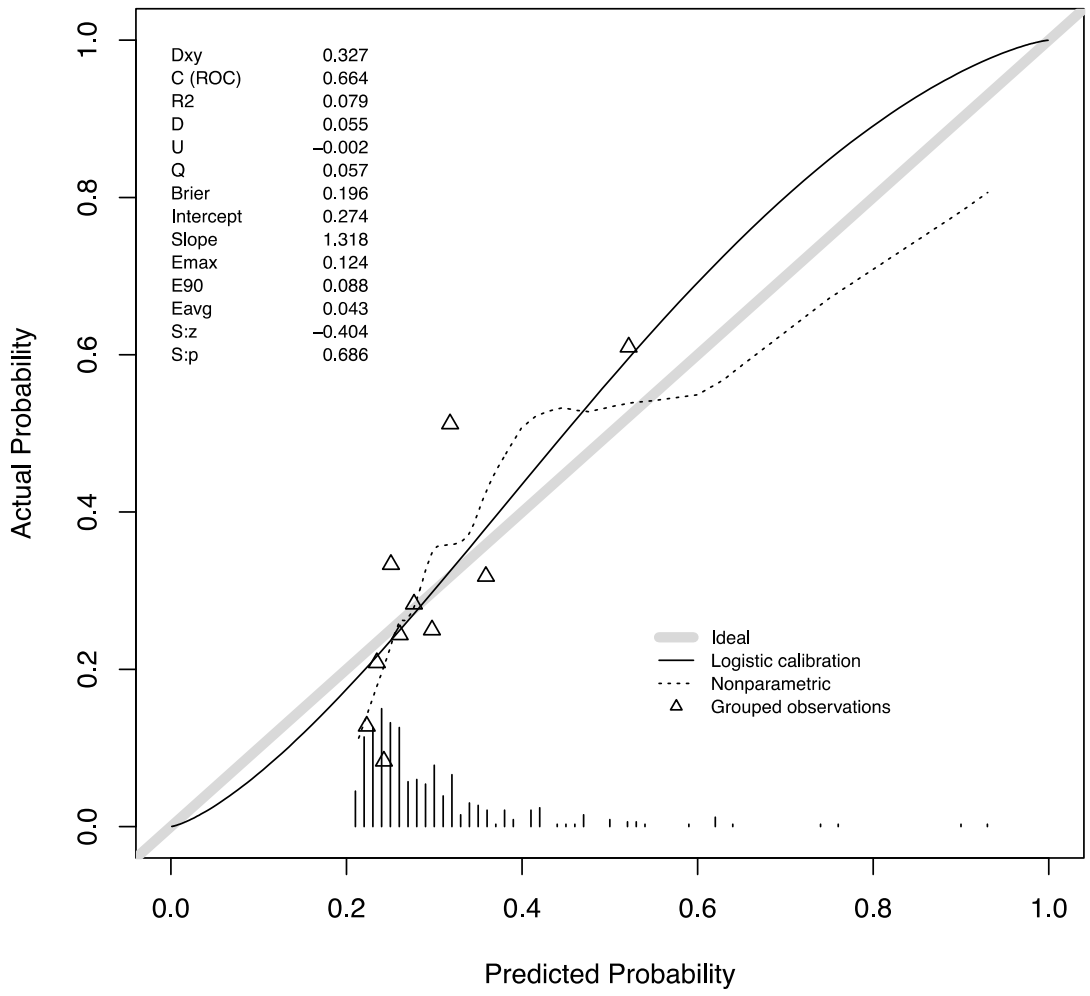

Figure 6.17 Calibration Plot for STS risk score only model with updated intercept

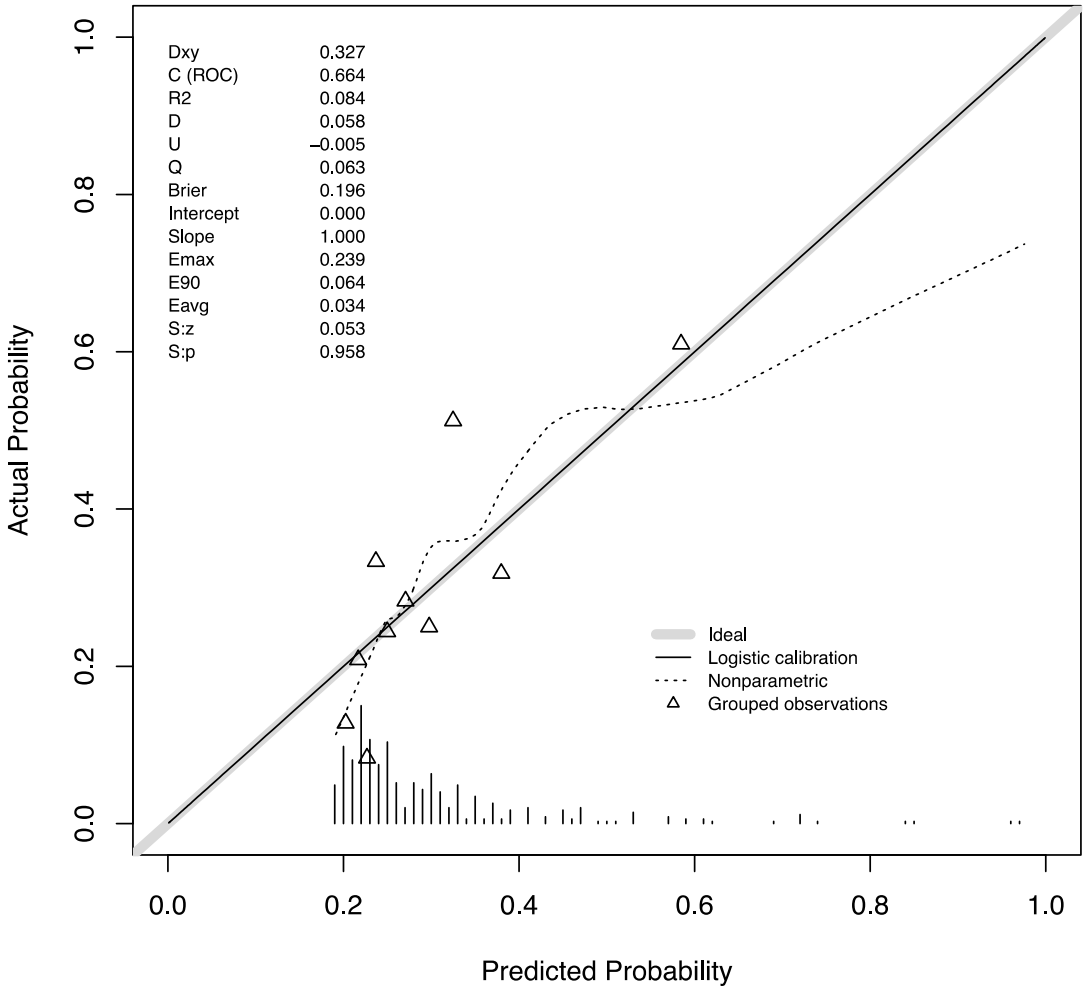

Figure 6.18 Calibration plot of STS risk score model with updated intercept and slope.

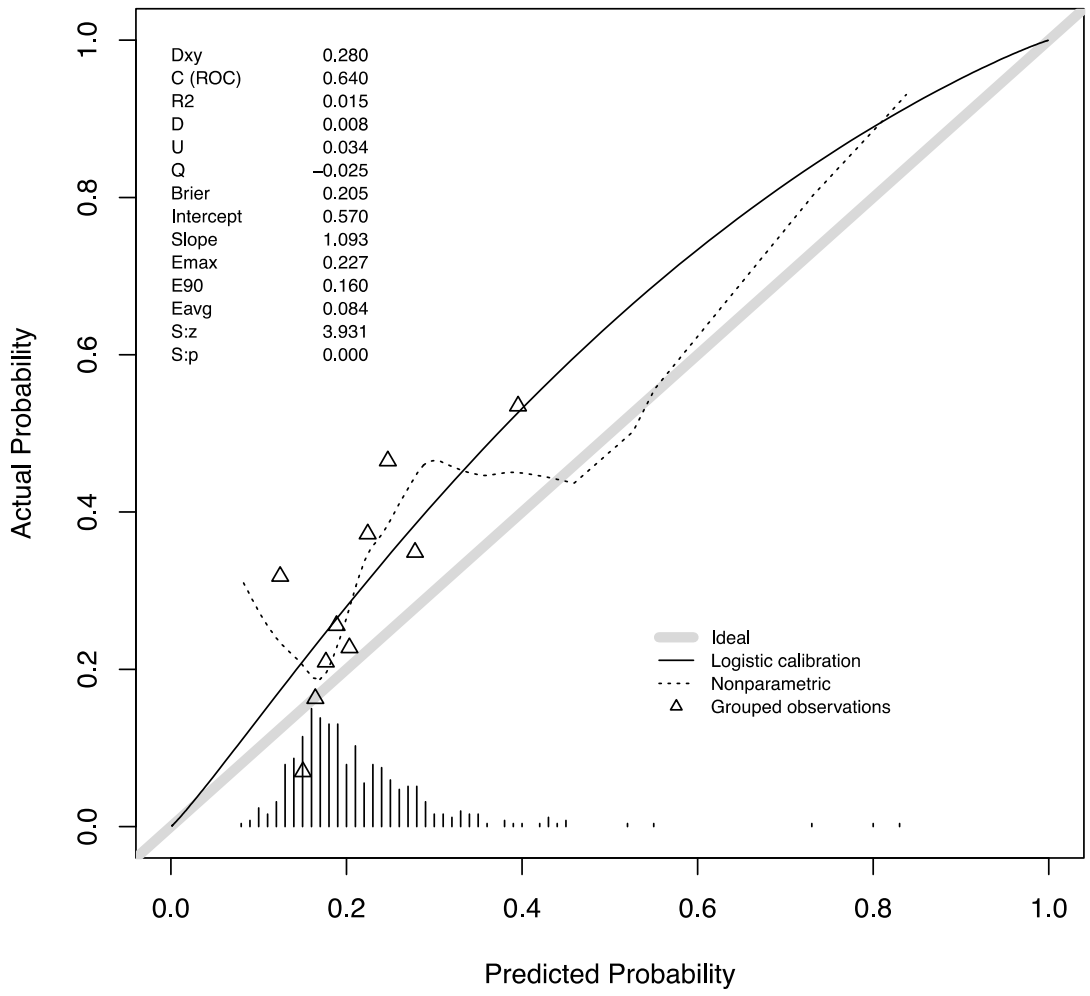

Figure 6.19 Calibration plot for model in the external validation set with impedance metrics prior to model updating

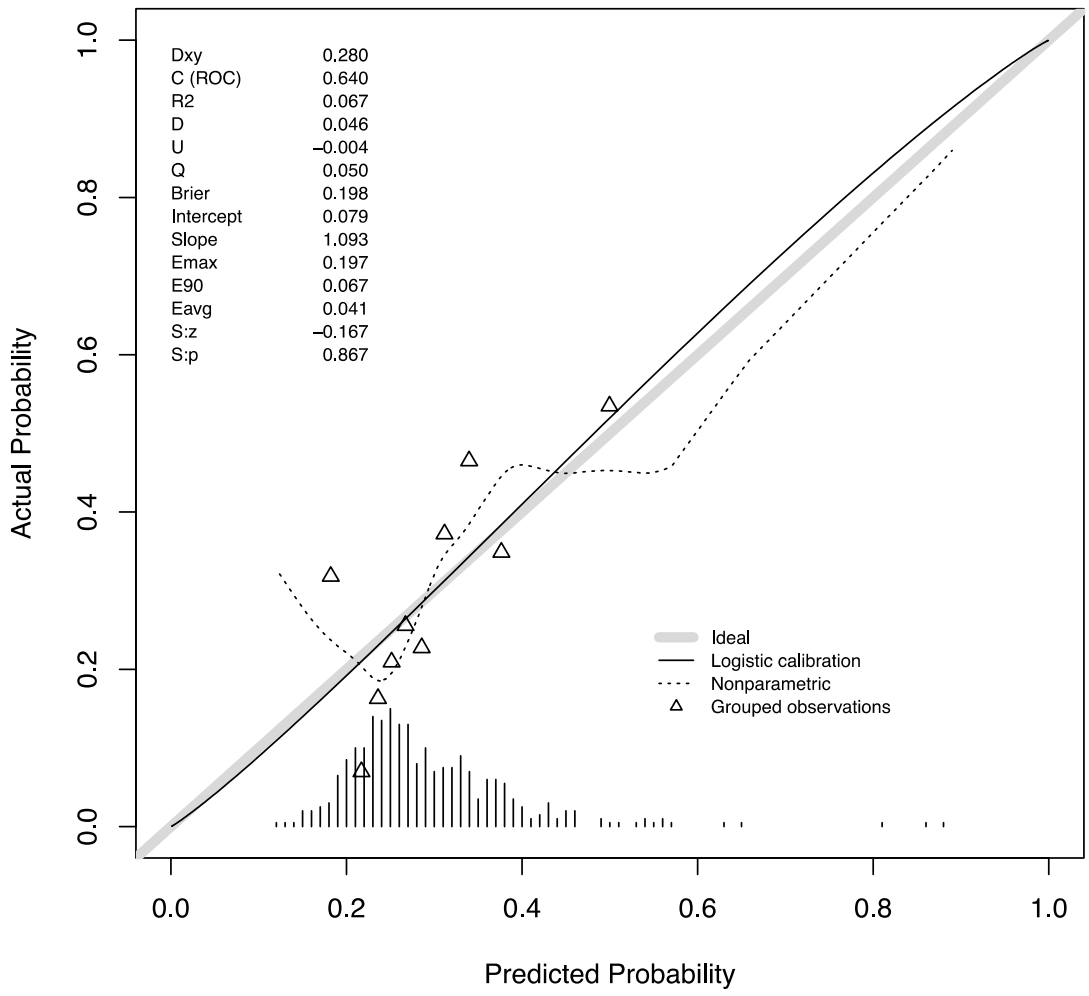

Figure 6.20 Calibration plot for model with impedance after update of intercept

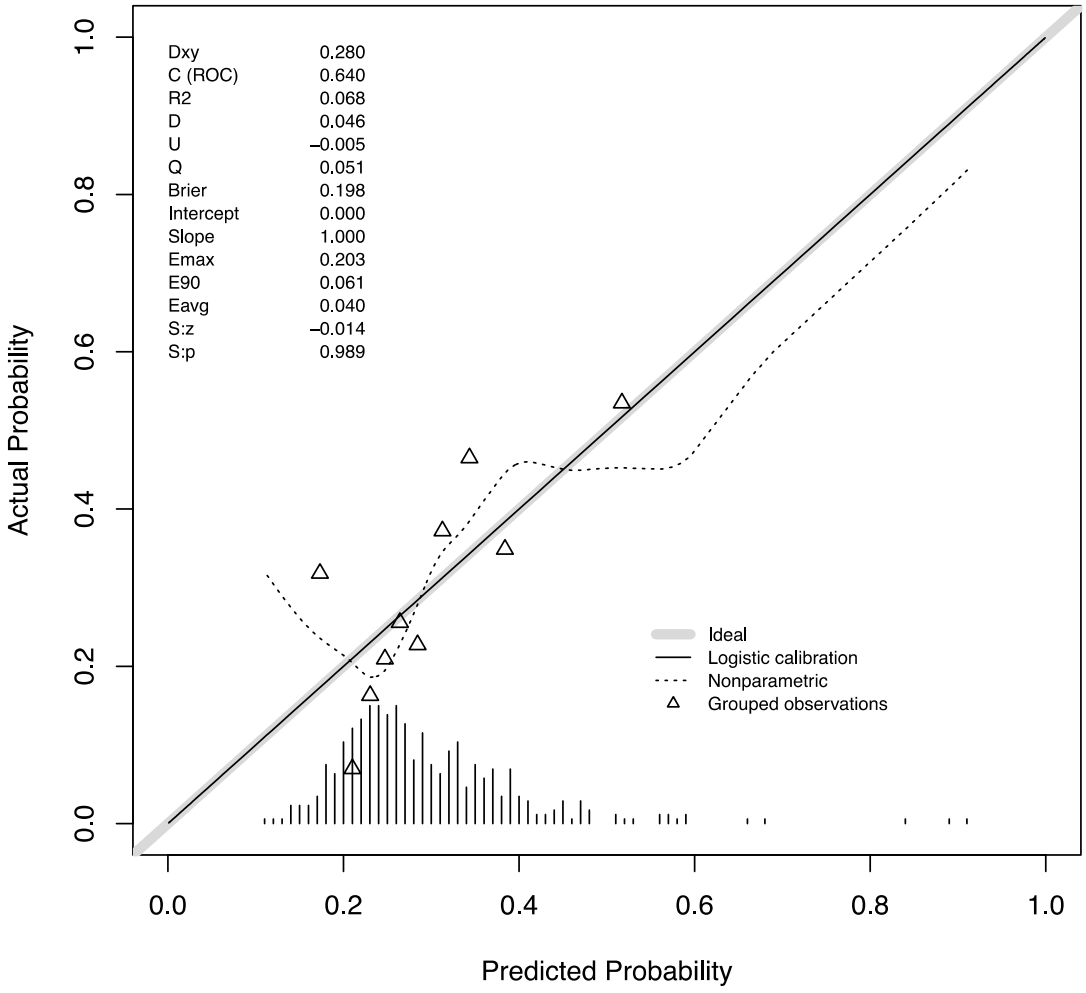

Figure 6.21 Calibration plot for model with impedance after update of intercept and slope

Chapter 7 Bibliography

1. Ben-Dor, I. *et al.* Correlates and causes of death in patients with severe symptomatic aortic stenosis who are not eligible to participate in a clinical trial of transcatheter aortic valve implantation. *Circulation* (2010) doi:10.1161/CIRCULATIONAHA.109.926873.
2. Chizner, M. A., Pearle, D. L. & deLeon, A. C. The natural history of aortic stenosis in adults. *American Heart Journal* (1980) doi:10.1016/0002-8703(80)90375-0.
3. Popma, J. J. *et al.* Transcatheter aortic valve replacement using a self-expanding bioprosthesis in patients with severe aortic stenosis at extreme risk for surgery. *Journal of the American College of Cardiology* **63**, 1972–1981 (2014).
4. Leon, M. B. *et al.* Transcatheter Aortic-Valve Implantation for Aortic Stenosis in Patients Who Cannot Undergo Surgery. *New England Journal of Medicine* **363**, 1597–1607 (2010).
5. Thaden, J. J., Nkomo, V. T. & Enriquez-Sarano, M. The Global Burden of Aortic Stenosis. *Progress in Cardiovascular Diseases* **56**, 565–571 (2014).
6. *2020 American Community Survey 5-Year Estimates*. https://data.census.gov/cedsci/profile?q=United%20States&g=0100000US.
7. *2017 National Population Projections Tables*. https://www.census.gov/data/tables/2017/demo/popproj/2017-summary-tables.html.
8. Keele, K. & Pedretti, C. *Leonardo da Vinci: Corpus of the Anatomical Drawings in the Collection of Her Majesty the Queen at Windsor Castle, 2 vols & facsimiles, London 1979-80*.
9. Vaslef, S. N. & Roberts, W. C. Early descriptions of aortic valve stenosis. *American Heart Journal* **125**, 1465–1474 (1993).
10. Harken, D. E., Lunzer, S. & Jacobey, J. A. Aortic Valve Replacement with a Caged Ball Valve. (1962).
11. Rossebø, A. B. *et al.* Intensive Lipid Lowering with Simvastatin and Ezetimibe in Aortic Stenosis. *N Engl J Med* **359**, 1343–1356 (2008).
12. Nishimura, R. a *et al.* 2014 AHA/ACC Guideline for the Management of Patients With Valvular Heart Disease: A Report of the American College of Cardiology/American Heart Association Task Force on Practice Guidelines. *Journal of the American College of Cardiology* **63**, (2014).
13. Baumgartner, H. *et al.* Echocardiographic assessment of valve stenosis: EAE/ASE recommendations for clinical practice. *European Journal of Echocardiography* **10**, 1–25 (2009).
14. Pio, S. M. *et al.* Discordant severity criteria in patients with moderate aortic stenosis: prognostic implications. *Open Heart* **8**, e001639 (2021).
15. Berthelot-Richer, M. *et al.* Discordant Grading of Aortic Stenosis Severity: Echocardiographic Predictors of Survival Benefit Associated With Aortic Valve Replacement. *JACC: Cardiovascular Imaging* **9**, 797–805 (2016).
16. Ahn, Y. *et al.* Classification of severe aortic stenosis and outcomes after aortic valve replacement. *Sci Rep* **12**, 7506 (2022).
17. Keshavarz-Motamed, Z. *et al.* Elimination of Transcoarctation Pressure Gradients Has No Impact on Left Ventricular Function or Aortic Shear Stress After Intervention

in Patients With Mild Coarctation. *JACC: Cardiovascular Interventions* **9**, 1953–1965 (2016).
18. ROSS, J. & BRAUNWALD, E. Aortic Stenosis. *Circulation* **38**, V-61-V–67 (1968).
19. Eveborn, G. W., Schirmer, H., Heggelund, G., Lunde, P. & Rasmussen, K. The evolving epidemiology of valvular aortic stenosis. The Tromsø Study. *Heart* **99**, 396–400 (2013).
20. Strange, G. *et al.* Poor Long-Term Survival in Patients With Moderate Aortic Stenosis. *Journal of the American College of Cardiology* **74**, 1851–1863 (2019).
21. Otto, C. M. *et al.* 2020 ACC/AHA Guideline for the Management of Patients With Valvular Heart Disease: Executive Summary: A Report of the American College of Cardiology/American Heart Association Joint Committee on Clinical Practice Guidelines. *Journal of the American College of Cardiology* **77**, (2021).
22. Collins, J. J. The evolution of artificial heart valves. *N Engl J Med* **324**, 624–626 (1991).
23. Arnold, S. V. *et al.* Predictors of Poor Outcomes After Transcatheter Aortic Valve Replacement: Results From the PARTNER (Placement of Aortic Transcatheter Valve) Trial. *Circulation* **129**, 2682–2690 (2014).
24. Arnold, S. V. *et al.* Predicting Quality of Life at 1 Year After Transcatheter Aortic Valve Replacement in a Real-World Population. *Circulation. Cardiovascular quality and outcomes* **11**, e004693 (2018).
25. Wessler, B. S., Weintraub, A. R., Udelson, J. E. & Kent, D. M. Can Clinical Predictive Models Identify Patients Who Should Not Receive TAVR? A Systematic Review. *Structural Heart* **4**, 295–299 (2020).
26. Lindman, B. R. *et al.* Blood Pressure and Arterial Load After Transcatheter Aortic Valve Replacement for Aortic Stenosis. *Circ: Cardiovascular Imaging* **10**, (2017).
27. Nichols, W. W., O'Rourke, M. F. & Vlachopoulos, C. *McDonald's Blood Flow in Arteries Theoretical, Experimental and Clinical Principles, sixth edition*. (Cambridge University Press, 2011).
28. O'rourke, M. F. Steady and pulsatile energy losses in the systemic circulation under normal conditions and in simulated arterial disease. *Cardiovascular Research* **1**, 313–326 (1967).
29. Song, N. *et al.* Pulsatile energy consumption as a surrogate marker for vascular afterload improves with time post transcatheter aortic valve replacement in patients with aortic stenosis. *Hypertens Res* (2022) doi:10.1038/s41440-022-01127-4.
30. Parker, K. H. An introduction to wave intensity analysis. *Med Biol Eng Comput* **47**, 175–188 (2009).
31. Westerhof, N., Segers, P. & Westerhof, B. E. Wave separation, wave intensity, the reservoir-wave concept, and the instantaneous wave-free ratio: Presumptions and principles. *Hypertension* **66**, 93–98 (2015).
32. Yotti, R. *et al.* Systemic Vascular Load in Calcific Degenerative Aortic Valve Stenosis. *Journal of the American College of Cardiology* **65**, 423–433 (2015).
33. Shim, Y. *et al.* Ejection load changes in aortic stenosis. Observations made after balloon aortic valvuloplasty. *Circulation research* **71**, 1174–1184 (1992).

34. Ben-Assa, E. *et al.* Ventricular stroke work and vascular impedance refine the characterization of patients with aortic stenosis. *Science Translational Medicine* **11**, (2019).
35. Chirinos, J. A. *et al.* Arterial Properties as Determinants of Left Ventricular Mass and Fibrosis in Severe Aortic Stenosis: Findings From ACRIN PA 4008. *Journal of the American Heart Association* **8**, (2019).
36. Karamanoglu, M., O'Rourke, M. F., Avolio, A. P. & Kelly, R. P. An analysis of the relationship between central aortic and peripheral upper limb pressure waves in man. *European heart journal* **14**, 160–7 (1993).
37. Carroll, J., Mack, M. J. & Vemulapali, S. STS-ACC TVT Registry of Transcatheter Aortic Valve Replacement. **76**, (2020).
38. Lindman, B. R. *et al.* Blood Pressure and Arterial Load After Transcatheter Aortic Valve Replacement for Aortic StenosisCLINICAL PERSPECTIVE. *Circulation: Cardiovascular Imaging* **10**, e006308 (2017).
39. Lancellotti, P. *et al.* Risk stratification in asymptomatic moderate to severe aortic stenosis: The importance of the valvular, arterial and ventricular interplay. *Heart* **96**, 1364–1371 (2010).
40. Hungerford, S. L. *et al.* A novel method to assess valvulo-arterial load in patients with aortic valve stenosis. *Journal of Hypertension* **39**, 437–446 (2021).
41. Baumgartner, H. *et al.* Recommendations on the Echocardiographic Assessment of Aortic Valve Stenosis: A Focused Update from the European Association of Cardiovascular Imaging and the American Society of Echocardiography. *Journal of the American Society of Echocardiography* **30**, 372–392 (2017).
42. Campos-Arias, D., De Buyzere, M. L., Chirinos, J. A., Rietzschel, E. R. & Segers, P. Longitudinal Changes of Input Impedance, Pulse Wave Velocity, and Wave Reflection in a Middle-Aged Population: The Asklepios Study. *Hypertension* **77**, 1154–1165 (2021).
43. Cooper, L. L. *et al.* Components of hemodynamic load and cardiovascular events: the Framingham Heart Study. *Circulation* **131**, 354–61; discussion 361 (2015).
44. Mitchell, G. F. *et al.* Transfer function-derived central pressure and cardiovascular disease events. *Journal of Hypertension* 1 (2016) doi:10.1097/HJH.0000000000000968.
45. Mitchell, G. F. *et al.* Changes in arterial stiffness and wave reflection with advancing age in healthy men and women: The Framingham Heart Study. *Hypertension* (2004) doi:10.1161/01.HYP.0000128420.01881.aa.
46. O'Rourke, M. F. & Nichols, W. W. High flow velocity and low systolic pressure compliance of the aortic wall or venturi effect within. *Journal of the American College of Cardiology* **66**, 595–596 (2015).
47. Yotti, R. *et al.* Reply: High flow velocity and low systolic pressure: Compliance of the aortic wall or venturi effect within. *Journal of the American College of Cardiology* **66**, 596–597 (2015).
48. Kadwalwala, M., Dehn, M., Downey, B., Patel, A. R. & Wessler, B. S. BLOOD PRESSURE CHANGES DURING ROUTINE TRANSTHORACIC ECHOCARDIOGRAPHY. *Journal of the American College of Cardiology* **79**, 1271 (2022).

49. Shoji, T., Nakagomi, A., Okada, S., Ohno, Y. & Kobayashi, Y. Invasive validation of a novel brachial cuff-based oscillometric device (SphygmoCor XCEL) for measuring central blood pressure. *Journal of Hypertension* 1 (2016) doi:10.1097/HJH.0000000000001135.
50. Kelly, R. & Fitchett, D. Noninvasive determination of aortic input impedance and external left ventricular power output: A validation and repeatability study of a new technique. *Journal of the American College of Cardiology* (1992) doi:10.1016/0735-1097(92)90198-V.
51. Bollache, E. *et al.* How to estimate aortic characteristic impedance from magnetic resonance and applanation tonometry data? *Journal of Hypertension* **33**, 575–583 (2015).
52. De la Torre Hernández, J. M. *et al.* Validation study to determine the accuracy of central blood pressure measurement using the SphygmoCor XCEL cuff device in patients with severe aortic stenosis undergoing transcatheter aortic valve replacement. *The Journal of Clinical Hypertension* jch.14245-jch.14245 (2021) doi:10.1111/jch.14245.
53. Lindman, B. R. *et al.* Evaluating Medical Therapy for Calcific Aortic Stenosis. *Journal of the American College of Cardiology* **78**, 2354–2376 (2021).
54. Ben-Assa, E. *et al.* The Role of Ventricular Stroke Work and Vascular Impedance in Defining Aortic Stenosis. in vol. 71 A2664–A2664 (2018).
55. Cramariuc, D. *et al.* Low-Flow Aortic Stenosis in Asymptomatic Patients. Valvular-Arterial Impedance and Systolic Function From the SEAS Substudy. *JACC: Cardiovascular Imaging* **2**, 390–399 (2009).
56. R Core Team. R: A Language and Environment for Statistical Computing. (2021).
57. RStudio Team. *RStudio: Integrated Development Environment for R*. (RStudio, PBC., 2022).
58. Michail, M. *et al.* Acute Effects of Transcatheter Aortic Valve Replacement on Central Aortic Hemodynamics in Patients with Severe Aortic Stenosis. *Hypertension* **75**, 1557–1564 (2020).
59. Lancellotti, P. *et al.* Outcomes of Patients with Asymptomatic Aortic Stenosis Followed Up in Heart Valve Clinics. *JAMA Cardiology* **3**, 1060–1068 (2018).
60. Zhu, D. *et al.* Left Ventricular Global Longitudinal Strain Is Associated With Long-Term Outcomes in Moderate Aortic Stenosis. *Circ: Cardiovascular Imaging* **13**, e009958 (2020).
61. Briand, M. *et al.* Reduced systemic arterial compliance impacts significantly on left ventricular afterload and function in aortic stenosis: implications for diagnosis and treatment. *Journal of the American College of Cardiology* **46**, 291–8 (2005).
62. Hachicha, Z., Dumesnil, J. G. & Pibarot, P. Usefulness of the Valvuloarterial Impedance to Predict Adverse Outcome in Asymptomatic Aortic Stenosis. *Journal of the American College of Cardiology* **54**, 1003–1011 (2009).
63. Levy, F. *et al.* Valvuloarterial impedance does not improve risk stratification in low-ejection fraction, low-gradient aortic stenosis: Results from a multicentre study. *European Journal of Echocardiography* **12**, 358–363 (2011).
64. Katayama, M. *et al.* Does valvuloarterial impedance impact prognosis after surgery for severe aortic stenosis in the elderly? *Open heart* **2**, e000241 (2015).

65. Segers, P. *et al.* Noninvasive (input) impedance, pulse wave velocity, and wave reflection in healthy middle-aged men and women. *Hypertension* **49**, 1248–1255 (2007).
66. Li, S. X. *et al.* Trends in Utilization of Aortic Valve Replacement for Severe Aortic Stenosis. *Journal of the American College of Cardiology* **79**, 864–877 (2022).
67. Pagoulatou, S. Z. *et al.* Acute Effects of Transcatheter Aortic Valve Replacement on the Ventricular-Aortic Interaction. *American Journal of Physiology-Heart and Circulatory Physiology* **2226**, ajpheart.00451.2020 (2020).
68. Spertus, J. V. *et al.* Integrating Quality of Life and Survival Outcomes in Cardiovascular Clinical Trials: Results From the PARTNER Trial. *Circulation: Cardiovascular Quality and Outcomes* **12**, 1–8 (2019).
69. Spertus, J. A., Jones, P. G., Sandhu, A. T. & Arnold, S. V. Interpreting the Kansas City Cardiomyopathy Questionnaire in Clinical Trials and Clinical Care: JACC State-of-the-Art Review. *Journal of the American College of Cardiology* **76**, 2379–2390 (2020).
70. Arnold, S. V. *et al.* How to Define a Poor Outcome after Transcatheter Aortic Valve Replacement: Conceptual Framework and Empirical Observations from the PARTNER Trial. 19 (2014).
71. Fok, H. *et al.* Dominance of the Forward Compression Wave in Determining Pulsatile Components of Blood Pressure. 8.
72. Nichols, W. W., Conti, C. R., Walker, W. E. & Milnor, W. R. Input impedance of the systemic circulation in man. *Circ. Res.* **40**, 451–8 (1977).
73. Chirinos, J. A. & Segers, P. Noninvasive evaluation of left ventricular afterload: Part 1: Pressure and flow measurements and basic principles of wave conduction and reflection. *Hypertension* (2010) doi:10.1161/HYPERTENSIONAHA.110.157321.
74. Chirinos, J. A. & Segers, P. Noninvasive evaluation of left ventricular afterload: Part 2: Arterial pressure-flow and pressure-volume relations in humans. *Hypertension* (2010) doi:10.1161/HYPERTENSIONAHA.110.157339.
75. Shahian, D. M. *et al.* The Society of Thoracic Surgeons 2018 Adult Cardiac Surgery Risk Models: Part 1—Background, Design Considerations, and Model Development. *Annals of Thoracic Surgery* **105**, 1411–1418 (2018).
76. Brien, S. M. O. *et al.* The Society of Thoracic Surgeons 2018 Adult Cardiac Surgery Risk Models : Part 2 — Statistical Methods and Results. (2018) doi:10.1016/j.athoracsur.2018.03.003.
77. Harrell, F. E. *Regression Modeling Strategies*. (Springer, 2015).
78. Arnold, S. V. *et al.* Prediction of Poor Outcome After Transcatheter Aortic Valve Replacement. *J Am Coll Cardiol* **68**, 1868–1877 (2016).
79. Operator's Manual SphygmoCor XCEL System v1.
80. Plunde, O. & Bäck, M. Arterial Stiffness in Aortic Stenosis and the Impact of Aortic Valve Replacement. *VHRM* **Volume 18**, 117–122 (2022).
81. O'Rourke, M. F. & Taylor, M. G. Vascular Impedance of the Femoral Bed. *Circulation Research* **18**, 126–139 (1966).
82. McDonald, D. A. & Taylor, M. G. The Hydrodynamics of the Arterial Circulation. *Progress in Biophysics and Biophysical Chemistry* **9**, 105–173 (1959).

83. Ben Zekry, S. *et al.* Flow Acceleration Time and Ratio of Acceleration Time to Ejection Time for Prosthetic Aortic Valve Function. *JACC: Cardiovascular Imaging* **4**, 1161–1170 (2011).
84. Gamaza-Chulián, S. *et al.* Acceleration Time and Ratio of Acceleration Time to Ejection Time in Aortic Stenosis: New Echocardiographic Diagnostic Parameters. *J Am Soc Echocardiogr* **30**, 947–955 (2017).